Alma Mater Studiorum – Università di Bologna

DOTTORATO DI RICERCA IN

CHIMICA

Ciclo 32 °

Settore Concorsuale: 03/A1

Settore Scientifico Disciplinare: CHIM/12

EXPLORING NEW MATERIAL AND ANALYTICAL METHOD FOR CHARACTERIZATION AND CONSERVATION OF ARTIFACTS

Presentata da: YIMING JIA

Coordinatore Dottorato **Supervisore**

DOMENICA TONELLI **ROCCO MAZZEO**

Esame finale anno 2020

Contents

Abstract

The removal of superficial layers on artworks including grease, dirty, various natural or synthetic varnishes that used in the past, is one of the most important mission in conservation of heritage [1]. Protective coatings and varnishes, such as terpenoid resins, waxes, siccative oil, and acrylic resins among others, would deteriorate under physical and chemical interactions with the surrounding environment, modifying the original appearance of artworks and compromising their conservation. Recently, many research efforts have been devoted to assess sustainable approaches for cleaning together with non-invasive techniques for evaluation the cleaning efficiency and effects of the treatments.

In the last decade, gel system applied for removal of aged varnishes or coatings from artwork surfaces have gained considerable popularity, in particular their ability to retain solvents, providing a more controlled and superficial cleaning action, respect to the traditional methods based on the use of neat organic solvents. In the previous study, we proposed new biocompatible and green cleaning systems of poly-3-hydroxybutyrate (PHB)-based gels with γ-valerolactone (GVL) as solvent, for the removal of terpenic and synthetic varnishes from oil and water sensitive egg tempera paintings [2],[3].

The application of green bio-based cleaning approaches for conservation field is beneficial not only for the artworks, but also for restorer and environment. In this dissertation, we focus on developing new green bio-based gel systems and evaluating both the cleaning efficiency and the release of residues on the treated surface, different micro or no destructive techniques, such as optical microscopy, TGA, FTIR spectroscopy, HS-SPME and micro-Spatially Offset Raman spectroscopy (micro-SORS) were tested, proposing advanced analytical protocols.

In the first part, a ternary PHB-DMC/BD gel system composed by biodiesel (BD), dimethyl carbonate (DMC) and PHB was developed for cleaning of wax-based coatings applied on indoor bronze. The evaluation of the cleaning efficacy of the gel was carried out on a standard bronze sample, which was melted and covered with a beeswax-based coating by restorers of Opificio delle Pietre Dure in Florence. Results obtained by μFTIR analysis showed an efficient removal of the coating. GC-MS was applied for evaluating the extract from the cleaned area of copper sheet mock-up, in order to quantitate the BD residues after wet cotton

swabs and gel cleaning. The PHB-DMC/BD gel was finally tested on a real case precious indoor bronze sculpture Pulpito della Passione attributed to Donatello, and showed good performance for removal of the aged wax containing coating.

In the second part, two new kinds of combined gels based on electrospun tissues and PHB-GVL gel were developed for removal of dammar varnish from painting. Electrospinning as a novel nanofiber producing technology which applied for producing high surface area and flexible fibre members, with large surface area, small aperture, biocompatibility and perfect mechanical properties. Thanks to their properties they have been already used in pharmaceutical and engineering researches [4]. The electrospun combined gels of PVA/PHB-GVL and nylon/PHB-GVL exhibited an outstanding mechanical property, which easy operation and peel off from the treatment surface. The cleaning tests were performed on different thickness dammar decorated painting mock-ups, results obtained by ATR analysis revealed the combined gels are efficient in cleaning over normal gel. TGA analysis showed that the combined gels prone to release larger amount of solvent than normal gel in the room temperature. SEM was applied for the characterization of morphologies both before and after used gels, a thick layer of dammar was observed on the after used electrospun combined gels, maybe because of their relative large solvent release and good absorption of swelling dammar varnish behavior, resulting in fast penetration of GVL into deep varnish layer. HS-SPME was applied for quantitative the amount of GVL residue after cleaning with the use of different gels, the results show that the combined gels have good retention ability in cleaning treatment over normal gel.

In the third part, green deep eutectic solvent was proposed to produce the rigid gel with agar for the removal of proteinaceous coating from oil painting. Deep eutectic solvent (DES) is a type of solvent composed of a salt with a hydrogen bond donor at room temperature that has a lower melting point than either of the individual components. In this research, an advanced DES-agar gel system consists of urea, choline chloride and agar was developed, rabbit glue and whole egg decorated oil painting mock-ups were selected for evaluating its cleaning efficiency, results obtained by ATR analysis showed the DES-agar gel has good cleaning performance. Further residues analysis demonstrated no DES residues were left on the surface.

Furthermore, we proposed micro-Spatially Offset Raman Spectroscopy (micro-SORS) as a

valuable alternative non-destructive method to explore the DES diffusion on painting mock-up. SORS-Raman is a new technique was recently developed, the technique combines conventional macroscale SORS with microscopy permitting the study of micrometer-scale turbid layers [5]. In this research, egg tempera was selected due to the interference of background fluorescence is much lower than oil painting, in addition, the DES residues can have a long term effects with proteinaceous binder paint. The defocusing micro-SORS measurements were acquired at imaged and defocused positions moving the objective away from the sample in vertical direction. The results revealed that the DES mainly distributed on the sample surface after different treatments of DES drop, DES cotton swab cleaning and DES agar gel cleaning, the DES was decreased with increasing of depth. Moreover, the DES agar gel cleaning has lower amount of solvent residues on the surface than the other applications. Further experiments demonstrated that after the diffusion and absorption process, the DES residues on the surface were too few and barely detectable. As a result, the noninvasive micro-SORS technique was successful applied for monitoring the liquid diffusion behavior in painting sub-layer, providing a great and useful instrument for noninvasive residues detection in the conservation field.

Chapter 1 The development of artworks cleaning and assessment methodology

1.1 Introduction

The cleaning of a painting means the removal of any unwanted material that has been deposited on its surface since it was created, including any coatings applied initially to protect the surface that have subsequently deteriorated. It may also be any accumulation on its surface either from atmospheric deposition or by accretions of material from specific activities, perhaps of historic interest [6].

Traditional cleaning of artworks including the use of neat solvents, applied with cotton swabs [7]. This cleaning method showed the disadvantages in unable control over capillary flow through the substrate. For painting, the capillary flow readily causes swelling and leaching of pigment layer and undesired removal of original substance. For other texture artworks, when use of solvent cleaning for removal of dirt or varnishes from particularly porous surfaces like stone or wood, free solvents with the dissolved materials may penetrate in the sub layer make impossible further removal procedures, resulting in a long term of risk for the artworks. To overcome the disadvantages of solvent cleaning system, gel system was proposed for removal of undesired varnishes in last decades. Comparison with solvent cleaning, the gel system has good solvent retention ability which provides more controllable cleaning, resulting a less affection to the original substance. In particular, the development of green and biodegraded cleaning system not only beneficial to the human health and environment but also reduce the risk for artworks. In the first chapter, various coating materials have been introduced, including the mostly used materials for finishing the artworks like nature source resins, waxes, drying oils and proteinaceous. The cleaning strategies described here are not limited to solvents or gels cleaning, but also include the latest progress of other general cleaning systems such as laser and biotechnology cleaning.

To understand the physical and chemical properties of artworks are the crucial points to implement any conservation or restoration of artworks. Nowadays, various analytical techniques could available to provide not only the artworks composition and physical structure, but also can be used to monitor the processes of degradation and deterioration

processes [8]. Microscopy-based techniques are applied to characterize the surface morphologies, such as OM, SEM and AFM, which can provide the different scales information from macro to nano scale. For spectroscopy and chromatography techniques such as FTIR, Raman, HPLC and GCMS can provide the organic and inorganic molecular information of the substances. In many cases, sampling is required for a micro invasive analysis to obtain more information, cross-section is usually prepared since they can be directly used to observe the layer structure of the artworks. Therefore, the design of a complementary, integrated protocol of analysis is often necessary in order to investigate as much as possible information from a small amount of sample. In this thesis we combined with the application of different micro or no destructive techniques, such as optical microscopy, SEM, TGA, FTIR spectroscopy, SPME and micro-Spatially offset Raman spectroscopy (micro-SORS), prosing advanced analytical protocols for evaluating the cleaning efficiency and residues of the new gel cleaning system.

1.2 Typical coating of artworks

"They make such a commotion about it, that it would seem that gloss is the only beauty, and varnish the apogee of art" Marco Boschini mentioned in 1660s [9].

"When a work is painted to the last degree of perfection, it can be considered from close to: it has the advantage of appearing stronger and three-dimensional" André Félibien wrote in 1680s [9],[10].

Varnishes serve as the protective coating and provide the color saturation and gloss for improving the painting's appearance. In detail, the rough surfaces of artworks were become smooth after applying a layer of varnish, resulting in reduced scattering and increased specular reflection of the light at surface, the darker changing is because of the pigment particles covered by the varnish result a higher refractive index than exposure in air. Most of the old master paintings especially those created before nineteenth century were applied the transparent layer for above reasons, but situation was gradually changed after the late of nineteenth century due to the new painting techniques and materials were developed, the use of varnishes are reduced.

Varnish resins such as dammar, sandarac, mastic, acaroid, and hard copal have been used in different periods for different purposes (different texture artworks). Among them, copal resins

could produce the hardest and most durable varnishes, whereas dammar resins are outstanding for their more transparent, pale and ageing resistance performances. Other resins are usually applied for special varnishes, such as sandarac for metal and paper, acaroid resins for metal and leather, mastic for protecting oil and watercolor paintings [11].

Resins collected in the liquid state and applied directly to the surface to be varnished without use of any solvents are called lacquers [11]. Historically, paint varnishes have undergone changes in composition and application. In the old recipe, oil species of natural resins such as sandarac, gum and mastic were prepared by boiling or solubilized in drying oil such as linseed, walnut oil, or poppy oil. The other varnishes such as wax, egg whites were used alone or mix with other materials. The oil varnishes have disadvantages in drying slowly, easy yellowing, rather viscous and hard to apply. Afterwards, spirit varnishes which prepared by natural resins consist of resins (mastic from the Pistacia genus, sandarac, rosin and seldom Venice Turpentine) in the volatile solvents (terpentine oil) become more and more popular. Since the dammar resin was introduced in Europe in the 19th century, the use of dammar with volatile solvent served as a protective coating gradually replaced the position of other kind of varnishes, become the main painting varnishes, due to their better performance in aging resistance and mechanical property than other varnishes like mastic and sandarac. After 19th century, the synthetic technique enhanced, the synthetic varnishes were also developed and widely used such as Paraloid B72, mainly because of their ageing resistance and relative simple composition advantages, however many of them showed the non-ideal physical properties, such as polyvinyl acetate and polycyclohexanone resins [12],[13].

However, varnishes applied on the surface are the most vulnerable parts of artworks, with time, aging and exposure to light would change the composition of varnishes, oxidized species and high molecular weight materials could produce due to the condensation and the light-induced radical reactions. These transformations, which depend on the environments including exposure time, light wavelength and thickness of the layer, giving the varnish different level of yellowish color and degradation [14]–[17].

1.2.1 Wax

Since the ancient Greeks and Romans waxes were started their important application as medium on panel and wall paintings. They were also considered to use as wax varnishes on

marble columns, paintings, wooden ships, ivories and metal surfaces for saturating the surface color or protection purposes, due to their advantages of low water vapor permeability and low gloss [18],[19]. Waxes are amorphous substances principally composed by long chain aliphatic molecules which contain 20-50 carbon atoms in each chain and they show the amorphous regions by chain-chain and tail-tail stacking and are surrounded by disordered chains [20]. Waxes as the non-polymer compounds with low molecular weight and high water repellency, the low cohesive and adhesive properties result they are easily penetrate into the porosity of the objects.

The common used waxes are widely produced from plants, animals and insects including wool wax, montan wax, carnauba wax and beeswax. They mainly consist of free fatty acids, free alcohols or sterols, and hydrocarbon. Among these different sources of waxes, beeswax is one of the mostly used medium or varnish for artworks, it is produced from hive bee, the main components of beeswax are straight chain, saturated hydrocarbons and esters. The derivative of beeswax like carthaginian or punic wax was produced by boiling the original beeswax with seawater and soda several times, and removal of the solution every time. In the old recipe, it has been applied as encaustic technique in painting. With regard to the varnish, a melting of waxes at below 100 ℃ was mostly used for finishing the artworks [21].

As waxes age, their chemical composition alters, as well as the crystalline structure, grain size, bulk mechanical properties, solubility, and workability due to the microchemical reaction during degraded procedure with chains cross-linked, oxidation and chain scission. The degraded processes of wax as a varnish for metal surfaces when exposure outside have been studied. A mechanism based on electrochemical corrosion was proposed. Figure 1.1 showed the aged procedure at different stages, stage 0 represents a fresh wax coating with high barrier properties. Stage 1b represents the coating failure process, due to the presence of trans-film pores that allow electrolyte permeation, this stage occurs almost immediately upon exposure outdoors. Stage 2 represents a coating that fails from extensive cracking and under-film corrosion. Stage 3 represents a completely degraded coating with little wax remaining and extensive corrosion of the substrate [22].

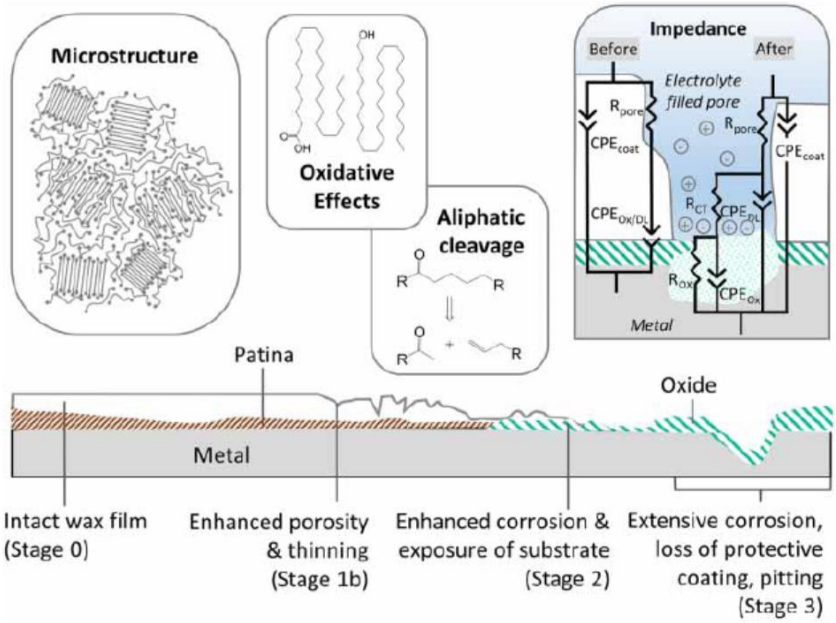

Figure 1.1 The degradation stages of wax coating on metal surface, insets detail the structural, chemical, and barrier properties of the system

1.2.2 Varnish resins

Resins are the sticky secretions from trees and play a role in protecting against herbivores and microorganisms, they would harden once exposed to air environment by evaporation of volatile fractions or partially oxidative polymerization of some components. The terpenoid resins are composed by different length linking of isoprene units (C_5H_8), the additional components including alcohols, aldehydes, esters and amorphous neutral substances. Terpenoids can divide into monoterpenoid, sesquiterpenoid, diterpenoid and triterpenoid which have 10, 15, 20 and 30 carbon atoms per molecular respectively. Different terpenoids showed different behavior in evaporation ability, the volatile fractions usually composed by monoterpenoid, sesquiterpenoid and part of diterpenoid, the nonvolatile fractions mainly composed by diterpenoid and triterpenoid acids, because of the mono- and sesquiterpenoid (figure 1.2) are liquids at room temperature, they usually serve as solvents (the feedstock of volatile terpentine oil) to dissolve the solid formulation of diterpenoid and triterpenoid. As a result, diterpenoid and triterpenoid such as dammar, sandarac, mastic, acaroid, and hard copal, have become the most commonly used materials for painting in history.

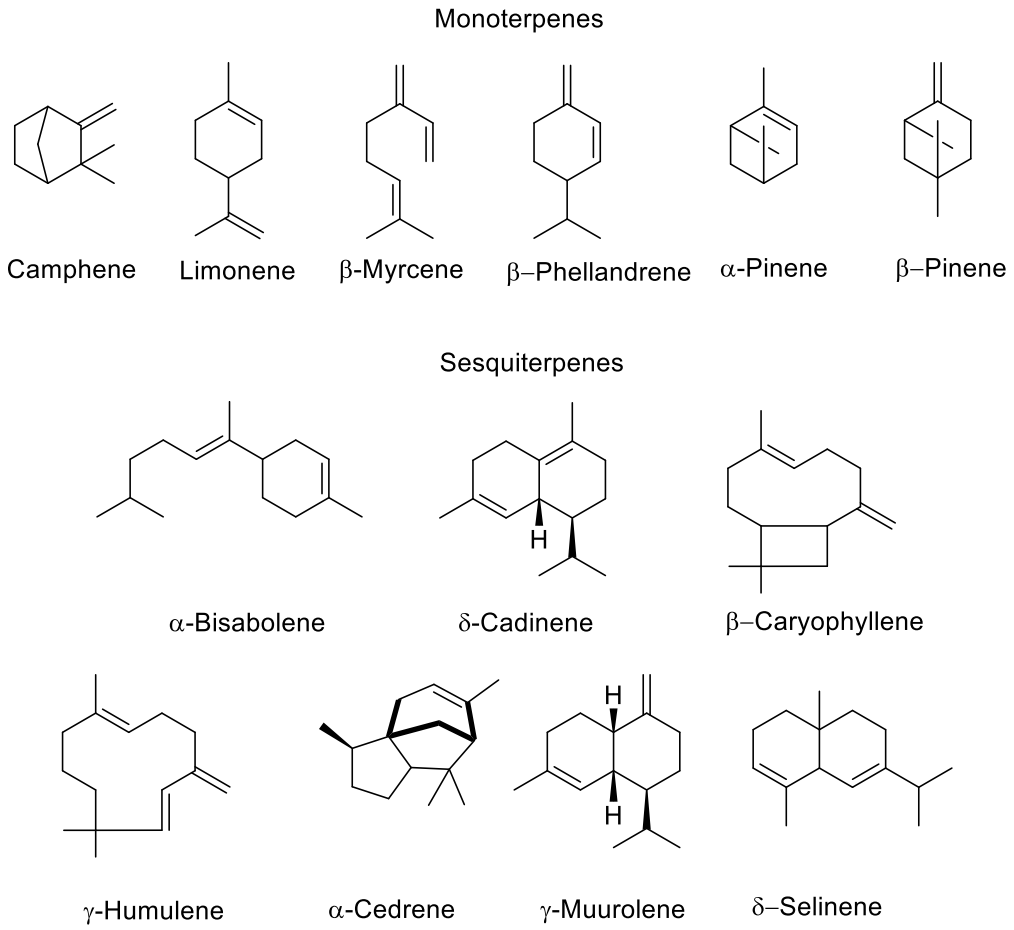

Figure 1.2 Structure of some common monoterpenoids and sesquiterpenoids constituting conifer and angiosperm resins that are used commercially

Sandarac and Copal resins

The diterpenoids are mainly produce from conifer resins, they are characterized by three main skeletal types including abietane, pimarane, and labdane, distributing in different conifer families such as Pinaceae (Abietane and pimarane type diterpenic acids), Araucariaceae (Labdane type compounds) (figure 1.3). The diterpenoid resins have been used for varnishes in the history, such as pin resin, Venice turpentine, Sandarac and Copals.

Sandarac is a commonly used varnish resin in the early stage, sandarac mainly produced from Tetraclinus articulate plant located in North African, it produces a hard, white, spirit varnish that may be brittle if not mixed with other resins, and the gloss varies according to the solvent. During the 12^{th}-15^{th} centuries, it was boiled with linseed oil to prepare the varnishes. After 16^{th} centuries, it was used as a spirit varnish with the volatile terpentine oil.

Copal has been used for painting medium and varnishes, copal mainly consists of diterpenoids producers from Araucariaceae and Leguminosae family widely distribution in Africa, Asia and south America, but after noticing its disadvantages of easy to turn dark and insoluble, they were not recommended as a final picture varnish in the 20th century [11].

Triterpenoid resins such as mastic and dammar, can be used alone or in a mixture with wax and oils, were the most popular varnishes in the past for artists and restorers because of their better adhesive, transparent, solubility and ageing resistance properties than diterpenoid resin varnishes.

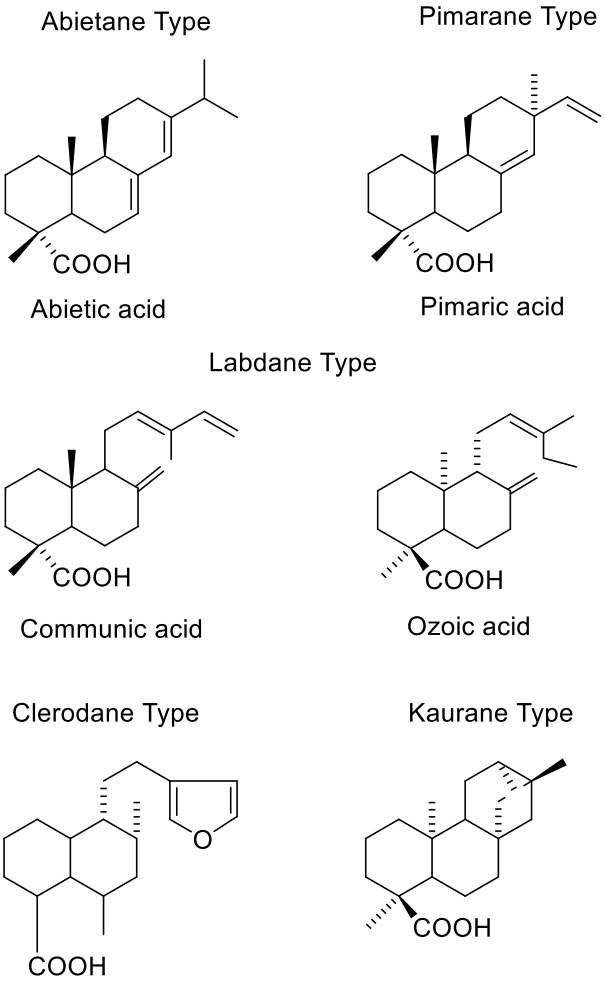

Figure 1.3 Some common diterpene resin acids

Mastic

Mastic is also a resin form conifer of the Anacardiaceae family, and produced by flowering plants (Pistacia lentiscus), mainly located in the Mediterranean region. More than 10 nonvolatile components of triterpenoid acids such as moronic, oleanonic, masticadienolic,

masticadienonic, and oleanolic acids have been identified, a considerable amount of a polymeric component (1,4-poly-β-myrcene) and some other compounds from the neutral fraction include dipterocarpol, lupeol, β-amyrin, β-amyrone, oleanonic aldehyde, and germanicol were also present [11]. Serve as a varnish, mastic has many advantages in terms of good transparency, gloss and solubility, but it is prone to brittle and degraded in moisture environment. It was an important varnish species used for oil varnishes and spirit varnishes during different periods [23],[24].

Dammar

Dammar is a nature triterpene resin producing from the Dipterocarpaceae trees which mostly distributed in the tropical and subtropical regions especially in Malaya and Indonesia (figure 1.4) [25],[26]. Dammar varnish known as a kind of spirit varnishes became widely used by artists and restorers since it introduced to the Europe during the nineteenth century and still be used today, due to its good performance in aging resistance and mechanical property over other varnishes like mastic and sandarac [13],[27].

The composition of dammar varnish has been well investigated by many researches with different analysis techniques, this triterpenoid species resin consists tetracyclic triterpenoids of the dammarane series and minor amounts of pentacyclic triterpenoids of the series of olanane, ursane and hopane, additional a small sesquiterpenoid (C_{15}) fraction and a small polymeric fraction [28],[29].

With aging, the composition of dammar become more complex, yellowing, cracking, brittle and the changing in solubility were observed in appearance, due to the oxidation in dammar resin is fast, it would take place over a short period around 6 months, no matter in light or darkness, regardless of the storage conditions [30],[31]. The oxidation is accompanied by partial polymerization and partial decomposition of the original constituents, and the autoxidation proceeds of radical chain reactions is shown in figure 1.5, when the light was not excluded, initiation through UV excitation of keto groups followed by alpha cleavage (Norrish reaction) has been proposed as a major initiation step.

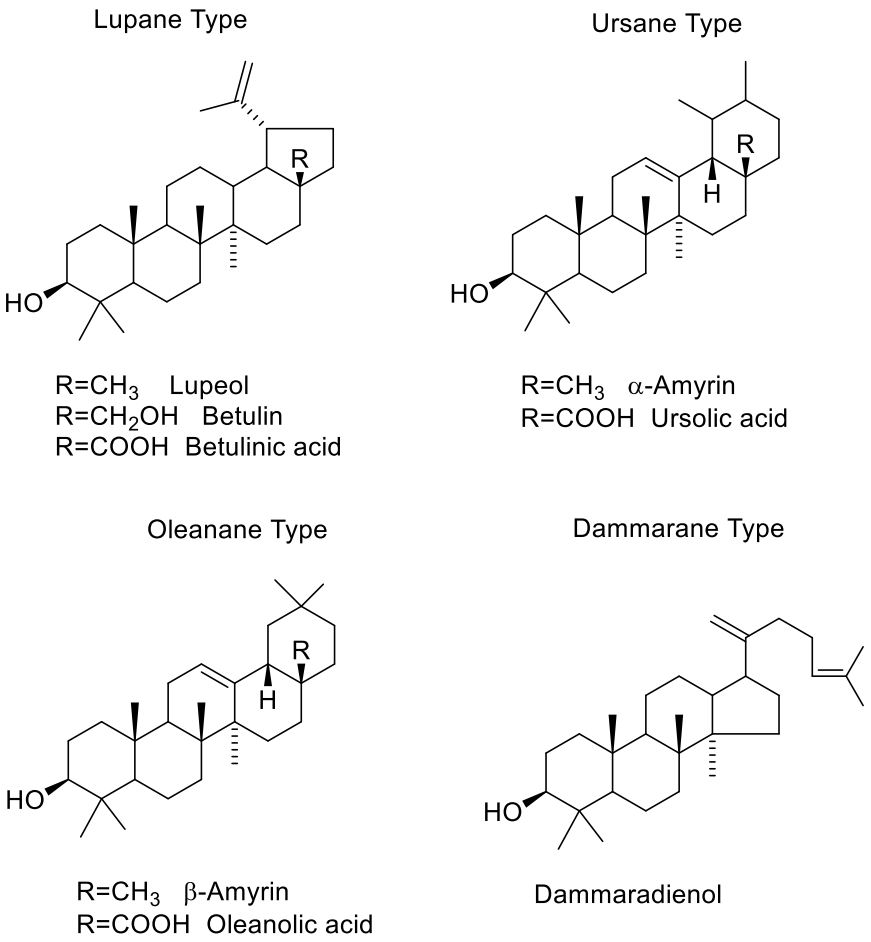

Figure 1.4 Examples of some structural types common in triterpenoid resin components in the large tropical families Burseraceae, Dipterocarpaceae, and Anacardiaceae

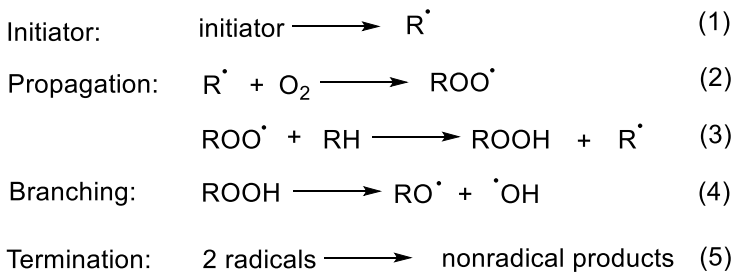

Figure 1.5 The proposed ageing process of dammar

Synthetic varnishes

Since the twentieth century, the development in chemistry enables to synthesize new polymers and provides highly degraded resistant property serve as varnishes. Among these materials, polyvinyl acetate was prepared by polymerization of vinyl acetate with a free-radical mechanism (figure 1.6a). Polyvinyl acetate could be swollen in water and showed an opaque white colour, however it will become transparent after drying. Due to the

advantages in light stable, it was widely used by artists and conservators since it was introduced in this field in 1932 [32]. Paraloid B-72 is another important synthetic varnish material mainly composed by ethyl-methacrylate copolymer (figure 1.6b). It shows good solubility in acetone, ethanol, toluene, xylenes and their mixture, after application, Paraloid B-72 showed stronger and harder than polyvinyl acetate without being extremely brittle.

Comparing with natural resins, synthetic resins have more simple chemical structures, which easier for studying their transformation and degradation mechanism, they also exhibited more uniform and regular chemistry property. However, the synthetic resins have much longer polymer chain and less poly-dispersity than natural resins, thus lead to high viscosities and difficult to operate uniform layer [33],[34]. Afterwards, many new with low molecular weight polymer species were developed for varnishes, such as ketone, hydrogenated hydrocarbon and urea-alderhyde [35]. Ketone serves as a varnish show similar appearance to the natural resins, but the coating seems brittle and easy degradation [36]. Hydrogenated hydrocarbon coating could provide high stable and photochemical degradation resistant property, but its low glass transition temperature (<33 ℃) usually results in a tacky condition and easy to be polluted [37]. Urea-alderhyde coating can overcome the disadvantages and display both photochemical stability and low viscosity which has the potential application in the future [38].

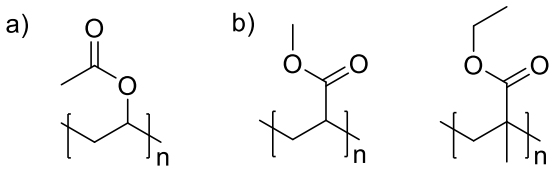

Figure 1.6 a) Structure of polyvinyl acetate (PVAC), b) Paraloid B72, copolymer structures of methyl acrylate and ethyl methacrylate

1.2.3 Siccative oil

Oil paints have been used for hundreds of years in the European tradition of panel and canvas painting since the fifteenth century. Siccative oils especially linseed oil were widely used as the medium for painting, also served as a binder or solvent to dissolve the varnishes. The artists believed that using the same medium in painting and final varnish could ensure a homogeneous constitution and reduce the crack. Due to their capacity of good optical and mechanical properties after drying, linseed oil has become the most commonly used siccative

oil. Linseed oil is natural fatty oil mainly consisting of mixtures of triglycerides, which composed by a glycerol molecule decorated with three fatty acid chains through ester group (figure 1.7). Typically, there are five types of fatty acids, including palmitic, stearic, oleic ($C_{18}H_{34}O_2$), linoleic ($C_{18}H_{32}O_2$) and linolenic acid ($C_{18}H_{30}O_2$), the different percentages were listed in table 1.1, linseed oil contains over 80% of unsaturated fatty acids demonstrated the drying and harden procedure is based on the chemical polymerization via the double bonds by a free radical mechanism, the higher concentration of linolenic acid lead to the faster drying capacity [39]. The polymerization reaction of siccative oils is a three-step radical chain reaction: induction, propagation and termination. The oxygen in the air is the initiator for the first step of the desiccation process. The oxidation and cross-linking take place between of fatty acids, mainly through the reactive methylene groups positioned between the double bonds in the polyunsaturated acids. These reactions lead to form a three-dimensional polymeric network of cross-linked triglycerides [40].

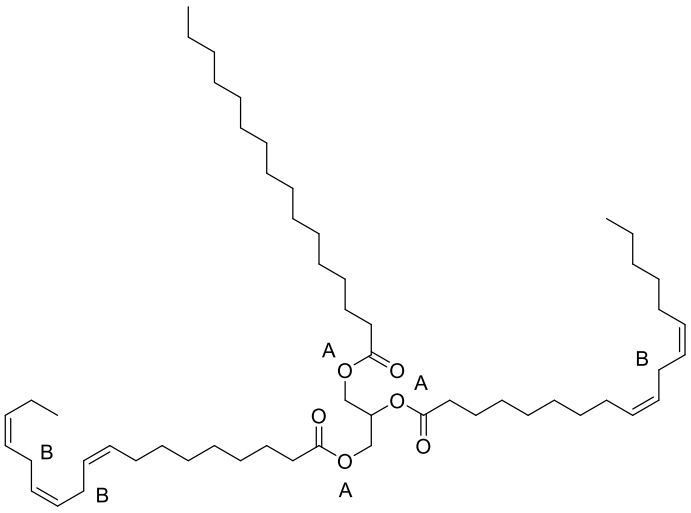

Figure 1.7 Typical structure of a linseed oil triglyceride, derived from palmitic, linoleic and linolenic acids. A=ester bond, B=reactive methylene

Table 1.1 Typical percentages of component fatty acids in linseed oil

Fatty acid	Abbreviation	Systematic name	%
Palmitic	C16	Hexadecanoic	6
Stearic	C18	Octadecanoic	4
Oleic	C18:1	Cis-9-octadecenoic	22

Linoleic	C18:2	Cis-9,12-octadecadienoic	16
Linolenic	C18:3	Cis-9,12,15-octadecatrienoic	52

The old recipe for preparing the protective varnishes was to mix natural resins such as colophony with drying oil and heat, the oil varnishes were widely used in sixteenth century to eighteenth century to protect against air and humidity, and obtain a glossier and more saturated appearance. The main chemical components of these resins are various terpene or terponiod products, when under heating with drying oil, the diterpenic resin would take place of isomerization, dehydration, oxidation, polymerization and decarboxylation reactions. As an example, the presence of colophony may promote oil hydrolysis and suggested the reaction of molecules from linseed oil and colophony with each other, linseed oil and colophony compounds are most probably reacting together to form hybrid species, consist of oligomericditerpenes and/or hybrid glyceride-diterpene [41],[42].

1.2.4 Proteinaceous

Proteins are large biomolecules composed of amino acids, containing both functional carboxylic acid group (-COOH) and basic amine ($-NH_2$) and a side chain (-R) that is specific to each amino acid. Proteins consist of long polypeptides built from series of up to 20 different amino acids, which the amino acids in a polypeptide chain are linked by peptide bonds (CO-NH). The number of amino acids and the sequence in which they are aligned in the chain identifies and gives specific structure and function to the proteins. The simplest protein is just consists of one polyamide with a primary structure of amino acid sequence. Secondary structure is local interactions between stretches of a polypeptide chain by hydrogen bonds, producing a spatial arrangement of the chain such as α-helix and β-pleated sheet and turns structures. Tertiary structure is the overall the three-dimension folding based on the secondary structure. Quarternary structure is the orientation and arrangement of several protein molecules to a single protein complex [43],[44].

Egg white contains about 88% of water, 11% of proteins, 0.2% of fat and 0.8% of ash [45]. The most abundant proteins in egg white are ovalbumin, conalbumin, ovomucoid and lysozyme. Whole egg is a complex mixture of proteins, water, carbohydrate, fat, ash and cholesterol. The main components of whole egg are egg-white (albumin) and egg-yolk [46]. Egg yolk consists

mainly of 68% low density lipoproteins, 16% high density lipoproteins, 10% of livetins and 4% of phosvitins [47]. Whole egg has been serves as a binder for pigments in tempera painting. This ancient technique was used for panel painting until the fourteenth century.

Animal glues are natural polymers derived from mammalian or fish collagen, mainly consist of gelatin and lower molecular weight residues of collagen, keratin, and elastin. They usually used in historic and artistic objects, such as painting ground, binders for pigments, and adhesives [48]. Glue can increase the tensile strength, but becomes stiffer and more brittle upon artificial ageing under UV light, fluctuating RH and temperature [49]. The use of glue as a medium has been quite common in the tempera paintings, it was widely used not only as binder for pigment, but also mixed with gypsum for the preparation of the ground layer in painting.

1.3 The cleaning strategy for artworks

1.3.1 Traditional wet cleaning

The varnish of a painting would become brittle, yellow and losing transparency after few decades, the cleaning process is to removal of the degraded varnish. Suggestions for the use of various kinds of solvents already existed in the early nineteenth century. Their effect on picture surfaces was described by Doerner in 1921, he mentioned “the strongest caustics, acids, and solvents are used without a second thought. Solutions with unknown composition, so-called secret solutions, are recommended to the public, as something anybody without any knowledge can use to clean pictures” [50]. In that period, there is no clearly concept for removal of varnishes or cleaning, but of scrubbing, washing, and refreshing pictures. Different organic or inorganic solvents like caustics, acids, soaps, solvents, and ethereal oils were used. Every ingredient from the kitchen was also put on the table: egg yolks, bread, vegetable juices, onions, garlic, and much more [51]. Afterwards, in the mid-nineteenth century, questions and concerns about new painting techniques and approaches to cleaning paintings were started by scientists, in order to find a new fundamental starting point for interventions.

Traditionally, solvents have been the most common choices for removing the discoloured and degraded varnish, spirits of turpentine and wine, lye soap, pot ash and alkaline, various methods with liquid were used to solubilized, saponification or alkaline hydrolysis for the

further removal of unwanted varnishes. Thus, more and more attention to the threat of painting when applied the solvents for cleaning due to the successful and failure experiences. A long time has been taken to recognize the risks inherent in exposing painted surfaces to cleaning agents, the systematic scientific studies of the effects of cleaning solvents on varnish and oil films were not attempted until Stout's investigations in the 1930s. Stolow measured the swelling of paint films by organic solvents, providing the first framework in which to compare our choice of solvents in 1956, the risk of leaching was also observed. Afterwards, Ruhemann described the critical study in using very small swabs to check each area and confine any potential damage at the level of visual resolution [52]. Conservators applied a variety of solvents to remove aged varnishes, the Teas diagram was the first three-dimensional map of solubility, providing a theoretical framework of categorizing solvents, helping simplified and logical way to predict effective solvents or solvent blends for a given resins [53],[54].

In Italy, after the second half of the twentieth century, the cleaning of paintings artworks was mainly performed with neutral organic solvents and acid or alkaline components, sometimes mixed together with water. One of the most important practical skills for restorer is dealing the cleaning treatment and solve some difficulties during the practice, based on a set of formulas and recipes (table 1.2) for removal of varnishes and retouchings [55].

Table 1.2 Some common mixtures employed in restoration. Note that the acronyms stem from the Italian name of the solvents. DMF=dimethylformamide; n/a=not applicable

Mixtures	Components	Ratio
2 A	Water + ammonia	1:1
3 A	Water + acetone + ethanol	1:1:1
4 A	Water + acetone + ethanol + acetone	1:1:1:1
AB	Water + butylamine	1:1
ABD	Water + butylamine + DMF	1:1:1
Benzine 80℃-100℃	Hydrocarbons	n/a
Nitro thinner	Mixture of esters, ketones, alcohols, and aromatic hydrocarbons	variable, depending on the producer
DA	DMF + amyl acetate	1:1

DAN	DMF + amyl acetate + nitro thinner	1:1:1
DIDAX	DMF + synthetic thinner + xylol + acetone (35 + 15 + 10 + 10 mL, respectively)	3.5:1.5:1:1
Petroleum ether	Hydrocarbons	n/a
White spirit	Hydrocarbons	n/a

However, the use of solvents applied over the surface may affect the pigments and medium in a nondesirable and nonreversible way, because it is difficult to control the penetration into the paint layers [56]. The solvent cleaning procedure involves several crucial issues, the diffusion of free solvents through works of art can produce the swelling or solubilization of sensitive original materials, such as pigments, dyes and binders. Once the pigments solubilized even a few amount in the solvents could lead to de-bonding of the medium, which may explain some blanching or color lifting phenomena. Usually, alcohols and water preferentially affect inorganic pigments, while ketones and less polar solvents preferentially affect organic pigments (dyes). Moreover, any solubilized contaminants, varnishes and adhesives can be diffused by solvents within the pores of the artifact, which means that part of the unwanted layers is prone to move deeper in the painting by capillarity. Finally, most of organic solvents commonly used in restoration are different level of volatile and toxic, hence potentially harmful both to restorers and environment.

The leaching of oil painting layer by solvents has been widely studied since 1950s [57], the soluble and non-cross linked components in the binding medium are the main leaching out components such as glyceride monomers and dimers. Subsequent studies have shown that a solution of varnish produced during the cleaning procedure can have a measurable leaching effect on a paint film [58]. In the meantime, the organic used in the cleaning could also promote the fatty acid carboxylates (metal soaps, formed by free fatty acid and metallic pigments) migrate in painting layer, lead to a significant impact on a painting's appearance [59]. Different periods painting samples from seventeenth to nineteenth centuries were cleaned by polar solvents, the results indicated a small but measurable extraction of fatty acids in some cases were detected in part of samples, and other no, suggested that for the old painting with hundreds of years age exposed to solvents in normal cleaning condition, leaching likely occurs at very low levels [60].

The leaching phenomenon has been also tested on egg tempera with solvents cleaning, the traditional solvents wet cleaning procedure (application of cotton swabs with light rolled over painting surface methods) were tested on both fresh and aged egg tempera (from the sixteenth-century painting) painting surfaces, aiming to evaluate the organic solvents effect with egg binder [61]. Different cleaning agents including the organic of ethanol or acetone, isooctane, and water were used. The results depended on their polarity, which isooctane mainly removes fatty acids and cholesterol, and water removes only amino acids. It was observed that the main leaching component is lipid, and more in the fresh samples, due to the unsaturated fatty acids has completely reacted in old painting. Besides, leaching phenomenon prefer in a layer without pigments than pigments layer. In addition, amino acids were also detected even in the old master painting.

Alkyd resins represent one of the most important classes of binding media of the twentieth century. The general paint rules that apply to alkyds are similar with classic oils such as ground, varnishes, as well as solvents applied for cleaning [62]. The leaching of alkyds painting after cleaning has been evaluated with six solvents or their mixture, including n-hexane, toluene, chloroform, diethyl ether, acetone, and ethanol. The results indicated the smaller components such as free fatty acids, dicarbonic acids, and oxidized products of fragmentation prone to have better solubility and readily tend to be susceptible to leaching. Under the cleaning with different solvents, the more polarity of the solvent mixture results in increased leaching of polar oily components, while the ethanol and its mixture proved to be more destructive to the painting. Besides, the main leaching component during the solvent cleaning was found to be a waxy rheological additive based on hydrogenated castor oil, which generally served as additive in modern paint systems [63].

1.3.2 Laser cleaning

The first attempted with laser cleaning in cultural heritage was by Schawlow in 1965, a ruby pulsed laser was tested for removal of ink pigments from paper without noticeably affecting the underlying paper [64]. Afterwards, since 1970s laser was started and widely used for removal of encrustations from stone sculptures and corrosions from metal objects, and show very good cleaning efficiency [65]. Laser cleaning relies on the ablation effect, as a result of short and strong pulse irradiation at stated wavelengths which are strongly absorbed by the

objects. Generally, Laser cleaning technique can be used alone or combined with traditional cleaning methods (laser application followed by solvent or scalpel cleaning) to obtain a more efficient and safe result [66]. Neodymium laser (Nd: YAG) is the most commonly used laser for cleaning the stone artworks. Excimer laser emitting in the ultraviolet is mainly used for the removal of degraded varnishes from paintings, due to the fact that varnish absorbs strongly in the UV that shows efficient material removal, with minimal light penetration to the sublayers [67]. Laser-assisted removal of degraded varnish coatings showed advantages of the high spatial resolution, accuracy, noncontact, material selectivity and immediate feedback associated with the process of laser ablation over other conventional cleaning methodologies applied for cleaning [68].

However, laser cleaning is an intrusive technique and should be used with good control methodologies, appropriate parameters could promote the laser cleaning effective, selective, and safe. Thus, for the removal of varnishes from painting artworks, laser application is one of the most delicate operations and requires a thorough study of the laser induced thermal, photochemical, and photomechanical effects in order to avoid the damage of paint layer [69]. The potential risks could occur once the coating layer has been removed, the radiation will penetrate the painting layer, if there are no prevention and control measures. The irradiation in sub-layer could induce discoloration of the painting depending on the pigment components affected by the laser radiation. It was suggested that photochemical modifications could occur from the radicals, ions and radicals inspired from the laser ablation could produce photo-oxidation products [70]. Evidence suggested the photo-oxidation may cause some components decomposition, depolymerization or cross-linking during the heating ablation process [67],[71]. Therefore, laser research is nowadays focus on the development and enhancement of the controllable removal of aged protective layers.

There are different types of laser have been used in laser cleaning of paintings, such as Excimer laser, Nd: YAG laser and Er: YAG laser. Excimer laser is a form of ultraviolet laser emitting the wavelengths in the Uv region, various wavelength depends on the molecules be used, for example: ArF (193 nm), KrF (248 nm), XeBr (282 nm), XeCl (308 nm) and XeF (351 nm) [72],[73]. The removal of degraded varnishes and over-paintings with minimum light penetration and thermal effects to the painting layer has been demonstrated based on the use of a KrF excimer laser operating at 248 nm with a nanosecond (ns) pulse duration [68],[74].

Other two different wavelength ultraviolet laser pulses at 398 and 265 nm both in the femtosecond (fs) and nanosecond (ns) durations, and single pulses in the ns domain at 213 nm were tested for the removal of shellac varnish from tempera paints. The results indicated that the irradiation of the coating with fs pulses would change the structure of the varnish and results in degradation of the pigment layer. While the cleaning with pulses of 15 ns at the highly absorbed wavelength of 213 nm enable a gradual control for the removal of varnish without noticeable modification of the pigment layer [75].

Nd: YAG (neodymium-doped: yttrium aluminium garnet, Nd: $Y_3Al_5O_{12}$) is a common type of laser which widely used for stone cleaning applications. The emitting light wavelengths mainly in the near infrared region, typically λ = 1064 nm (ω). For many applications, the infrared light is frequency-doubled, -tripled or more using nonlinear optical materials to obtain various wavelengths of λ = 532 nm (2ω), λ = 355 nm (3ω), λ = 266 nm (4ω), and λ = 213 nm (5ω) [76]. The infrared irradiation tends to active photothermal transformation, enable breaking inorganic component bonds. The effects with organic components are less due to the energy is insufficient to break the covalent bonds, this type of laser could also exhibit good performance for cleaning painting artworks. Research has been applied Nd: YAG laser for removal of terpenic resin from painting mock-up, in the case of without any liquid assists, the main alterations observed were blanching or darkening (linseed binder) effects, which were precursors of ablation of the paint layer observed at higher fluences. The damage situation was strongly related to the type of pigments, especially lead white, cinnabar, and minium, they are sensitive to laser heating. However, the side effect was significant reduced when lead white was mixed with some pigments such as red ochre or lapislazuli [77]. Cleaning tests were performed for removal of black carbon layers and darkened varnishes from egg tempera mock-ups, with the appropriate parameters which under the threshold, the complete cleaning without any observable damage was achieved, also for green earth and lapislazuli mixed with lead white (figure 1.8) [78]

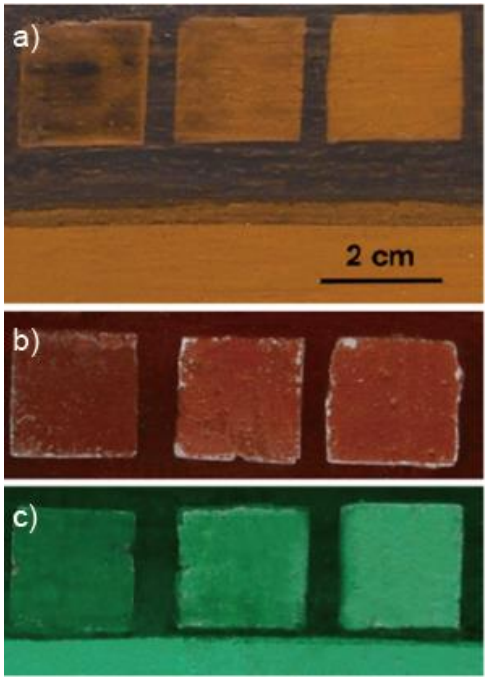

Figure 1.8 LQS1 Nd: YAG (1064 nm/120 ns) laser gradual removal of different coating from egg tempera mock-ups, a) black crust on yellow ochre in egg tempera, b) and of doped dammar on red ochre, c) and malachite

Er: YAG laser (erbium-doped yttrium aluminium garnet laser, erbium YAG laser) emits light wavelength of 2940 nm in mid-infrared region, this wavelength light is highly absorbed by O-H bond especially in aqueous solvents, which could prevent the penetration in presence of components contain O-H groups. If the treated objective doesn't have O-H group, the addition of hydroxylated solvents could also achieve the function in limiting the radiation and heat penetration [79]. Er: YAG laser equipment with threshold conditions of energies lower than 20 mJ at 15 pps assisted by wetting polar agents such as water/ethanol mixture (U1), can be safely used for selectively collecting thin layers from paintings [80].

1.3.3 Microemulsions and micelles cleaning

Amphipathy compounds contain a polar group and an aliphatic tail, could solubilize both in water and organic solvents such as the surfactants. Once the concentration is higher than critical micelle concentration (CMC), the amphipathy molecular will aggregate to form micelles. Micellar and microemulsive solution were produced by surfactant when above the CMC concentration (figure 1.9). Microemulsions were firstly used for cleaning objective in

1991 by Ferroni and his cooperator, dodecane-in-water which sodium dodecylsulphate (SDS) as a surfactant and 1-pentanol as a co-surfactant, was selected for removal of the candle wax deposits. The new cleaning system showed high efficiency in cleaning the wax, afterwards, it got more and more attention, and a series of advanced microemulsions and micellar were developed by researchers [81].

Micellar and microemulsive systems for removal of aged coating from artworks were more developed in last decades, these small nano-sized droplets play an important role for confinement of organic solvent, controlling the release of solvent during the application. Both microemulsions and micellar solutions are optically transparent appearance and thermodynamically stable. The differences of microemulsions and micellar are mainly in the former presents a second liquid component termed the dispersed phase that is insoluble in the solvent, which is termed the continuous phase. The dispersed phase forms microdroplets in the continuous phase, which are stabilized by adsorption of the surfactant at the interface between the microdroplets and the solvent [81].

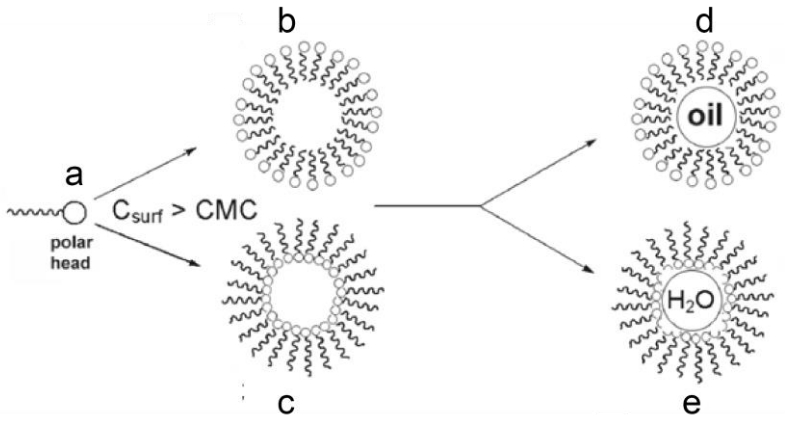

Figure 1.9 Different types of aggregates formed by surfactant molecules: (a) surfactant molecule; (b) spherical micelle; (c) reversed micelle; (d) oil-in-water microemulsion; (e) water-in-oil microemulsion

Oil in water (o/w) microemulsions and micellar solutions based on the blend of surfactant of sodium dodecylsulphate and 1-pentanol was reported for removal of vinyl and acrylic resin from wall paintings. The microemulsions and micellar showed the advantages in reduced the amount of organic solvent and minimized the diffusion in the painting layer, due to form a hydrophilic barrier that can prevent the hydrophobic materials penetrate in the board [81]. A

new nanofluid miceller system produced by water, SDS, 1-pentanol, ethyl acetate, and propylene carbonate was developed (figure 1.10) [82]. This miceller system blended with cellulose pulp poultice, and applied with a rice paper barrier for removal of acrylic and vinyl/ acrylic copolymers coating from mural painting. A mechanism of the cleaning was also proposed with the coating was swollen in the micelles provided extracts, and the swollen coating would separate with surface once the micelles turn small and re-organize the structure with the solvents outflow.

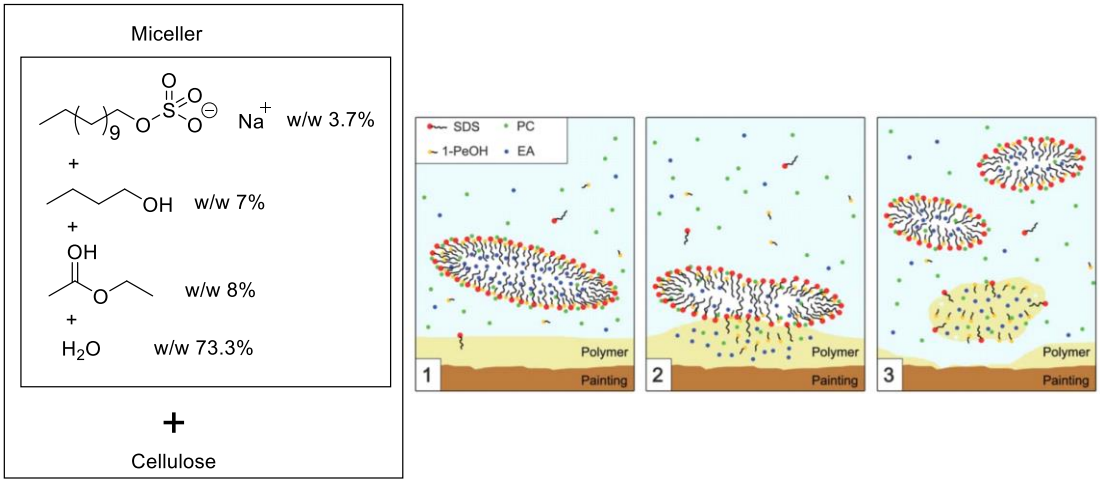

Figure 1.10 The components of micelles (left); the proposed mechanism of interaction between the micelles of the micelle system and the polymer coating (right)

An environmentally-friendly nonionic/cationic (insensitive with divalent metal ions) type of ternary o/w microemulsion consists of diethyl carbonate (oil phase), N, N-Dimethyldodecan-1-amine oxide (surfactant) and water was proposed [83]. The microemulsion was blended with cellulose pulp poultice, and applied with a rice paper barrier for removal of acrylic polymer coating from mural painting (figure 1.11).

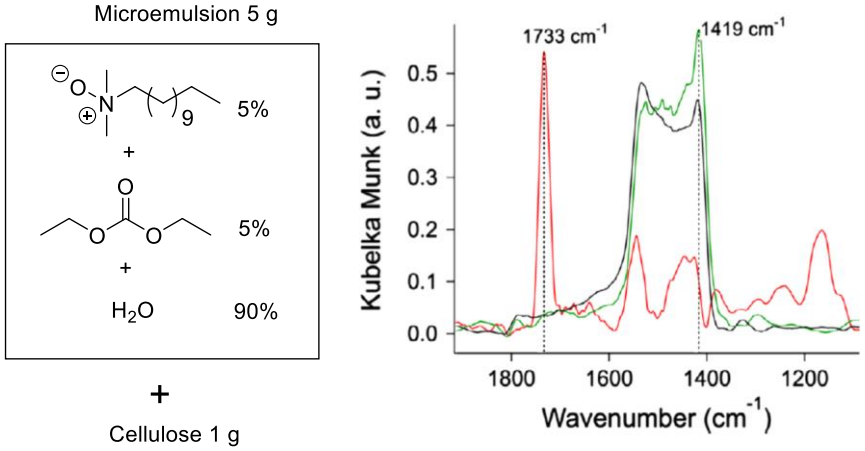

Figure 1.11 The components of Microemulsion (left); FT-IR spectra on the fresco mock-up (right), Black line: untreated fresco surface; Red line: area coated with Primal AC33®; Green line: green line: after cleaning

1.3.4 Biotechnology cleaning

The tools of biotechnology have a great and largely untapped potential for the conservation and restoration of in cultural heritage field [84]. Enzymes are composed by proteins with specific amino acids sequences and unique three dimensional configuration that allows the recognition with certain specified materials in active position, that have been described many times as a lock and key system [85].

Since the 1970s, the enzymes have been found the application in conservation field for the removal of unwanted substances in a controlled condition. Enzymes, in particular hydrolytic enzymes have been proved the possibility in removal of the proteinaceous coating and starch-containing materials. In the certain conditions with aqueous medium and appropriate pH, the aged and insoluble protein-based materials, starch-based glues, and oil-bound overpaints enable be effectively removed with proteases, amylases, and esterases, respectively [85]. Figure 1.12 showed an application of enzyme for cleaning of the discolored polychrome stone sculpture, in order to remove the degraded materials that has been applied for consolidation and protective purposes [86]. Human saliva is 99.5% water, but also contains many important substances, including electrolytes, mucus, antibacterial compounds and various enzymes, especially α-amylase and lipase. The use of saliva to clean degraded surfaces has been widely used by conservators for its flexibility and efficiency. For instance, lipases has been succeed apply for removal of aged drying oil layer and Paraloid B72 in a controlled way, due to the ability of hydrolyzing some ester groups to form free carboxylic acid groups [87]. The mechanism of the saliva cleaning process has been describe as enzymes catalyze degradation action and liquid washing action [88].

However, enzymes are sensitive with temperature, pH and many heavy metal ions, they could induce enzymes denaturation and lose the activity. The denaturation factors have to be considered when apply the enzymes for cleaning. For instance, heavy-metal ions, such as lead, mercury, antimony, and cadmium, are known to be powerful enzyme inhibitors under homogeneous phase catalysis. But these kinds of metals served as pigments such as lead

white, minium, orpiment, and cinnabar, were widely used for the pigments, this could be a limitation factor effect the cleaning efficiency when use the enzymes on these heavy metal pigments contained artworks [86].

The residues problem should be another important issue in using enzymes, proteinaceous tends to darken during aging and affects the artworks appearance; moreover, the residual enzymes could become reactivated sometime following conservation treatments, in this case, many efforts have been applied for removal of the residues [89].

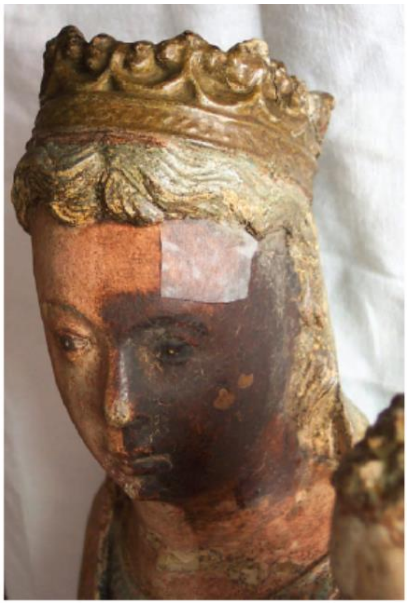

Figure 1.12 Application of an enzyme solution, absorbed onto a cellulose tissue, on a polychrome stone sculpture to remove a discolored oily and proteinaceous coating

In the varnishes application history, nature or synthetic resins were mostly used for coating layer, these organic materials can serve as substrates for microorganisms and accelerate the deterioration process [90]. Biological cleaning consists on the use of living organisms to remove degraded coating, environmental pollutants or other exogenous substances, through biodegradation process due to their metabolic ability to use organic and inorganic compounds for growth [91]. Moreover, biocompounds have the ability to counteract the growth of contaminating microorganisms those are potentially dangerous to the painting, these advantages highlight the potential usefulness of application of microorganisms to prevent bio-deterioration of artworks [92]. Biorestoration method for removal of altered organic materials on stone and fresco artworks has been developed and evaluated. An innovative

biological cleaning for removal of the unwanted layer (collagen) from mural painting consisted of the direct application onto frescoes surface with whole bacterial cells of the Pseudomonas stutzeri A29 strain (bioaugmentation), afterwards a purified Protease enzyme was applied for the final cleaning (figure 1.13). This new technique with microbial cultures for cleaning showed advantages in nondestructive and only removal of the extraneous substances or altered compounds from the fresco, the selected bacteria has non-specific activity, while further treatment with enzymes solution ensure completely removal of all the organic residues, moreover, the use of safe microorganisms (not pathogenic bacteria or yeasts, not spore-forming bacteria) are no harm for both the restorers and the environment [93]. More recently, the same group applied a new agar-gauze bio-gel system for loading seudomonas stutzeri A29 bacterial cells, and made the cleaning more controllable, after 3-12 h, the degraded lipid and protein residues were succeed removed from wall painting fresco (figure 1.13) [94].

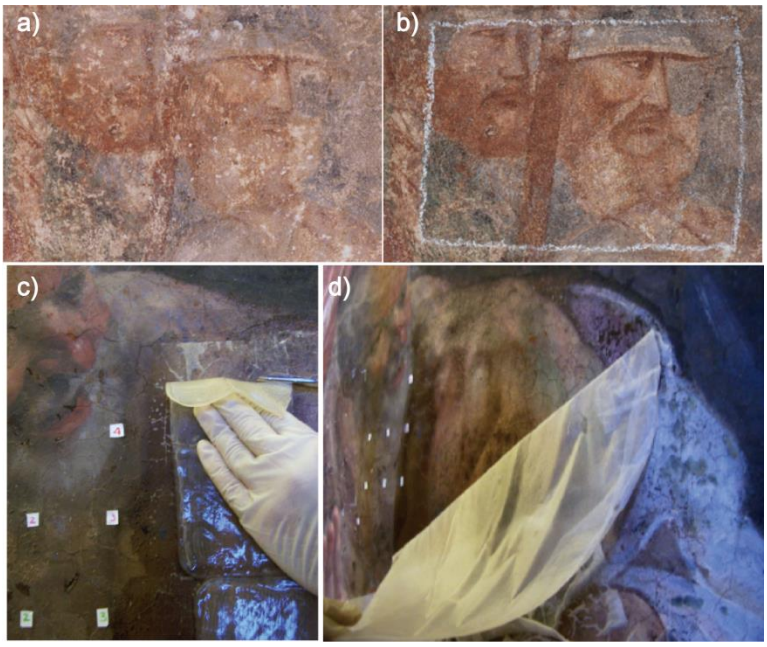

Figure 1.13 Bio-cleaning with Pseudomonas stutzeri strain A29 cells and Protease enzyme on fresco of Conversione di S. Efisio e battaglia (14th century) at Pisa Camposanto Monumentale, (Italy), before (a) and after treatment (b); Agar-gauze bio-gel with Pseudomonas stutzeri A29 on La Navicella wall painting fresco, Vatican Museums, Rome, before (c) and after treatment (d)

1.3.5 Gel cleaning system

In 1980s, Wolber firstly introduced the aqueous gel for cleaning painting surface, the method was dispersion of the cleaning material such as solvent, enzyme, resin soap, surfactant or pH buffer in an aqueous gel. Due to the capacity of the gel, it can better control and reduce the capillary flow induced by the liquids. The more degradation upper varnish enables gradual swelling and safety be removed, in the meantime, the solubilized matter including varnish and dirt would be absorbed by the gel, limiting the transportation within the pores of the painting [95]. As a result, many efforts have been focused in the development of gel cleaning system to retain the liquid component and controlling its spreading and vertical diffusion. Due to the differences of construction driving forces, the gels were divided into categories of physical gels and chemical gels. The physical gels were usually developed by weak interaction driving force including hydrophobic, electrostatic, van der Waals interactions and hydrogen bonds which formed between polymer chains and solvents, such as the organization of traditional used solvents with cellulose ethers, carboxymethyl cellulose, and polyacrylic acid. However, the intrinsic limit of these gels is that they may leave gel residues on the surface after cleaning, requiring further washing with organic solvents in a free-form due to the sticky and difficult handing mechanical property [7],[96].

While chemical gels are refer to those gels based on covalent bands to form a strong 3D cross-link network, most of this kind of gel has good mechanical property and easy to operate, they can load of different cleaning agents, and prone to leave less gel residues on the treatment surface [97],[98], such as the hydrogels based on semiinterpenetrating networks of poly-(2-hydroxymethyl methacrylate) and poly-(vinylpyrrolidone), poly vinyl alcohol based gels, and polymethyl metacrylate organogels have been developed for the cleaning the artifacts [95],[98].

In this case, many gels were developed with good mechanical property and showed outstanding cleaning efficiency for various texture artworks. A hydrophobically modified hydroxyethylcellulose hydrogel was reported with the advantages of high viscosity, readily removal of residue, high water capacity and transparent appearance [99]. Microemulsion cleaning agent of p-xylene in water (consist of sodium dodecylsulphate, 1-pentanol, p-xylene and) was dispersed in the rigid gel for removal of degraded poly-(ethylmethacrylate-co-methylacrylate) coating and natural varnishes on mural painting and wood craft.

A borate cross-linked partially hydrolyzed Poly-(vinyl acetate) gel was developed and showed better loading organic solvents capacity than fully hydrolyzed Poly-(vinyl acetate) gel, up to 50% of organic solvents [100]. In the meantime, the highly viscosity and elastic properties suggested the peel-able and shape flexibility advantages. Different common used organic cleaning agents like acetone, 1-propanol, methyl ethyl ketone, and N-methyl-2-pyrrolidinone could disperse in the gel for various cleaning objective. The cleaning application demonstrated they were efficiency in cleaning aged Paraloid B72 varnishes from wood painting or mural painting (figure 1.14).

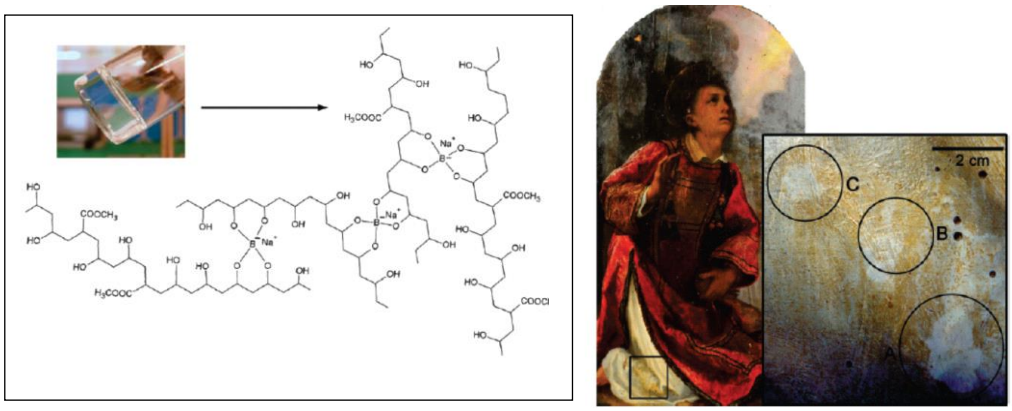

Figure 1.14 Structure of the partially hydrolyzed Borate Cross-Linked PVAc gel (left); area A represents loading 50 wt % 1-propanol in the gel for 1 min cleaning, area B and C represent 30 wt % 1-propanol in the gel for 1 min cleaning (right)

A full chemical organogels was reported which synthesized by a free radical copolymerization reaction, with methyl methacrylate (MMA) and a cross-linker of dimethacrylate react in present of initiator of azobisisobutyronitrile [95]. The chemical gel was used for loading of four typical used organic solvents during restoration, including methyl ethyl ketone (MEK), cyclohexanone (cyclo), ethyl acetate (EA) and butyl acetate (BA). The EA and BA loaded gels were showed good performance for removal of Paraloid B72 from easel paintings and canvas (figure 1.15).

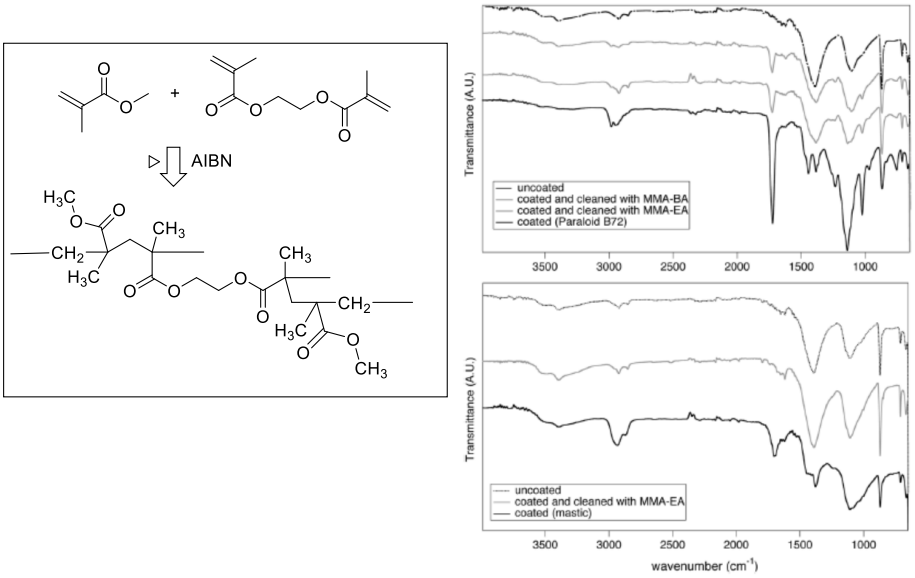

Figure 1.15 The framework of the organogel (left); ATR-FTIR spectra of canvas painting mock-ups coated with natural (mastic) or synthetic (Paraloid B72) coatings, and cleaned using the PMMA organogel gels (right)

A new with good mechanical and loading properties semi-interpenetrating p(HEMA)/PVP hydrogel was developed which was synthesized through free radical polymerization of 2-Hydroxyethyl methacrylate using 2,2-Azobis-(2-methylpropionitrile) as an initiator and N,N'-Methylenebisacrylamide as cross-linker, and the hydrophilic PVP as the loaded component [101]. Two different microemulsion cleaning systems, including nonionic surfactant based micellar cleaning system which consists of N,N-Dimethyldodecan-1-amine oxide (surfactant), 1-butanone, ethyl acetate, butyl acetate and water, another one is ionic microemulsion cleaning system which composed by water, SDS, 1-pentanol, ethyl acetate, and propylene carbonate, they were loaded in the hydrogel for the removal of aged natural resins (dammar) varnishes (figure 1.16).

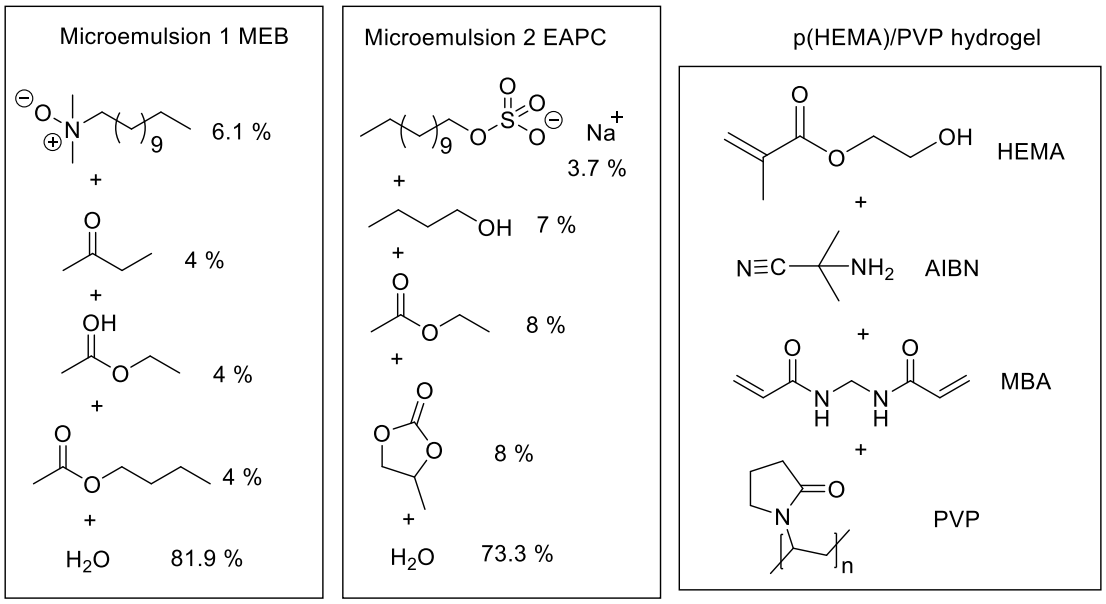

Figure 1.16 The components of nonionic surfactant based microemulsion(left); ionic surfactant based microemulsion(middle); loaded p(HEMA)/PVP hydrogel (right)

Recently, semi-interpenetrating p(HEMA)/PVP hydrogel system was synthesized through free radical polymerization of 2-Hydroxyethyl methacrylate using 2,2-Azobis-(2-methyl -propionitrile) as an initiator and N,N'-Methylenebisacrylamide as cross-linker, PVP as the loaded component [102],[103]. A microemulsion cleaning agent composed by water, SDS, 1-pentanol, ethyl acetate and propylene carbonate was loaded in the stiff gel for the safe and efficient removal of adhesive tapes from backside of a canvas painting and paper artworks (figure 1.17).

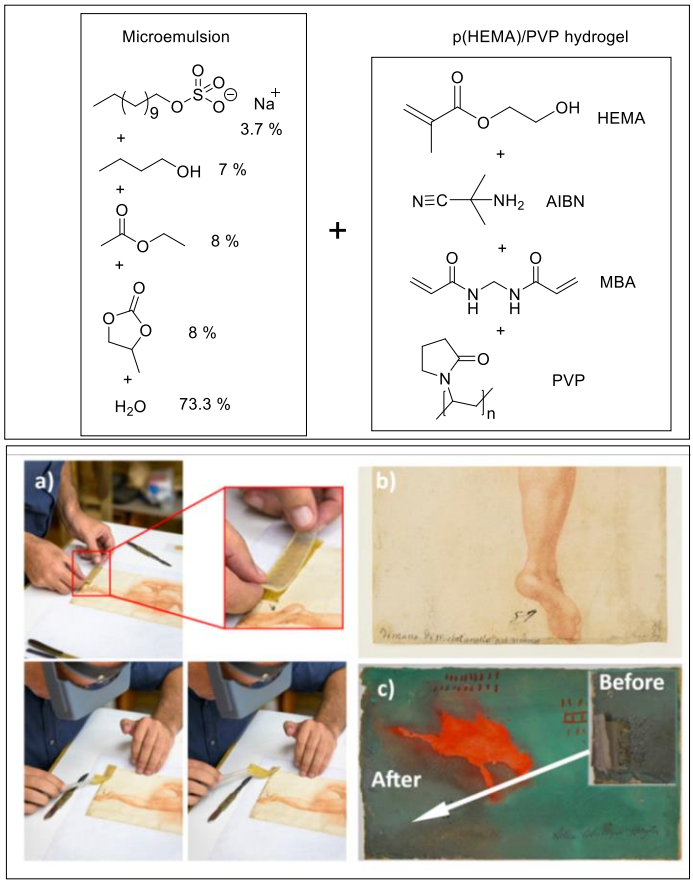

Figure 1.17 The components of microemulsion loaded p(HEMA)/PVP hydrogel (up); (a) Removal of adhesive tapes from the bottom of the 16th century drawing. (b) Detail of the drawing after removal of the pressure-sensitive tape. (c) Before and after removal of pressure-sensitive tape with drawing of Helen Phillips Hayter

More recently, a new kind of hydrogel based on poly-(vinyl alcohol) and poly-(vinyl pyrrolidone) was developed which prepared by using both cast-drying and freeze-thawing methods [104]. The gel showed optimal mechanical strength and displayed good adhesion to rough surfaces. Which could be future applied for loading different cleaning agents for removal of degraded varnishes (figure 1.18).

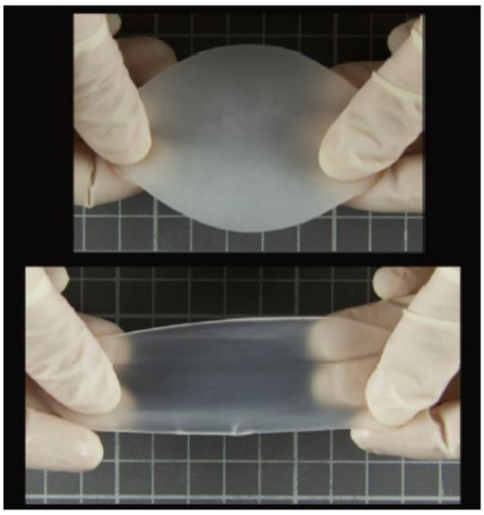

Figure 1.18 The hydrogel of PVA/PVP (3:1), showed the properties of elastic, semi -transparent, and allows an easy manipulation

1.4 Cleaning of artworks: state of the art

Historically, artists have been protected painting or other artworks surfaces with varnish, a system that provides color saturation and gloss to improving the painting's appearance, prevents the air contamination or light directly contact with the painting layer. Cleaning starts with the decision to protect the surface, due to the varnish layer is the most vulnerable part, varnishes are most susceptible to UV radiation, air pollution, and moisture, and as the varnish ages, it becomes more polar and brittle and more soluble in aqueous mixtures.

In the last decades, the crucial concerning about the gel cleaning has been investigated and summarized by Narayan Khandekar in his review [105].

1. Concern over the mechanism of cleaning. The precise role of each component in a gel formulation is in question. Whether it contributes in one or more ways to the cleaning process and whether it works on its own or in tandem are areas that have received an initial examination but are still open to further investigation.

2. Gel residues. What the residues are, how they will react with the paint/varnish film over time and how they will themselves change over time are all questions that have been addressed in the research to date.

3. Leaching of the paint film. Leaching as a result of aqueous gel cleaning has been compared with that caused by solvents applied in a traditional way. Closely related is solvent penetration of paint films through gel application. Although gels reduce capillary movement

of solvents, a comparison of the diffusion of free and gelled solvents has yet to be carried out exhaustively.

There are many researches have been focus on the long-term changes after cleaning by solvents and gels. The investigation of the effects by cleaning agents could helpful in developing a theoretical basis for minimizing risks during cleaning [56]. In the oil painting, the present fatty acids from painting layer were used as the indicators for monitoring the risk of cleaning, evaluating the leaching out fatty acids by extracting the attachments from swab is feasible [106]. Recently, an evaluation of leaching induced by waster or organic solvents applied for the removal of gel residues was studied by extracting the swabs method [107]. Some kind of physical gels show less viscosity, they are not rigid and prone to leave gel residues after treatment, such as cellulose ethers or polyacrylic acid based gels, further wet cleaning is required to remove the residues, which could cause detrimental effects like swelling or leaching of binders or pigments. More recently, the application of unilateral NMR on the after treatment surface for investigating the solvents and gels cleaning was reported, unilateral NMR exhibited a good performance in monitoring the water residue as well its penetration behavior by water and hydrogel cleaning and efficiency in analyzing the thickness of varnish layer and to monitor the effect of the cleaning [108],[109].

Concerning the mechanism of cleaning is an important issue to understand how does different gel component work. Most of the solvent cleaning agent based gels showed the advantages in controlling the solvent release lead to a gradual layer by layer removal of the varnishes, as well as the easy operation with some kind of high viscosity and rigid gel. The solvent plays an important role in swelling the varnishes, and further cotton swab for complete removal of the swelling varnish and residues. Micelle and microemulsion cleaning system composed by amphiphilic surfactant with water and organic solvents have been showed good solvent retention ability and cleaning efficiency. Micelle and microemulsion act as solvent containers and interact with the polymer film leading to varnish swelling and detached from the surface and to its segregation in a liquid droplet, which phase separates from the aqueous bulk. After the removal process the micelles become smaller in size and undergo a structural re-arrangement due to the depletion of the organic solvents (figure 1.19) [82],[110].

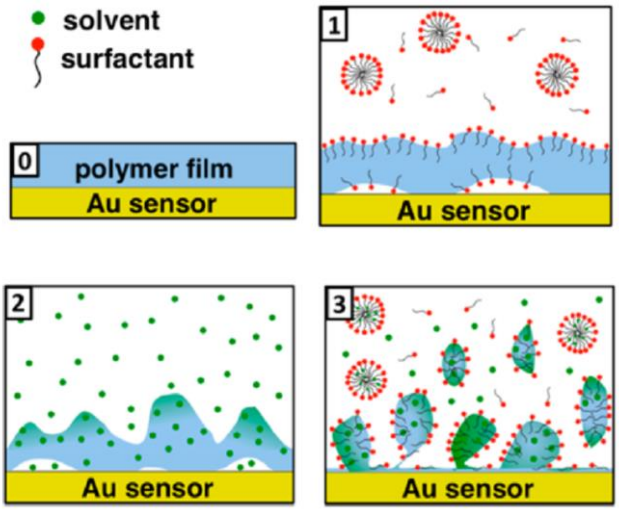

Figure 1.19 Schematic representation of the possible mechanism of polymer removal by Nanostructured Fluids, (0) Polymer film on gold sensor before cleaning. (1) Morphological reorganization of the film induced by amphiphilic aggregates. (2) The good solvent penetrates through the film inducing a significant swelling of the coating. (3) The combined action of both surfactant and solvent promotes the detachment of the film from the surface

Toxicity eventually became a great concern in the 1990s, and it was the main reason for initiating the information campaign on new methods and techniques both in conservation schools and among restorers and conservators [111]. Some high toxicity nitro diluents and of butyl amine not only induce some heath problem, but also a serious of affection by their long retention time inside the paint layers and their very poor selectivity. It was obviously not generally known for how long these toxic substances could remain in the environment and circulate within the human body, even after their use had been stopped or discontinued. At the time, no epidemiological analyses were carried out in this field that would have made these points clearer. Thus, the search for less toxic materials and a more reasonable and cautious use of traditional ones (such as diethanolamine and hydrocarbons) were undertaken and are currently ongoing [112].

The Kamlet-Taft parameters are the most comprehensive and widely used solvent scales to understand and predict of solvent behavior. Solvents are identified by their polarity and polarizability π^* and their basicity or hydrogen-bond accepting ability β (figure 1.20) [113]. Jessop has made the plots which divided the general and green solvents into protic solvents

and aprotic solvents and allowed comparison the solubilization power with each other (figure 1.21) [114]. The green solvents including, water, methanol, ethanol, 2-propanol, 1-propanol, 1-butanol, t-butanol, heptane, ethyl acetate, isopropyl acetate, acetone and methyl ethyl ketone, two carbonate solvents of diethylcarbonate and propylene carbonate, two liquid polymers of poly-(ethylene glycol) and poly-(propylene glycol), several CO_2-expanded solvents, superheated water, and several recently proposed green or biomass-derived organic solvents such as ϒ-valerolactone, 2-methyltetrahydrofuran, glycerol, glycerol ethers, ethyl lactate and cyclopentyl methyl ether. These polar parameters of green solvents are useful for searching an appropriate cleaning agent for the varnish removal.

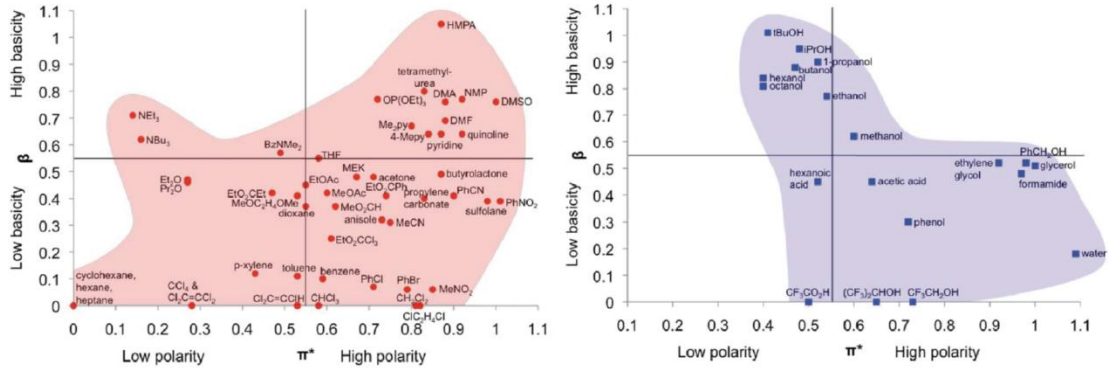

Figure 1.20 Plots showing (left) common aprotic solvents and (right) common protic solvents as a function of their π* (polarity and polarizability) and β (basicity or hydrogen-bond accepting ability) values

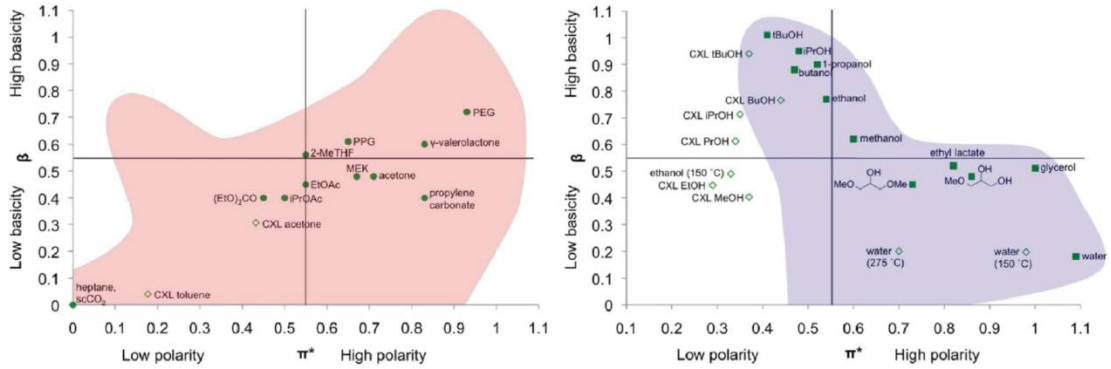

Figure 1.21 Plots showing (left) green aprotic solvents and (right) green protic solvents as a function of their π* (polarity and polarizability) and β (basicity or hydrogen-bond accepting ability) values

Chapter 2 PHB-DMC/BD gel for the removal of wax coating from indoor bronze surfaces

2.1 Introduction

The patina of indoor metal objects is a complex system characterized by the presence of inorganic products and organic coatings. Traditionally, at the end of the casting process, the bronzes were cleaned and the rough surface usually treated to obtain the desired surface finish [115]–[117]. Artificial coatings may be obtained by treating the bronze surface with different chemical solutions, such as chlorides, nitrates and sulphates in order to obtain a color or a selective range of shades of colors. Usually, wax, lacquer, or varnish were applied to saturate the surface color and protect the patina and the metal surface from corrosion [19],[118],[119]. Among these different materials, natural wax such as beeswax is one of the mostly used coating for indoor bronzes, thanks to its properties such as low water vapor permeability and low gloss properties [120]. Waxes were possible applied as a form of maintenance or conservation treatments. As a result, one of the most common objectives today in restoration of bronze is the removal of degraded and aged coatings from objects.

Waxes are mainly composed of long chain aliphatic molecules containing 20-50 carbon atoms, they are surrounded by disordered chains with amorphous regions by chain-chain and tail-tail staking [20]. Usually non-polar solvents, such as dodecane, can be used to solubilize the wax [121]. Some alkaline compounds could also be used to remove the waxes from the surfaces, and then treated with weakly acidic solutions to neutralize their action. This application has been limited due to its aggressiveness for the artwork and environment [122]. Additionally, traditional cleaning methods were based on the application of neat solvents. This cleaning approach may induce some drawbacks mainly owing to the unrestricted action of the solvent, which leads to its penetration into porous matrices, producing undesired phenomena [56],[123]–[125].

In the last decade, chemical and physical gels used for the removal of aged varnishes or coatings from artwork surfaces have gained considerable popularity. The main reason is the gel enable to retain solvents and provide a controlled and efficient superficial cleaning action [82],[121],[126]–[128].

For the cleaning of metal objects, different type of thickeners and confining systems such as micellar solutions or microemulsions, were reported [129]. Recently, a new poly(vinyl) alcohol-based film has been proposed for the removal of corrosion products from historical bronzes [129]. On the other hand, limited attention has been devoted to the impact that such cleaning systems might have on environmental and human safety.

To introduce powerful and sustainable alternatives for cleaning artworks, we have recently developed new biocompatible cleaning systems for paintings based on the use of fully green components [2],[3]. In particular, in the previous studies we have demonstrated the efficiency of poly-3-hydroxybutyrate (PHB)-based gels with γ-valerolactone (GVL) as solvent, for the removal of terpenic and synthetic varnishes from oil and water sensitive egg tempera paintings.

In the present study, bio-based materials were selected to produce new organogels that able to solubilize aged wax coatings from indoor bronzes with a controlled action. To this purpose, PHB was selected as thickening agent and mixed with biodiesel (BD) and dimethyl carbonate (DMC). PHB can be obtained from bacteria through aerobic conversion of various carbon sources, and it is characterized by thermal and mechanical properties comparable to synthetically-produced degradable polyesters and similar to polypropylene (PP) [130]. PHB-based gels can be obtained when the solution formed by heating the polymer in a proper solvent and is then cooled [2]. Therefore, this behavior implies that the solvent used has to be able to solubilize the polymer, while at the same time has to allow the formation of the crystalline phase which holds the structure of the gel together. However, PHB is a highly crystalline polymer, whose solubilization can be guaranteed by just a few green solvents, among the previously attempted solvents able to provide PHB based gels, there are many polar molecules.

Biodiesel is a mixture of alkyl esters with long chain fatty acids, biodegradable and produced by renewable sources [131]. BD was tested and proved its ability in the removal of wax coating, making it a perfect candidate to produce a gel system active against non-polar coatings. However, PHB was completely insoluble in BD, and for this reason it was not possible to obtain a gel by only using these two components.

To overcome this drawback, new solvents mixtures were evaluated, with the aim of

expanding the range of possible formulations that can be used, and possibly allowing the ability to tune the hydrophobic/hydrophilic character of the obtained gels for tailored applications. To this aim, DMC was selected as additional solvent because it is soluble in BD and previous works have demonstrated that it is able to solubilize PHB at 70-90 ℃ and to form a gelly phase when cooled down to room temperature. Moreover, DMC also has the advantage of being the same solvent used for the extraction and purification of the polymer from bacterial debris [132],[133]. DMC is characterized by a low toxic solvent, it is fully biodegradable and not classified as volatile organic compound (VOC) (EPA). In addition, DMC has a high vapor pressure of 7.57 kPa at 25 ℃, that guarantees a lower residual amount on the treated surface.

The performance of the triplet DMC, BD and PHB to provide gel was thus assessed and its performances were evaluated both on standard samples and on the indoor bronze surfaces of the *Pulpito della passione* (1460 A.C.) attributed to Donatello to validate this innovative cleaning system.

2.2 Materials and methods

Reagents	Grade of purity.	Manufacturer
Dimethyl carbonate (DMC)	99%	Sigma-Aldrich
poly-hydroxybutyrate (PHB)	-	Sigma-Aldrich
Cyclohexane	99.5%	Sigma-Aldrich
Biodiesel (BD)	-	Novaol, Ravenna (IT)
Methyl nonadecanoate	-	Sigma-Aldrich
Beeswax	-	C.T.S.

Rheological measurements, the oscillatory shear measurements were carried out on a Paar Physica UDS200 rheometer working at 25 ℃ (±0.1 ℃ Peltier temperature control system) using plate-plate geometry (25 mm diameter). Frequency sweep measurements were carried out at 5% strain. The storage and loss moduli (G’ and G’’, respectively) and complex viscosity

were measured over the frequency range 0.1 to 100 Hz. Rheological measurements were performed on a set of 3 replicates for each type of gel system studied and the trend show no significant differences.

Wide-angle X-ray scattering technique (WAXS) was carried out at room temperature with a PANalytical X'Pert PRO diffractometer equipped with an X'Celerator detector (for ultrafast data collection). A Cu anode was used as X-ray source (K radiation: λ = 0.15418 nm, 40 kV, 40 mA), and ¼° divergence slit was used to collect the data in 2θ range from 2° to 60°.

Scanning Electron Microscope (SEM) ZEISS EVO 50 EP in Environmental mode with ≈100 Pa pressure in the chamber, was applied to characterise the microstructure of the gels, the gels were dried under air condition.

Thermogravimetric analysis (TGA) was performed to identify the capacity of the gel network to retain the solvent, by evaluating the evaporation rate of solvent or gel under set up condition. In this research, TA Instruments model STD-600 was used. Analyses on gels (about 25 mg) and neat solvents (sample weight about 25 mg) were performed under nitrogen flow, an isothermal run at 40 ℃ for 90 min was selected as the one most like the exposition condition of the restorer during cleaning practice. TGA measurements were performed on a set of 3 replicates for each type of gel system studied and the trend shows no significant differences.

Gas chromatography mass spectrometry (5977 Agilent GC-MS) for quantification the solvent residues after cleaning. In this case, 1 cm^2 of copper sheets were treated with both gel and neat biodiesel and then extracted with cyclohexane (10 mL) under sonication for 20 min. The cyclohexane is commonly used for analyzing and synthesizing fatty acid methyl esters (main biodiesel constituents) by GC-MS. Thus, cyclohexane has been selected as a suitable solvent and its ability to solubilize biodiesel has been tested before the analysis. The GC-MS analyses of cyclohexane were performed using an Agilent HP 6850 gas chromatograph connected to an Agilent HP 5975 quadrupole mass spectrometer. The injection port temperature was 280 ℃. Analytes were separated on a HP-5 fused-silica capillary column (stationary phase poly (5% diphenyl/95% dimethyl) siloxane, 30 m, 0.25 mm i.d., 0.25 μm film thickness), with helium as the carrier gas (at constant pressure, 33 cm s^{-1} linear velocity at 200 ℃). Mass spectra were

recorded under electron ionization (70 eV) at a frequency of 1 scan s^{-1} within the 12-600 m/z range. The temperature of the column was increased from 50 to 180 ℃ at 50 ℃ min^{-1} and then from 180 to 300 ℃ at 5 ℃ min^{-1}. Methyl nonadecanoate (0.05 mL of a solution 1000 ppm) was used as internal standard for the quantitation, assuming a unitary response factor for all the methyl esters. Chromatographic analysis has been carried out on 3 sample replicas for each cleaning procedure.

Dino-Lite Premier2 digital microscope type AD4113T-I2 V with ×40 magnification was used to record the morphological changes of the treated surfaces.

To evaluate the presence of wax residues after the cleaning, an Infrared Microscope Thermo Scientific Nicolet iN10MX was used in total reflection mode to record spectra in the range between 675 and 4000 cm^{-1}, with a spectral resolution of 4 cm^{-1} and an optical aperture of 150×150 μm. To obtain representative data, spectroscopic analysis was performed on 3 different areas treated with the same cleaning procedure and 4 spectra were recorded before and after treatment.

Bruker Alpha portable FTIR spectrometer was applied to monitoring the cleaning procedure on the real case of study, with reflectance mode sampling and spectral range 400-7000 cm^{-1}. The instrument has a measurement spot of 6 mm in diameter and working distance of approximately 15 mm. 256 scans were acquired for each spectrum at a resolution of 4 cm^{-1}.

2.3 Gel synthesis and characterization

2.3.1 Synthesis of PHB-BD/DMC gel

Considering the solubility of PHB in DMC, with different ratio of DMC and Biodiesel of solvent mixture could influence of the hardness of the gel, in order to find a best condition gel for cleaning, various ratio of DMC and biodiesel were tested, the gel can't be formed if DMC:BD more than 1:3 (v/v). In the present research, we synthesized two formulations of peelable gel (Table 2.1), with the synthesis step of solubilizing poly-hydroxybutyrate (PHB) into mixtures of dimethyl carbonate (DMC) and biodiesel (BD) with the ratio of polymer with solvent mixture of $PHB_{mg}/solvent_{mL}$=100/1, in a closed vial, by stirring at 110 ℃ for 5 min in an oil bath, until all the PHB powder dissolved in the solution and became transparent, then

cooled down to room temperature in a Petri dish, the thickness of gel is around 0.3 cm.

Table 2.1 Composition of the gel formulations

Gel	PHB mg	DMC mL	Biodiesel mL
PHB-DMC/BD(3:1)	400	3.0	1.0
PHB-DMC/BD(1:1)	400	2.0	2.0

2.3.2 Discussion

In order to evaluate the ability of DMC and biodiesel mixture solvent to produce a gel in the presence of PHB polymer, two formulations of gel have been obtained by varying the ratio between DMC and BD (table 2.1). Preliminary tests showed that BD can dissolve wax, while DMC is used mainly as a tool to promote gel formation and does not seem to contribute to the cleaning. Due to the fact that BD has the ability of removal wax and DMC could form gel with PHB through intermolecular interaction. Both the gels were thickened and formed at the end of the procedure, leading to a gel with a whitish, opaque aspect (Figure 2.1). In both cases the polymer was able to swell up roughly 10 times its starting dry weight (400 mg PHB vs. 4 mL solvent mixture) after the gel formation, demonstrating an interesting attitude in acting as solvent carrier to be used for conservation purposes. Both gels were characterized by different technic to select the most suitable one as cleaning system. Indeed, materials appropriate for the cleaning treatments should be easy to be handle and to be removed from the artwork surface, and they should have to guarantee an adequate stability over time. Hence, different technic including microstructure, rheological behaviour and thermal properties were characterized to evaluate the gel performance and stability.

Organogels are stable as long as the solvent, or a fraction of it, does not evaporate. The PHB-DMC/BD gels showed a good stability over the time. Thus, the shelf life of the gels was estimated at a time interval of two weeks by keeping the gel closed between two Petri dishes in a room environment. At that time the gel has unchanged mechanical properties and still has good cleaning efficiency. Furthermore, previous studies have demonstrated the possibility of recycling PHB after its use in gel formulations.

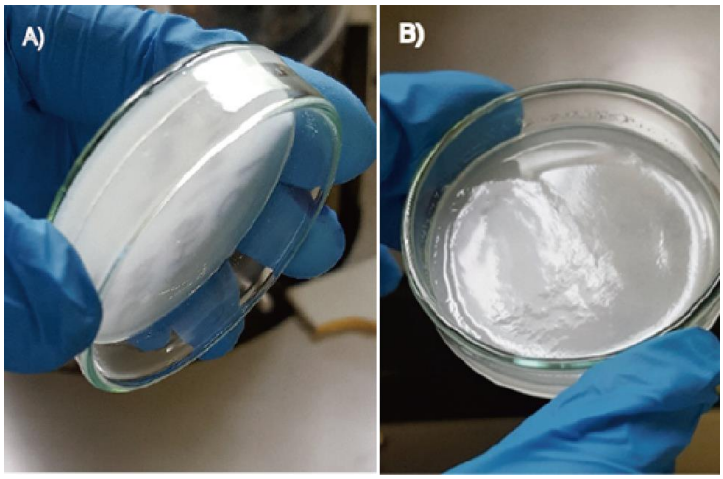

Figure 2.1 The aspect of A) PHB-BD/DMC (3:1) gel; B) PHB-BD/DMC (1:1) gel

2.3.3 Gel characterization

2.3.3.1 Rheological measurements

The mechanical properties of the two gels were investigated with rheological measurements. Figure 2.2 shows the complex viscosity as a function of the applied shear rate. For both samples, a decrease in complex viscosity was observed with increasing frequency. However, the gel containing a higher amount of DMC (DMC/BD 3:1) display a viscosity which is higher by an order of magnitude if compared with the DMC/BD 1:1 gel. This means that the gel is more rigid than the previous formulation and that the simple modification of the solvent system hardly impacts the system properties. Both samples displayed also a high storage modulus (figure 2.2b), indicating good mechanical proprieties in terms of gel stiffness, allowing an easy handling and removal of the gel. The gels presented a gel-like behaviour and in all the cases storage modulus G' was higher than that of the loss modulus G''. The storage modulus quantifies the elastic behaviour of the gels to measure the deformation energy stored in gels during the shear process, while the loss modulus corresponds to the viscous component of gels and shows the dissipation ability of the polymer network. This feature proves the ability of DMC to form the gel, building a 3D network. The stiffness and rigidity are positively correlated with G' and G''. The DMC/BD 3:1 gel has higher modulus than the DMC/BD 1:1, making the latter less stiff. Considering that PHB is insoluble in BD, the higher viscosity recorded for the gel with a higher DMC fraction might tentatively be attributed to a stronger ability to interact with the more akin solvent system, and such a stronger interaction

would in turn hinder the polymer chain mobility. On the bases of this outcome, the DMC/BD 3:1 based gel seems more suitable for cleaning purposes than DMC/BD1:1 based gel, since stiffer formulations could be easier to peel off and usually leave a lower (up to none) extent of residues after application.

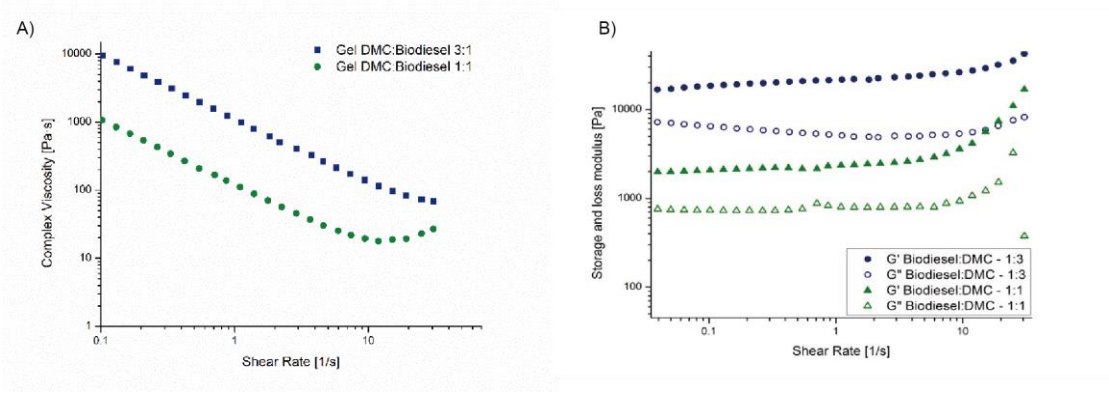

Figure 2.2 Complex viscosity A) and Storage and loss modulus B) as a function of frequency for PHB-DMC/BD (3:1) gel (blue) and PHB-DMC/BD (1:1) gel (green)

2.3.3.2 X-ray powder diffraction

While the capacity of both mixtures of solvents for producing a gel-like structure was proved, the effect on the polymeric component was assessed in terms of ability to crystallize. Wide-angle X-ray scattering technique was used to evaluate the crystallinity of the gels under investigation. As shown in figure 2.3, black diffractogram is referred to the pristine PHB polymer, prior gelation, while spectra in figure 2.3A refer to the diffraction pattern of freshly prepared DMC/BD gels. Fresh gel samples DMC/BD 3:1 and DMC/BD 1:1 diffractograms showed both the presence of narrow reflections typical of a crystalline phase besides the obvious amorphous halo expected for a wet sample, where the solvent is still most of the analysed volume. The comparison of such reflections with the pristine PHB powder spectrum revealed a good agreement of the 2θ positions, confirming once again, that the presence of a gel-like phase is strongly connected to the ability of the solvent system to allow polymer crystallization, without contemporary forcing its complete precipitation in a solid phase precipitate. Moreover, DMC/BD 3:1 wet gel (diffractogram b) seemed to be characterized by a broader amorphous halo. When gels are dried of the solvent system, the analysis of the PHB recovered still displayed reflections positioned accordingly with those of pure PHB. However,

WAXS diffractograms recorded after the complete drying of the gels (Figure 2.3B) showed a broad amorphous halo, suggesting that the polymer is not prone to re-crystallize again with a similar morphology like the pristine polymer, as observed in the presence of GVL [2]. Such a hindering effect towards crystallization ability might be due to the sequential volatilization of the solvent that promotes a preliminary evaporation of the DMC, thus leaving the polymer in the presence of a non-solvent which not allow mobility and reorganization of the polymeric chains in a crystalline fashion. Additionally, the different solvent systems can affect the ability to recrystallize after liquid phase removal, and the presence of a smaller fraction of BD worsen the quality of the PHB crystals, as observed by the comparison of the shape and intensity of the diffractogram peaks.

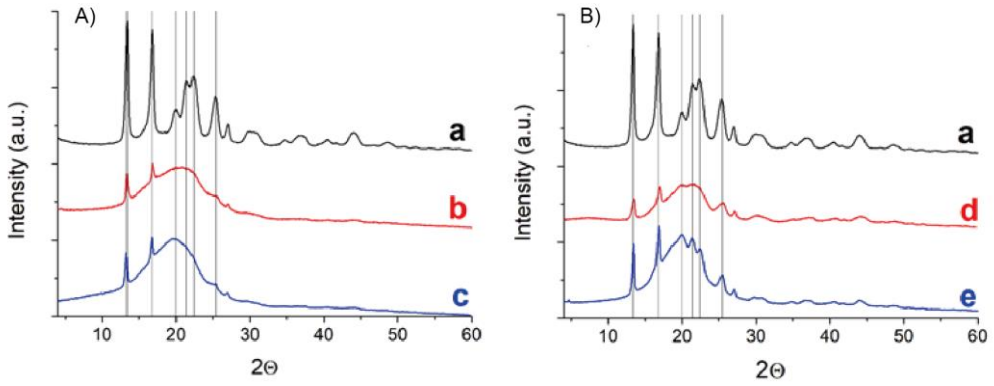

Figure 2.3 WAXS diffractograms of pristine PHB powder (a) compared with A) wet gels PHB-DMC/BD (3:1) (b) PHB-DMC/BD (1:1) (c) and B) dried gels PHB-DMC/BD (3:1) (d) PHB-DMC/BD (1:1) (e). Vertical lines are drawn to guide the eye about the position of pristine PHB (a) crystal phase reflections

2.3.3.3 Scanning electron microscope

Micrographs of dried gels were taken with SEM. The SEM images of PHB-DMC/BD gels with different DMC and BD ratio of 3:1 and 1:1 are shown in Figure 2.4. From the results, both the systems display a compact irregular surface, with some morphology typical of plastic deformation. The surface of the gel DMC/BD 3:1 displays a rugged and voids structure, whereas the gel DMC/BD 1:1 shows a light protuberance and dense surface without any pores. The gel DMC/BD 3:1 also shows a finer structure with micro-indentations typical of a more homogeneous material. This behaviour well compares with the WAXS study previously

discussed, that shows a more amorphous system for the dried DMC/BD 3:1 gel, results of a less microcrystalline structure in the gel and readily form a more homogeneous gel phase.

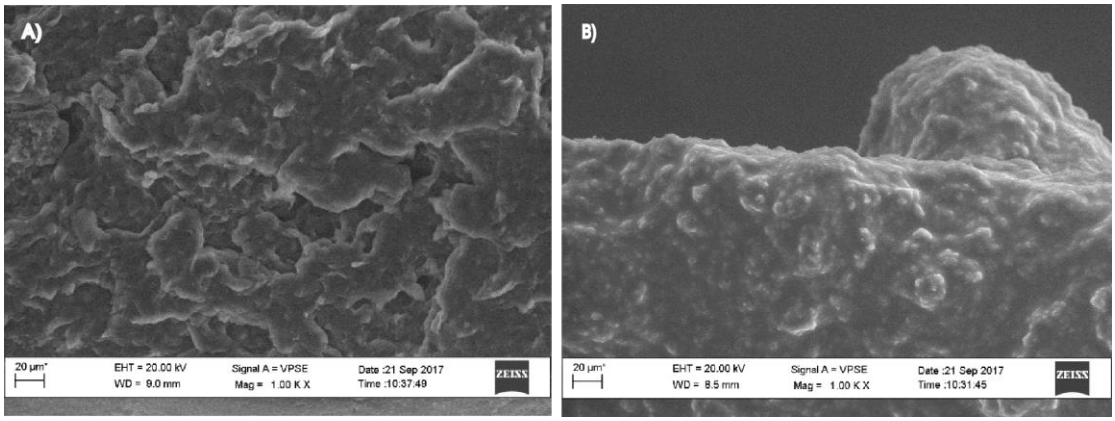

Figure 2.4 SEM micrographs of dried gels A) PHB-DMC/BD (3:1) and B) PHB-DMC/BD (1:1)

2.3.3.4 Thermogravimetric analysis

Once the structure and morphology of the proposed gels has been investigated, their ability to slow down solvent evaporation was evaluated. The capacity of the gel network to retain the solvent and thus reduce the evaporation rate, was evaluated by thermogravimetric analysis (TGA) using a TA Instruments STD-600 apparatus, in comparison to the pure solvent behavior, i.e. in conditions that rule out any possible thermal degradation contribution to the recorded material weight loss. Analyses both on gels and neat solvents were performed under nitrogen flow with the weight around 25 mg. An isothermal run at 40 °C for 90 min was selected as the one most like the exposition condition of the restorer during cleaning treatment. In the applied conditions the weight loss can only be attributed to some solvent evaporation, which is mainly ascribed to DMC, since the biodiesel has a low volatility and high boiling point. The relative weight loss was calculated for each sample, referring to the sole liquid components. This is due to the reason that the polymer (PHB) will never volatilize in the applied conditions, and results are resumed in Table 2.2. The results which illustrated in Figure 2.5, clearly show that the solvent is kept more effectively in the gels while applying the same measuring conditions. The bars in green show the difference between the weight of DMC present in the pristine gel (discarding the PHB fraction) and the actual weight loss recorded during the thermogravimetric measurement, considering only the solvent fraction.

The blue bars represent the difference between the weight of DMC in the sole solvent mixture and the total weight loss recorded during the application of the isotherm in TGA. The solvent retention within the gels is higher for every ratio of dimethyl carbonate and biodiesel. The higher of the biodiesel fraction, the more efficient of the retention of DMC in the gel system. This is a useful feature that can be used to modify the evaporation properties of highly volatile materials (such as DMC), which are generally more complicated to use, while also ensuring greater gel stability.

Table 2.2: Evaluation of the gel's retention power based on TGA results

Sample	Solvent fraction [%wt]	DMC in solvent mixture X_{DMC} [%wt]	TGA weight loss WL_{TGA} [%wt]	$_{DMC}$ [b] [%wt]
Gel PHB-DMC/BD(3:1)	90.9	78.9	67.3[a]	15
Gel PHB-DMC/BD(1:1)	90.5	55.5	38.2[a]	31
DMC/BD(3:1)	100	78.9	72.3	8
DMC/BD(1:1)	100	55.5	51.7	7

[a] Evaluated discarding polymer fraction of the gel

[b] Evaluated as $\Delta_{DMC} = 100 * \frac{(X_{DMC} - WL_{TGA})}{X_{DMC}}$

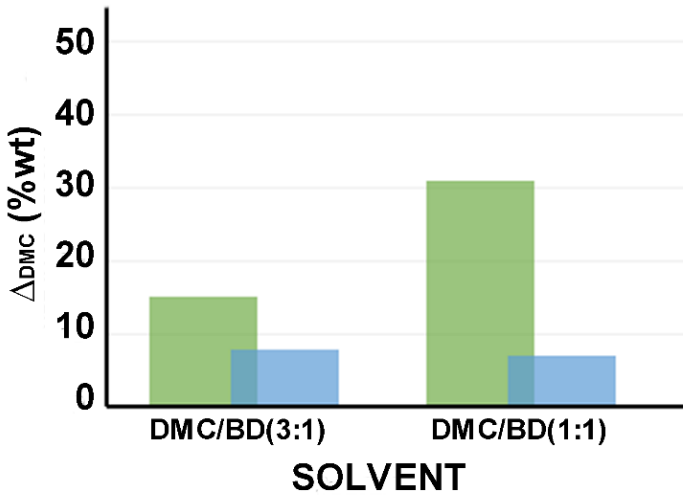

Figure 2.5 Comparison of the solvent evaporation in the gel systems (blue bars) and in pure solvents (green bars) based on TGA experiments

2.3.4 Discussion

In this section, gel characterizations were performed with different techniques and aim to verify the mechanical property, structure and morphology, and solvent retention of the PHB-DMC/BD gel. Two formulations of gel with different ratio of DMC and BD were compared in above experiments. Rheological measurements showed the DMC/BD 3:1 gel has higher modulus than the DMC/BD 1:1 which indicated the former has higher viscosity and rigid phase. SEM micrographs showed the DMC and BD ratio of 3:1 gel displayed more rugged and voids structure which could provide large contact surface. Wide-angle X-ray scattering technique was applied to evaluate the crystallinity of the gels, indicated the gel phase is related to the crystallization ability of the solvent. After drying the gel, the polymer couldn't re-crystallize to the polymer pristine. In order to understand the solvent retention capacity of the two gels, TGA isothermal run at 40 °C for 90 min condition was applied, the lost solvent in this condition is DMC due to the other liquid of biodiesel has low volatility and high boiling point. After calculation, the higher is the biodiesel fraction, the more efficient is the retention of DMC in the gel system.

As a result, DMC and BD ratio of 3:1 gel was selected for further cleaning experiments, considering the better mechanical property and diversity of the morphology. Moreover, the lower amount of difficult volatilization component (biodiesel) presence, the easier for removal of all the residues after application, lead to a low risk to the artworks after cleaning.

2.4 The cleaning work on bronze

2.4.1 Mock-ups preparation

Standard bronze samples have been prepared by the restorers of Opificio delle Pietre Dure (Florence), following ancient recipes (figure 2.6a). In more detail, the metal surface of a fresh cast bronze has been brushed with silver nitrate solution and heated with blue flame, until the surface turn to black. Then, a thin layer of beeswax was brushed under soft flame, after polishing with a piece of towel until the surface become glossy, the FTIR in total reflection and the bands vibrational assignments were showed in figure 2.7a and table 2.3.

Copper sheets were also used for the evaluation of the cleaning approach. Copper sheets were

prepared by applying a thin layer of beeswax with soft brush after oxidation of the surface with flame (figure 2.6b), the FTIR in total reflection and the bands vibrational assignments were showed in figure 2.7b and table 2.3.

Finally, the Pulpito della Passione (1460 A.C.) exhibited in the church of Basilica di Lorenzo and attributed to Donatello was submitted to the green gel cleaning procedure for the removal of an aged wax-based coating (figure 2.6c).

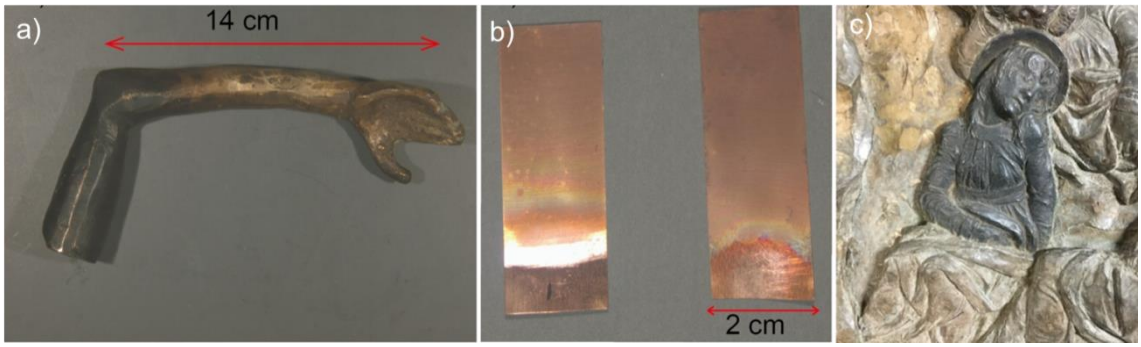

Figure 2.6 a) Bronze mock-up sample made by Opificio delle Pietre dure in Florence; b) Copper sheet mock-up coated by beeswax; c) Pulpito della passione (Donatello, 1460, Florence)

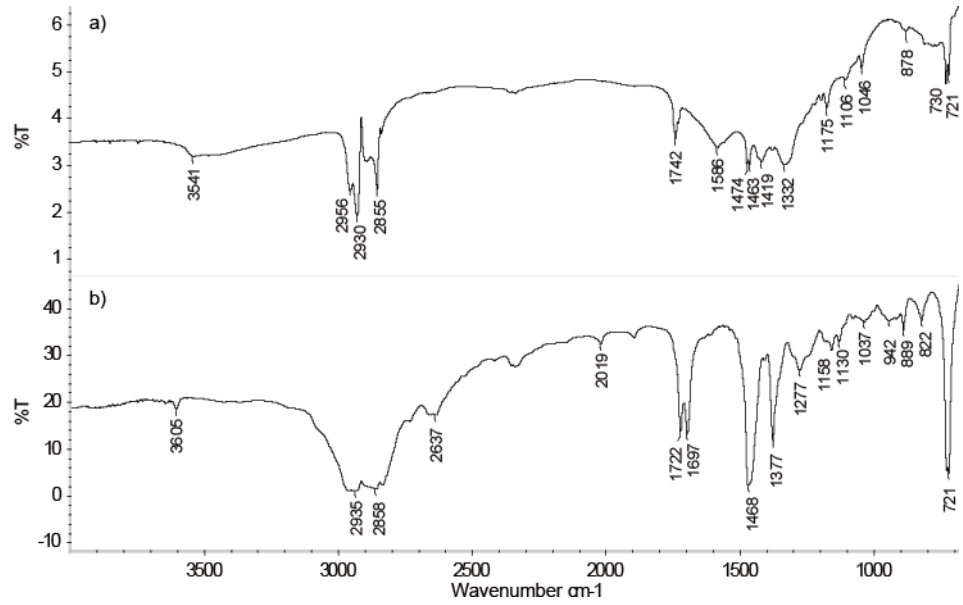

Figure 2.7 Total reflection spectra of bronze mock-up sample made by Opificio delle Pietre dure in Florence a) and beeswax covered copper sheet mock-up b)

Table 2.3 Principal vibrational assignments of beeswax covered bronze mock-ups

Bronze arm prepared by Opificio delle Pietre dure	Assignment	Copper sheet mock-up	Assignment
3541 cm^{-1}	v O-H	3605 cm^{-1}	v O-H
2930 cm^{-1}	v_a C-H_2	2935 cm^{-1}	v_a C-H_2
2855 cm^{-1}	v_s C-H_2	2858 cm^{-1}	v_s C-H_2
1742 cm^{-1}	v C=O	1722 cm^{-1}	v C=O
1586 cm^{-1}	v_a COO^-	1697 cm^{-1}	v COOH
1474 cm^{-1}	δ C-H_2	1468 cm^{-1}	δ C-H_2
1463 cm^{-1}	δ C-H_2	1377 cm^{-1}	δ C-H_3
1419 cm^{-1}	v_a O-NO_2	1158 cm^{-1}	v C-O
1332 cm^{-1}	v_s O-NO_2	889 cm^{-1}	wag =C-H
1175 cm^{-1}	wag CH_2	822 cm^{-1}	wag =C-H
1106 cm^{-1}	v_s C-C	721 cm^{-1}	γ C-H_2
1046 cm^{-1}	v N-O		
730 cm^{-1}	γ C-H_2		
721 cm^{-1}	γ C-H_2		

2.4.2 Evaluation the cleaning efficiency on mock-up

The sample allowed us to assess the applicability of the gel on substrates presenting morphologies and compositions comparable to a real case of study. The evaluation of the cleaning efficiency of the gel was carried out on a standard bronze sample, which was melted and covered with a beeswax-based by restorers of Opificio delle Pietre Dure in Florence (figure 2.8a). PHB-BD/DMC gel was applied sandwiched in between two piece of rice paper for 5 min in contact with the surface. A light pressure provided a good adhesion of the gel with the treated area. Rice paper is used to avoid the risk of PHB residues left on the treated surface and further to control the solvent release, without compromising the adhesion of the gel even on curved or vertical surfaces. Then the gel was removed, and the surface further cleaned with neat DMC and dry cotton swabs. For comparison with the gel cleaning, the neat solvent of biodiesel has been used for cleaning with cotton swabs. In more detail, the cotton

was soaked in biodiesel and applied to the surface to be treated with a slight mechanical action for a minute. Then, a cotton swab soaked with dimethyl carbonate has been used to remove the residues of biodiesel for a few seconds.

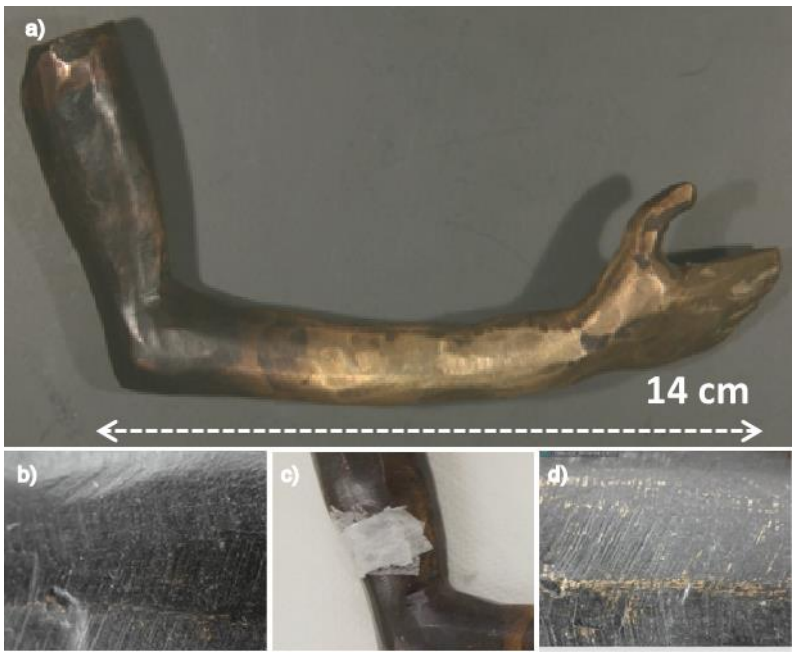

Figure 2.8 a) Bronze mock-up sample made by Opificio delle Pietre dure in Florence; Dino-lite microscope images b) before; c) the application of PHB-DMC/BD (3:1) gel and d) after cleaning by PHB-DMC/BD (3:1) gel for 5 min

DMC/BD 3:1 gel was selected for evaluation the performance of the cleaning system on the bases of rheological measurements result as the most suitable cleaning system for restoration purposes. FTIR with total reflection mode was applied to evaluate the presence of wax residues after the cleaning. All the areas were also documented with microphotographs to determinate the changes in morphology (figure 2.8b and 2.8c) with dino-Lite Premier2 digital microscope. Results were obtained by μFTIR analysis and showed an efficient removal of the wax coating in all areas in which the gel was applied. Thus, the diagnostic bands of wax at 1474 and 1465 cm^{-1} referred to CH_2 scissoring, the doublet at 731 and 721 cm^{-1} referred to CH_2 rocking, as well as the C=O stretching band at 1742 cm^{-1} were no longer visible after PHB-DMC/ BD gel application (figure 2.9).

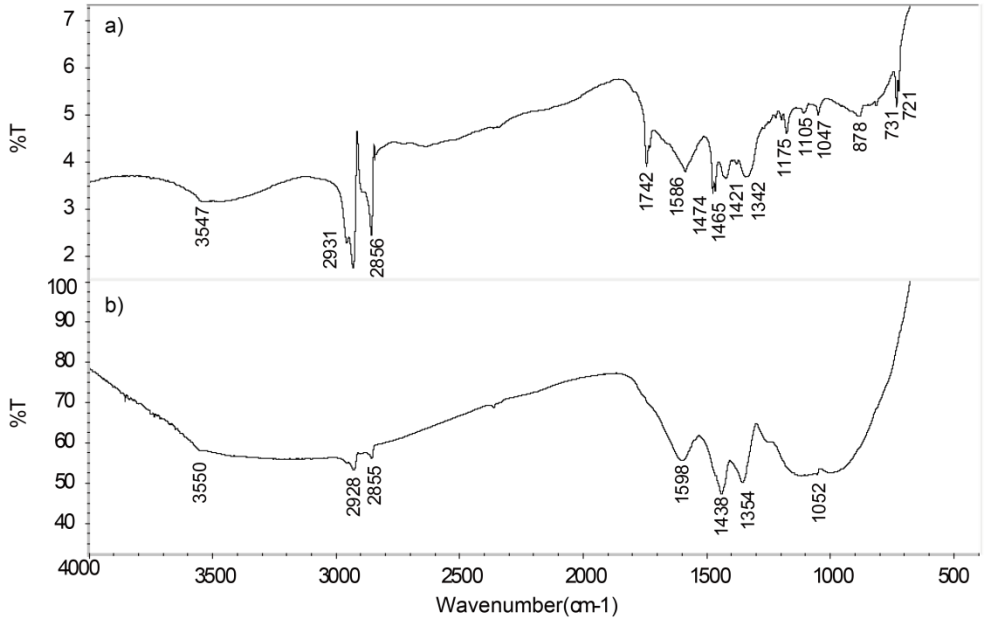

Figure 2.9 Total reflection spectra of bronze mock-up sample made by Opificio delle Pietre dure in Florence collected from a treated area with PHB-DMC/BD (3:1) gel, a) before cleaning; b) after cleaning

On the other hand, bands that characterized to the original metal patina were better identifiable. The broad band around 1590 cm^{-1}, ascribable to copper carboxylate salts and possibly formed due to the interaction between fatty acids of wax with copper salts, become more intense. In addition, the O-H stretching at 3550 cm^{-1}, the N-O stretching at 1052 cm^{-1} and O-NO_2 symmetric stretching at 1342 and 1421 cm^{-1} may be referred to the copper hydroxyl nitrate ($Cu_2(OH)_3NO_3$), formed during the procedure of manufacture, based on the use of a silver nitrate solution. The weak bands ascribed to the C-H stretching are still present although with a significantly lower intensity. These bands could be related to the presence of organic materials used as a coating penetrated into the porosity of the substrate as well as to the presence of copper carboxylates. After the cleaning procedure, the surface appeared to be less uniform and details on the manufacturing have become visible. In addition, no bands related to the presence of BD residues were detected.

Comparative tests, performed with neat BD solvent applied with a cotton swab, seem to confirm the ability of BD in the removal of wax coating (Figure 2.10). However, while the CH_2 rocking bands at 721 and 729 cm^{-1} disappeared, wax and BD residues cannot be excluded due to the presence of bands at 1746 cm^{-1} (C=O stretching bands), at 1195 and 1175

cm^{-1} (O-CH_3 stretching and C-O-C symetric stretching) (figure 2.10b). This result can be explained by the less controlled action of BD wet cleaning, which was not confined to the gel matrix, and by a less effective cleaning action of the neat solvent.

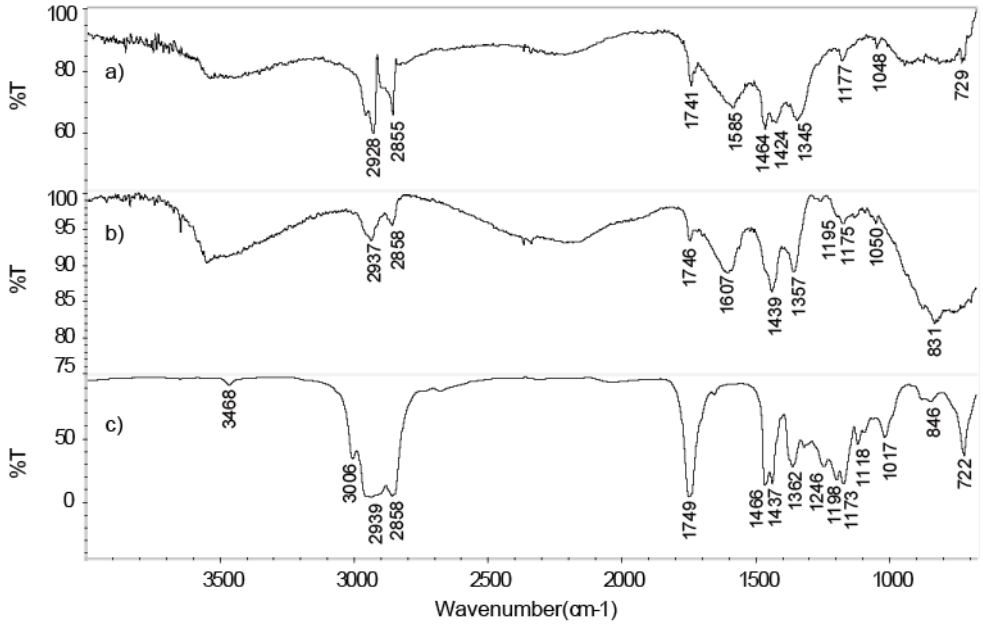

Figure 2.10 Total reflection spectra of bronze mock-up sample made by Opificio delle Pietre dure in Florence collected from a treated area with neat BD, a) before cleaning; b) after cleaning; c) BD reference spectrum

2.4.3 Evaluation the biodiesel residues

The evaluation of solvent retention by the treated surface is a crucial point in the development of new cleaning systems. Indeed, the persistence of solvent on the treated surfaces may lead to harmful interaction, alterating the substrate and inducing further corrosion phenomenas. To better investigate the amount of residual biodiesel after cleaning, quantitative GC-MS analysis of biodiesel methyl esters (methyl esters of palmitic, linoleic, oleic and stearic acid) were carried out on *ad-hoc* samples obtained by covering an oxidated copper sheet with a layer of beeswax and treated with PHB-DMC/BD gel or neat BD, the same cleaning procedure was performed as the bronze arm. Cutted 1 cm^2 of copper sheets which treated with gel and neat biodiesel and then extracted with cyclohexane of 10 mL under sonication for 20 min. Gas chromatography mass spectrometry was applied for quantification the presence of solvent on treated surface. As shown in figure 2.11a, after cleaning by neat BD solvent with

cotton swab, the GC-MS analysis indicated that the major contains of biodiesel including C_{17}, C_{19} and 9,12-octadecadienoic acid methyl ester were clearly visible and detectable with the retention time of 16.8, 18.5 and 18.7 min. The analysis performed on three sample replicas treated with the same procedure allowed to quantified the amount of BD in the substrate after the cleaning procedure, after cacultaion there are 0.15 ± 0.03 mg/cm^2 amount of BD residues still present on the surface after cacultaion. However, no BD residues were detected after the application of DMC/BD gel for 5 or 15 minutes, in the 15 min cleaning, no wax retention time bands were observed any more, revealved that the wax coating was completely removed by the gel. On the other hand, the length of gel application time could be more efficient to remove the thick layer of wax coating mock-up without leaving BD resudes, confirming the gel capacity in solvent retention, in accordance with FTIR investigations.

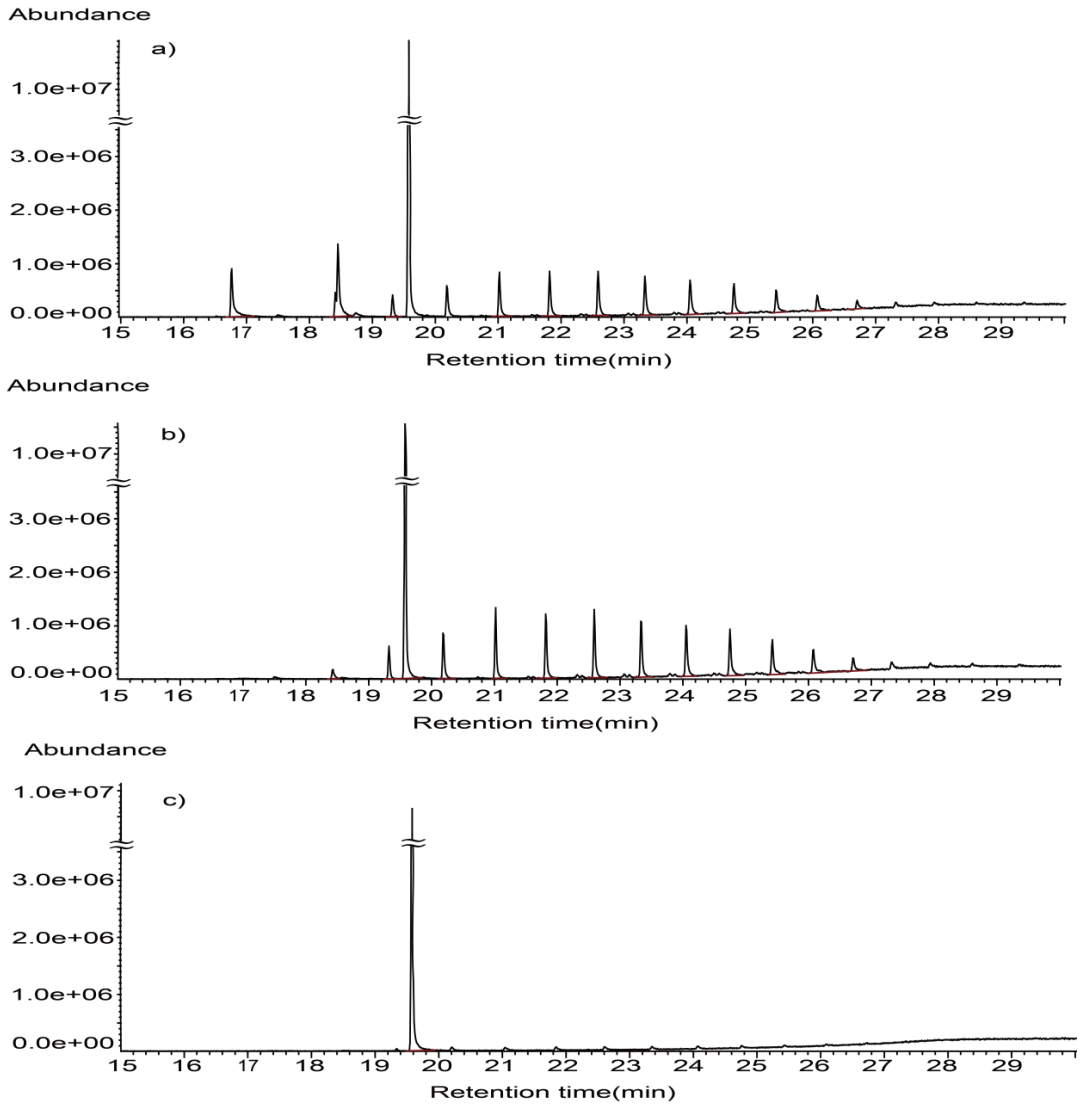

Figure 2.11 Chromatograms of a) Cleaned sample with neat BD; b) Cleaned sample with PHB-DMC/BD (3:1) gel for 5 min; c) Cleaned sample with PHB-DMC/BD (3:1) gel for 15 min

2.4.4 The cleaning on real case sample

After the preliminary evaluation of the gel performances in terms of cleaning efficancy and solvent retention, the PHB-DMC/BD gel was finally applied on the Pulpito della Passione attributed to Donatello for the real cleaning test. The metal surface presented a wax-based coating, probably applied during a past restoration campaign. The coating appeared extremely altered, possible due to the degradation phenomena that occurred over time (Figure 2.12).

Figure 2.12 Detail of the Pulpito della passione (Donatello, 1460, Florence), before (left) and after (right) the cleaning with PHB-DMC/BD (3:1) gel

PHB-DMC/BD gel was sandwiched in between two sheets of rice paper and applied for 15 minutes on a representative area of a bas-relief surface. On-site spectroscopic investigations were carried out to monitor the cleaning effects using a portable FTIR spectrometer in total reflection mode both acquired before and after the cleaning treatment (figure 2.13). The untreated surface showed peculiar bands ascribable to the fatty materials present on the surface. In particular, the C=O stretching band at 1736 cm^{-1}, CH_2 scissoring band at 1480 cm^{-1},

C-O stretching band at 1188 cm^{-1}, and CH_2 rocking band at 786 cm^{-1} were visible. In addition, the presence of calcium carbonate at 716 cm^{-1} and 879 cm^{-1} probably ascribable to atmospheric deposition, and calcium oxalates (band at 1331 cm^{-1}) were also detected. After the gel application, only traces of calcium oxalates were still visible, while the other bands contributed to the organic coating were completely disappeared, no BD residues bands were observed, this result demonstrated the high efficiency of the proposed organogel system in removing the wax-based coating and without leaving solvent residues.

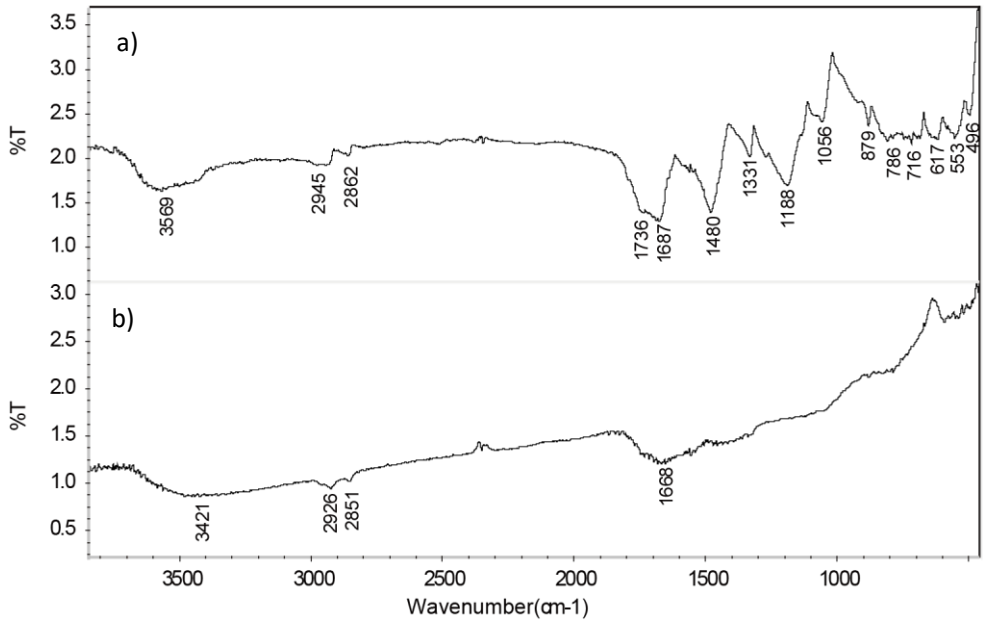

Figure 2.13 Total reflection spectra collected from the Pulpito di Donatello on the treated area of with PHB-DMC/BD (3:1) gel a) before cleaning; b) after cleaning

2.4.5 Discussion

In this section, the evaluation of the cleaning efficiency of the gel was carried out on a standard bronze sample, which was melted and covered with a beeswax-based coating by restorers of Opificio delle Pietre Dure. An ad hoc analytical protocol was implemented to evaluate both the cleaning efficiency and the release of residues on the treated surfaces. μFTIR analysis demonstrated the performance for removal of the beeswax coating by the gel. BD residues after cleaning by gel and neat BD with cotton swab were quantified through GC-MS with the extraction method, after calculation, 0.15 ± 0.03 mg/cm^2 amount of BD was presence on the neat BD treatment area, however no residue was detected after

PHB-DMC/BD gel cleaning, demonstrating the solvent retention ability of the gel. In order to evaluate the gel performances in cleaning of aged wax coating, the PHB-DMC/BD gel was finally applied on the Pulpito della Passione attributed to Donatello. Portable FTIR analysis showed the high efficiency of the proposed system in removing the wax-based coating, without leaving solvent residues.

Chapter 3 PHB gels combined with electrospun tissues for the removal of dammar varnish from paintings

3.1 Introduction

In the present research, electrospun fabrication mats were first time applied in conservation field to couple with green organogel of poly-3-hydroxybutyrate with γ-valerolactone (PHB-GVL gel) for removal of dammar coating from painting. Electrospinning is use of electric field to the droplet of fluid, leads to the droplet deformation and finally to the ejection of a charged jet from the tip of the cone accelerating towards the counter electrode leading to the formation of continuous fibers [134]. The fibers formed with a diameter of 50-500 nm, and the fibers morphology related to the fabrication parameters, including solution concentration, applied electric field strength, deposition distance and deposition time [135]. Electrospinning as a novel nanofiber-producing technology for producing fibre member with high surface area and flexible properties also including large surface area, small aperture, biocompatibility and perfect mechanical properties. Thanks to their properties they have been already used in pharmaceutical and engineering researches [4]. In the culture heritage field, electrospun membrane has been used for conservation of paper relics by directly covering a thin layer of PVDF fibres on paper surface, it can help to isolate the environment affect such as dust, water and mould, moreover, the porous able to provide the gases exchange between artwork and environment [136]. In this research, in order to improve the mechanical properties of organogels, as well as their cleaning efficacy, we proposed new gel composites based on the combination of electrospun polymer as PVA and nylon with PHB-based gels.

3.2 Materials and methods

Reagents	Grade of purity.	Manufacturer
γ-valerolactone (GVL)	99%	Sigma-Aldrich
poly-hydroxybutyrate (PHB)	-	Sigma-Aldrich
polyvinyl alcohol (PVA)	87-89% hydrolyzed	Sigma-Aldrich

nylon	-	Sigma-Aldrich
γ-butyrolactone	≥99%	Sigma-Aldrich
Rabbit glue	-	C.T.S
Dammar	-	Kremer
Gypsum	-	Phase Italia
Red ochre	-	Kremer

Optical microscopy in visible and ultraviolet light (Olympus Optical Microscope BX51, Tokyo, Japan) was applied on cross section before and after cleaning procedure to evaluate the thickness of varnish.

Electrospinning tissues and gels morphology were observed with a Philips 515 scanning electron microscope (SEM) at an accelerating voltage of 15 kV. Prior to SEM analysis, the gels were dried in oven at 40 ℃, samples were sputter-coated with gold, this very thin gold layer made the surface electrically conducting, but it did not alter the fine features of the sample.

Thermogravimetric analysis (TGA) was used to determine the thermal stabilities of, electrospinning mats, dry gels and fresh gels. The thermograms were recorded from room temperature to 700 ℃ at a heating rate of 10 ℃/min under N_2 atmosphere on a TA Instruments TGA-Q500.

The Single Cantilever is used for clamping the combined gels and PHB-GVL gel in one side and the dynamic mechanical analysis (DMA) is set to Controlled Force Mode. The dimensions of the prepared gels (length, width and thickness) were measured by a digital caliper with an accuracy of 1 μm and used by the DMA system during the initialization phase to calculate the initial stiffness of the samples. The gels were positioned in the machine at room temperature. The alignment of the sample was appropriate when the width of the specimens was parallel to the clamps/support. A good positioning is essential to avoid unsymmetrical loadings. The test parameters are same between the gels.

Headspace Solid Phase Microextraction (HS-SPME) sampling method was applied for extraction of GVL from painting mock-up (sampling a small painting fragment) for quantification the amount of cleaning agent residue after treatment.

It consists in an equilibrium sampling method among the concentration of the analyte in the sample, in the headspace above the sample and in the polymer coating on the fiber. According to the partitioning equation of analytes between the sample matrix and the extraction medium (equation①), the amount of analyte absorbed by the coating at equilibrium is linearly related to its concentrations in the sample

$$\mathbf{n} = \frac{K_{fs} V_f C_0 V_s}{K_{fs} V_f + V_s} \qquad ①$$

Where n is the mass of an analyte absorbed by the coating; V_f and V_s are the volumes of the stationary phase (coating) and the sample, respectively; K_{fs} is the partition coefficient of the analyte between the coating and the sample matrix; and Co is the initial concentration of the analyte in the sample.

In this research the sampling method HS-SPME was employed for the evaluation of solvent retention into the substrate after cleaning treatments. Analyses were performed by directly exposing a Carboxen-Polydimethylsiloxane (CAR/PDMS) fiber into the headspace of sealed vial containing the sample. The sample consisted in a fragment around 1.0 mg which collected from the surface of the painting mockup after 2 h and 24 h from cleaning treatments. Then the sample was placed into 20 mL HS vial, spiked with 1 μg of internal standard of γ-butyrolactone and sealed with a silicone/PTFE septa and aluminum cap (Thermo Fisher Scientific, Waltham, MA, U.S.A.). The SPME fiber was inserted into the headspace vial and the sample was thermally heated to 150 ℃ for 30 min. After reaching the extraction time, the fibre was inserted into the injector of a 5977 Agilent gas chromatograph connected to a 7820A Agilent quadrupole mass spectrometer (Agilent Technologies, Inc., Santa Clara, CA, U.S.A.). Analytes were thermally desorbed at 250 ℃ for 15 min and separated with a DB-FFAP polar column (30 m length, 0.25 mm i.d, 0.25 μm film thickness), using helium as carrier gas. The thermal program was: 100 ℃ to 250 ℃ at 10 ℃ min^{-1}. The abundances of the individual compounds were quantified from the m/z 86 for γ-butyrolactone, 100 for γ-valerolactone mass chromatograms. Calibration curves were performed for each solvent in the

concentration range 500-8000 ppm and were drawn by regression method. The areas corresponding to this range of concentration of standard solutions are in accordance with those obtained by sample measurements. The curves, obtained by applying the same procedure described above to standard solutions, showed a good linear response ($R^2 > 0.99$) in the considered concentration range.

Thermo Scientific Nicolet iN10 Infrared Microscope in total attenuated reflectance (ATR) mode was performed directly over the surface after treatment, without any sample preparation, in order to implement the non-invasive analysis for assess the cleaning efficiency and the residues after treatment. A Thermo Nicolet (Thermo Fisher Scientific, Waltham, MA, USA), iN™10MX imaging microscope, fitted with a mercury-cadmium-telluride (MCT) detector cooled by liquid nitrogen, was used for spectroscopic analyses. Measurements were performed using a slide-on ATR objective, equipped with a conical germanium crystal, in the range 4000-675 cm^{-1}, at a spectral resolution of 4 cm^{-1} with 128 scans and an optical aperture of 150×150 μm. Spectroscopic analysis was performed on 3 different areas treated with the same cleaning procedure and 4 spectra were recorded before and after treatment.

3.3 Electrospun combined organogel preparation and characterization

3.3.1 Fabrication of PVA and nylon electrospun mats

The electrospinning apparatus (figure 3.1), made in-house, was composed by a high voltage power supply (Spellman SL 50 P 10/CE/230), a medical syringe containing the polymeric solution that connected to a stainless steel blunt ended needle (inner diameter: 0.84 mm), and a grounded aluminum rotating mandrel as collector (length=12 cm, diameter=5 cm). The polymeric solution was dispensed through a teflon tube to the needle that was vertically placed on the collecting plate. The collecting time was set at 2-3 h to obtain handling mat. PVA was dissolved in EtOH/H_2O (1/1 v/v) at a concentration of 10% and stirred until all the polymer dissolved in the solvent at room temperature. PVA electrospinning tissue was fabricated using the following conditions: applied voltage 16 kV, needle to collector distance 18 cm, solution flow rate 1.5 mL/h, at room temperature and relative humidity RH 20-30%, the collecting time was 2 h. Nylon was dissolved in HFIP at a concentration of 20% and

stirred until all the polymer dissolved at room temperature. Nylon electrospinning tissue was fabricated using the following conditions: applied voltage 20 kV, needle to collector distance 15 cm, solution flow rate 0.5 mL/h, at room temperature and relative humidity RH 20-30%, the collecting time was 3 h. All the electrospinning tissues obtained were kept in room temperature overnight in order to remove residual solvents.

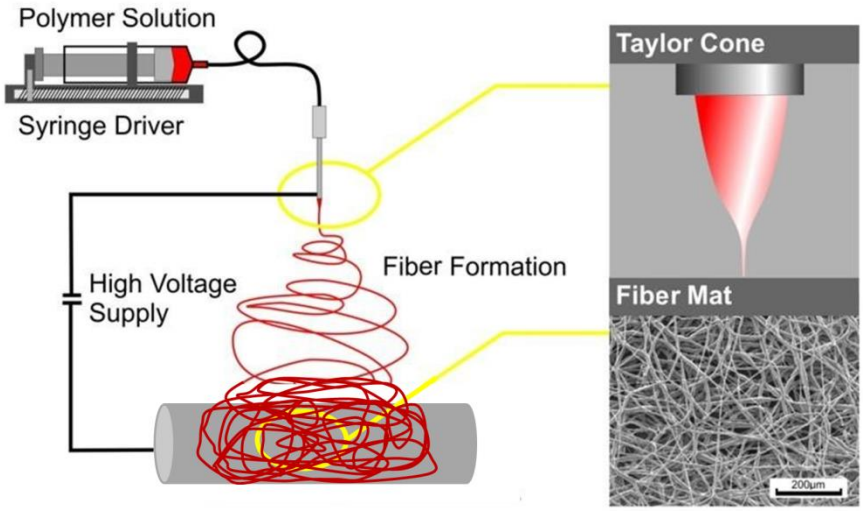

Figure 3.1 Schematic illustration of the basic setup for electrospun mat fabrication. The key components of the electrospun system including the grounded target (mandrel), high voltage source, injection syringe, and nozzle. Fiber deposition can be regulated by controlling the motion of the target mandrel and source solution with respect to one another. A rotating mandrel was used in our system as a ground target. A syringe mounted in a syringe pump was used as a reservoir for the electrospun source solution. The polarity of the system depicted in this image is arbitrary and, depending on the material to be processed, can be reversed [137].

3.3.2 Preparation of electrospun combined organogel

The green gel was synthesized by solubilizing 300 mg poly-hydroxybutyrate (PHB) into 3 mL γ-valerolactone (GVL), in a closed vial, by stirring at 110 ℃ for 5 min in an oil bath, until all the PHB powder dissolved in the solution and became transparent (precursor gel solution), then cooled down to room temperature in a Petri dish, the thickness of gel is around 0.3 cm.

PVA/PHB-GVL gel was synthesized by dropping 200 μL precursor PHB-GVL gel solution on a 1×1 cm square PVA electrospun mat, then covered another same size mat on the top, make a

slightly pressure, cooled down to room temperature.

Nylon/PHB-GVL gel was synthesized by dropping 200 μL precursor PHB-GVL gel solution on a 1×1 cm square nylon electrospun mat, then placed another same size mat on the top, make a slightly pressure, cooled down to room temperature.

3.3.3 Gel characterization

3.3.3.1 Thermogravimetric analysis

The TGA and DTG graphs of PHB-GVL fresh gel, PHB-GVL dry gel and pristine PHB are shown in Figure 3.2. There are two degradation steps that occurred in the TGA curves for PHB-GVL gels. In PHB-GVL fresh gel, the first degradation was referred to GVL solvent, and its weight loss was from 25 ℃ to 140 ℃. The PHB contributed to the second degradation step, and the temperature for its weight loss was from 210 ℃ to 261 ℃. The maximum decomposition temperature of GVL and PHB in PHB-GVL fresh gel was located at 129 ℃ and 244 ℃ respectively. By contrast, the maximum decomposition temperature of dry PHB-GVL gel was 246 ℃, which mainly referred to PHB decomposition, the maximum decomposition temperature of PHB in gel was lower than the pristine PHB (264 ℃), demonstrating the thermal stability was reduced maybe due to the chain scission during the gel formation process.

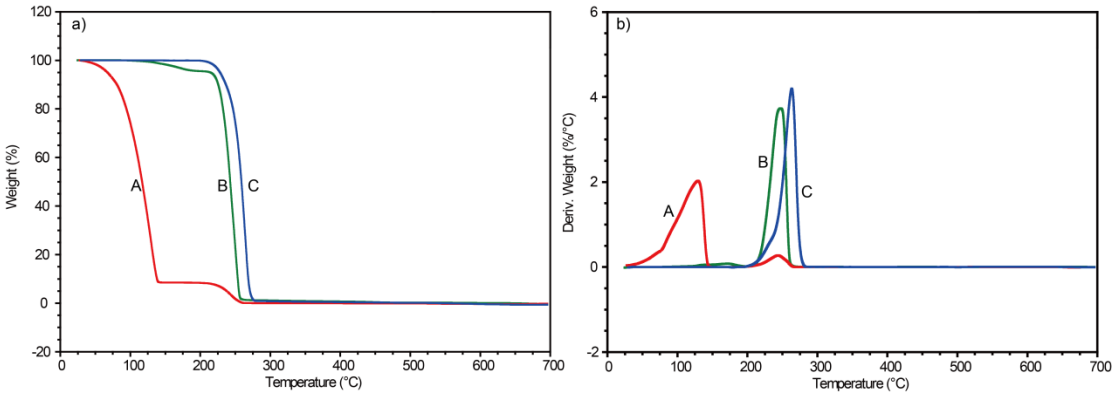

Figure 3.2 a) TGA and b) DTG of (A) PHB-GVL fresh gel, (B) PHB-GVL dry gel and (C) pristine PHB

The TGA and DTG of PVA/PHB-GVL fresh gel, PVA/PHB-GVL dry gel, pristine PHB and

PVA tissue are shown in Figure 3.3. There are nearly four degradation steps that occurred in the TGA curves for PVA/PHB-GVL fresh gel. In the fresh gel, the first degradation was referred to GVL solvent, and its weight loss was from 25 ℃ to 155 ℃, in the dry gel, the first degradation also contributed to GVL, because of the presence of a few amount of GVL in the gel. The PHB polymer contributed to the second degradation step, and the temperature for its weight loss was from 202 ℃ to 241 ℃. The last two degradation steps were from 210 ℃ to 480 ℃ that attributed to the decomposition of the PVA tissue. In this region, from 210 ℃ to 370 ℃ the structural degradation of the PVA tissue occurs, while the degradation above 370 ℃ could be ascribed to the decomposition of the cleavage backbone of the carbonaceous matter. DTG curve showed the maximum decomposition temperature of PHB in the PVA combined gel was lower than pristine PHB which could because of the polymer chain scission occurred in the gel formation process [138]. Moreover, there is an overlap weight loss temperature region with PHB and PVA, which in this region both including the weight loss of PHB and PVA, this might also affect the maximum decomposition temperature of PHB in the combined gel.

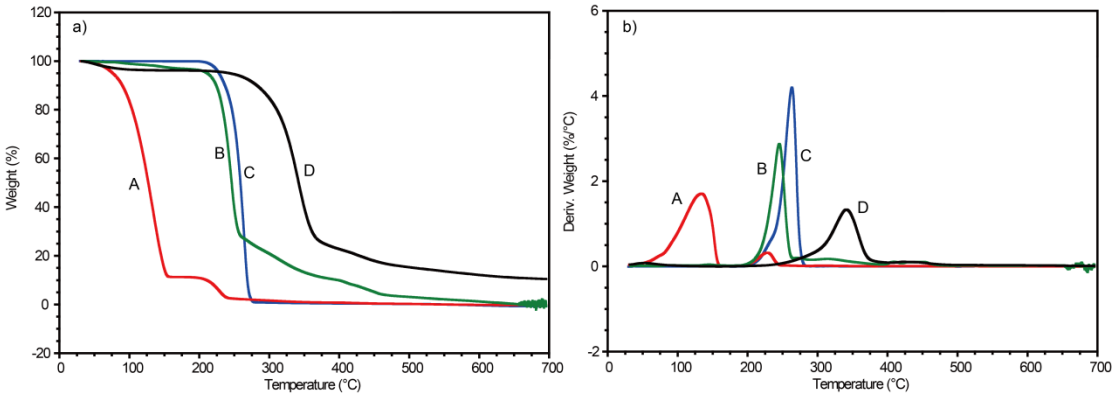

Figure 3.3 a) TGA and b) DTG of (A) PVA/PHB-GVL fresh gel, (B) PVA/PHB-GVL dry gel, (C) pristine PHB, and (D) PVA tissue

The TGA and DTG of nylon/PHB-GVL fresh gel, nylon/PHB-GVL dry gel, pristine PHB and nylon tissue are shown in Figure 3.4. There are three degradation steps that occurred in the TGA curves for nylon combined gel. The first degradation was referred to GVL solvent in both combined gels, and its weight loss was from 25 ℃ to 142 ℃. The second degradation step was observed at 191 ℃ to 270 ℃ which contributed to PHB polymer. The third degradation step was from 330 ℃ to 500 ℃ referred to the weight loss of nylon. DTG curve

showed the maximum decomposition temperature of nylon in combined gel has a slight decrease than the tissue alone, might be a result of the thermostability of nylon decreases during gel formation.

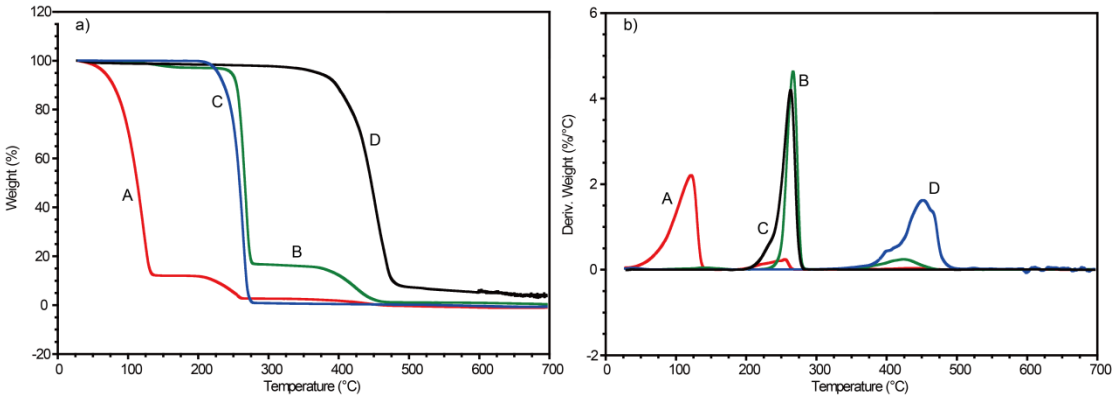

Figure 3.4 a) TGA and b) DTG of (A) nylon/PHB-GVL fresh gel, (B) nylon/PHB-GVL dry gel, (C) pristine PHB, and (D) nylon tissue

3.3.3.2 Scanning electron microscope

The SEM morphology of PVA and nylon electrospun nanofibres, as well as the after immersion in hot GVL solvent for 1 min at 100 ℃ is shown in Figure 3.5. It can observed that all the two kind of samples exhibit long and randomly oriented ultrafine fibres, and the three-dimensional randomly arrayed fibrous mesh maintained the highly porous fibrous structure, with diameters ranging from hundreds of nanometers to approximately 1 μm. During the electrospun combined gel synthesis procedure, the hot precursor PHB-GVL gel solution can reach 100 ℃, when in contact with the PVA and nylon mats. In order to understand if the fibre structure would change under extreme conditions, we immersed the PVA and nylon mats in a hot GVL solvent at 100 ℃ for 1 min. The SEM result showed that after the hot GVL solvent treatment, the morphology and diameter of the mats didn't have any change.

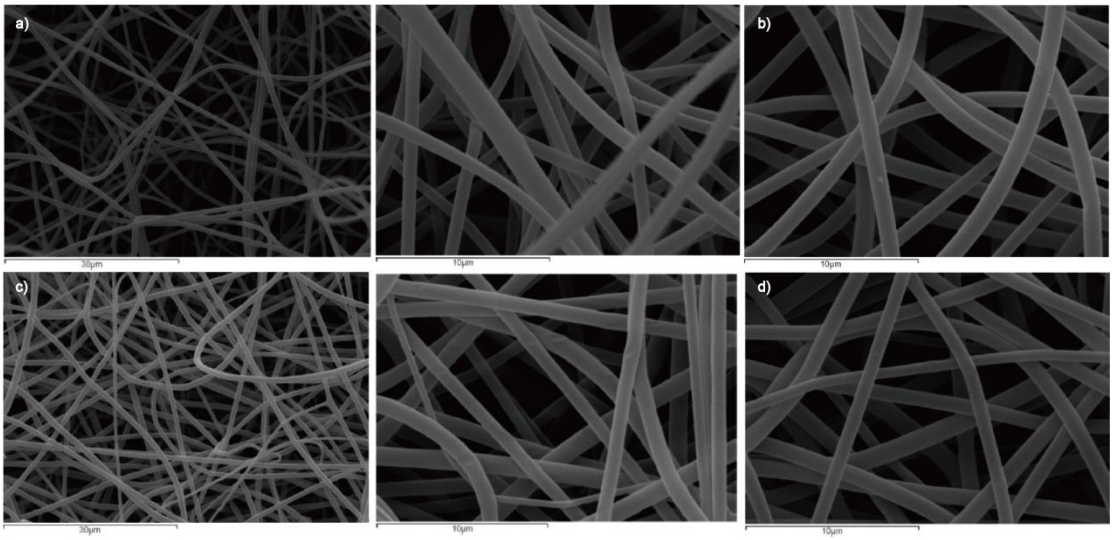

Figure 3.5 SEM micrographs of the obtained electrospun mats, a) different magnifications of PVA mat; b) nylon mat after immersion in hot GVL solvent; c) different magnifications of nylon mat; d) PVA mat after immersion in hot GVL solvent

SEM images were obtained to characterize the morphology of air-dried gels which performed under oven at 40 ℃ conditions. In particular the air dried PHB-GVL gel and combined materials with PVA and Nylon were observed considering both the surface and the cross sections (figure 3.6). The PHB-GVL gel showed a relatively smooth surface (figure 3.6a) with many tiny random cracks without any pores, a fracture was observed which could be formed by the shrinkage during the drying process, fibre like microstructures were presence in between the fracture. Observing the surface of the PVA/PHB-GVL and nylon/PHB-GVL gel, the porous texture of the fibers are partly filled together tightly with the gel layer, showing a sandwich like structure (figure 3.6d and f). The rough surfaces with some deep and interconnected porous may seem to allow a bigger contact area between the gel and the varnish to be removed (figure 3.6c and e). Moreover, the different texture may favour the diffusion of the varnish components within the gel matrix during the cleaning process.

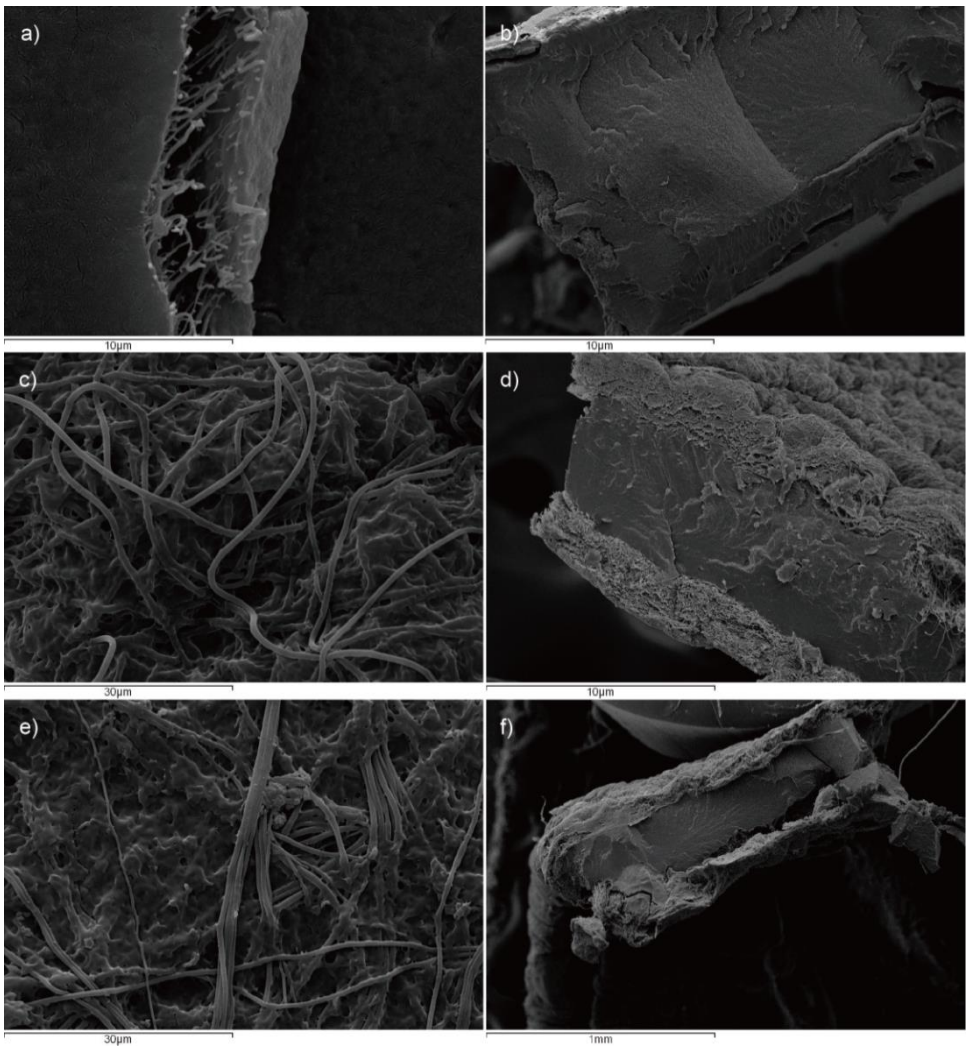

Figure 3.6 SEM micrographs of the gels, PHB-GVL gel a) surface and b) cross section; nylon/PHB-GVL gel c) surface and d) cross section; PVA/PHB-GVL gel e) surface and f) cross section

3.3.3.3 Gel evaporation behaviour

The solvent evaporation of the gels was studied through TGA to provide information about the solvent release and to understand the role played by the tissues plays in the combined materials. Combined gels and PHB-GVL gel were exposed at room temperature environment for 5 days, in the applied condition the weight loss can only be attributed to GVL evaporation process. An analytical balance was also used to check the weight changes during the exposure period. The results were resumed in table 3.1, the PVA/PHB-GVL gel, nylon/PHB-GVL gel and PHB-GVL gel weight loss is 40.6%, 57% and 14% respectively, which revealed that the

electrospun tissue could increase of the solvent release. These results were confirmed by the TGA analysis performed on the fresh gels and after 5 days exposure gels, as shown in figure 3.7, the GVL content of PVA/PHB-GVL gel decreased from 90% to 83.6%, 39.8% of GVL has been evaporated in the process. The composition of GVL in nylon/PHB-GVL gel decreased from 88% to 84.2%, 56.1% GVL has been evaporated. While in the PHB-GVL gel only few changes of GVL composition from 91.2% to 89.7%, 14.1% of GVL has been evaporated during the 5 days evaporation. From these results, the electrospun combined materials appears more prone to speed up the solvent release at room temperature condition, indicating that the tissue lead to a faster solvent release due to the high surface area and rich of porous structure which could be observed in the SEM images. Generally, the slower of solvent release the lower of risk to the artworks, but an appropriate increase of solvent release in a controllable way could be more effective in cleaning of the varnish in particular the thick coating layer. This may for instance help to reduce the mechanical swab operation time result.

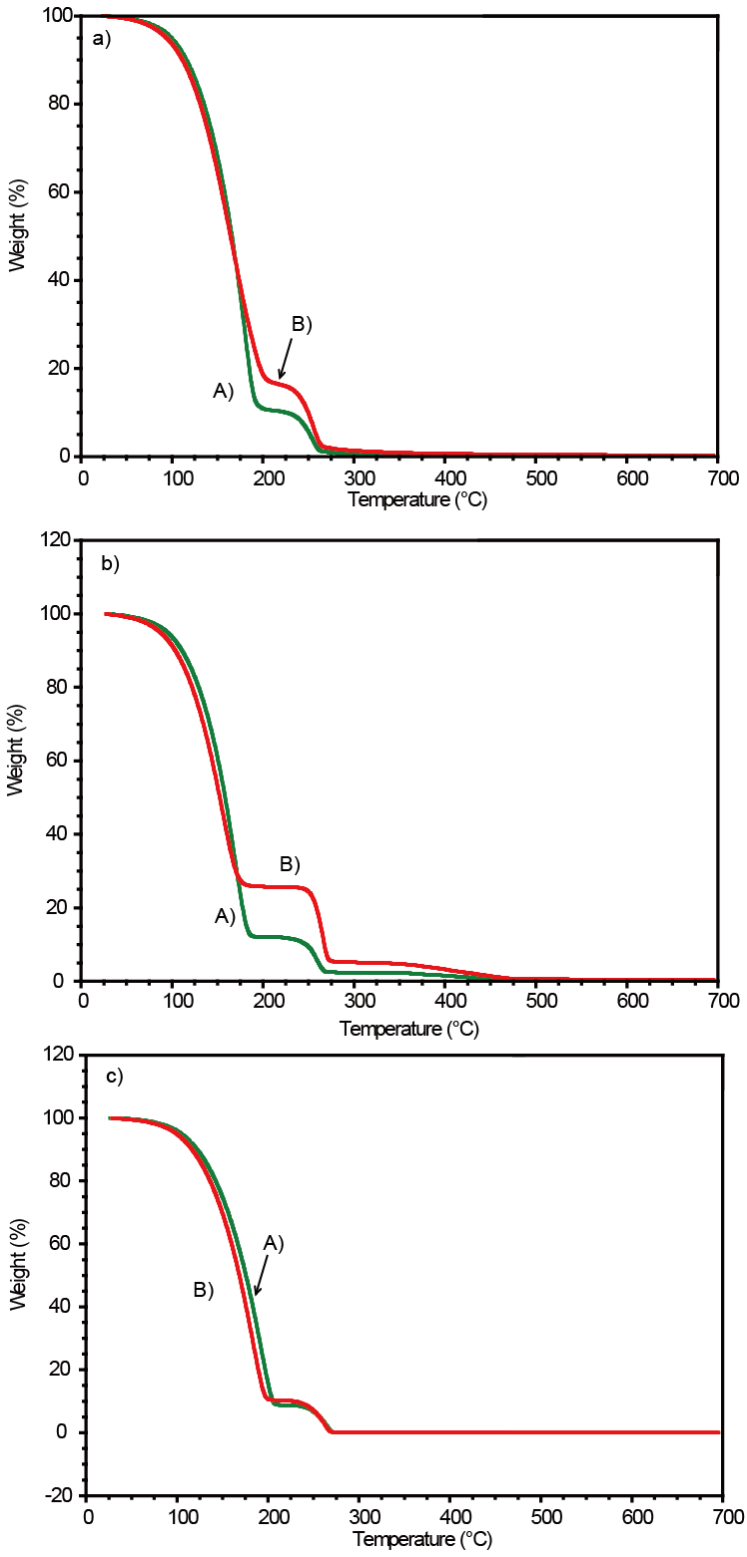

Figure 3.7 a) TGA of A) PVA/PHB-GVL fresh gel, B) PVA/PHB-GVL gel after 5 days exposure; b) TGA of A) nylon/PHB-GVL fresh gel, B) nylon/PHB-GVL gel after 5 days exposure; c) TGA of A) PHB-GVL fresh gel, B) PHB-GVL gel after 5 days exposure

Table 3.1 The weight loss change of different gels obtained by balance and TGA

Gel	Fresh gel GVL%	Gel after 5 days GVL%	Lost weight balance%	Lost weight calculation% [a]
PVA/PHB-GVL	10.5	16.4	40.6	39.8
Nylon/PHB-GVL	12.0	25.8	57.0	56.1
PHB-GVL	8.8	10.3	14.0	14.1

[a] $Evaporation\ GVL = m_{fresh} \times R_{fresh\ gvl} - m_{after} \times R_{after\ gvl}$

m_{fresh} is the fresh gel weight; $R_{fresh\ gvl}$ is the ratio of GVL from TGA; m_{after} is the gel weight after 5 days; $R_{after\ gvl}$ is the ratio of GVL after 5 days from TGA

3.3.3.4 Gel mechanical property

The mechanical properties of the PHB-GVL gel and combined gels were investigated via Dynamic mechanical analysis. Figure 3.8 and 3.9 show the single cantilever test of the out-of-plane bending behavior. Force/displacement trend can suggest the relevant bending behavior between different gels. As it can be seen, with increasing of bending force, the displacement significantly increased which related to the curing ability of the material, the PHB-GVL gel was damaged when implemented a very low force (figure 3.8a), revealing a limited mechanical property. On the other hand, combined materials show better resistance to bending force (figure 3.8b and c), especially nylon/PHB-GVL gel showed the best flexural rigidity of all (figure 3.9a), demonstrated the good mechanical property of combined gels.

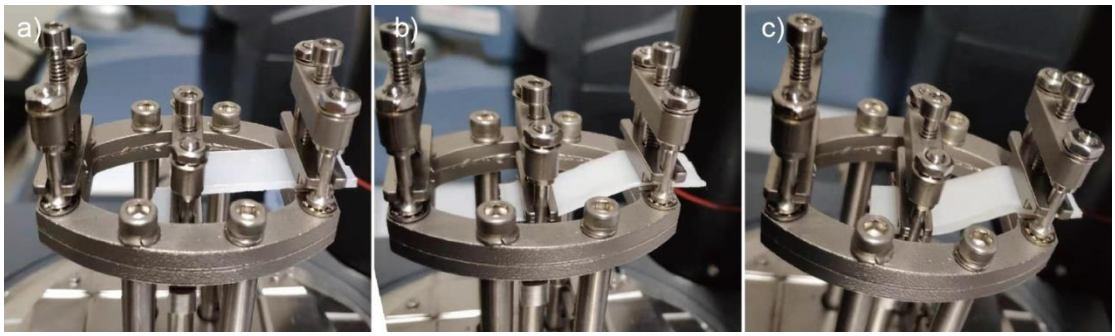

Figure 3.8 single cantilever tests of a) PHB-GVL gel, b) nylon/PHB-GVL gel, c) PVA/PHB-GVL

gel

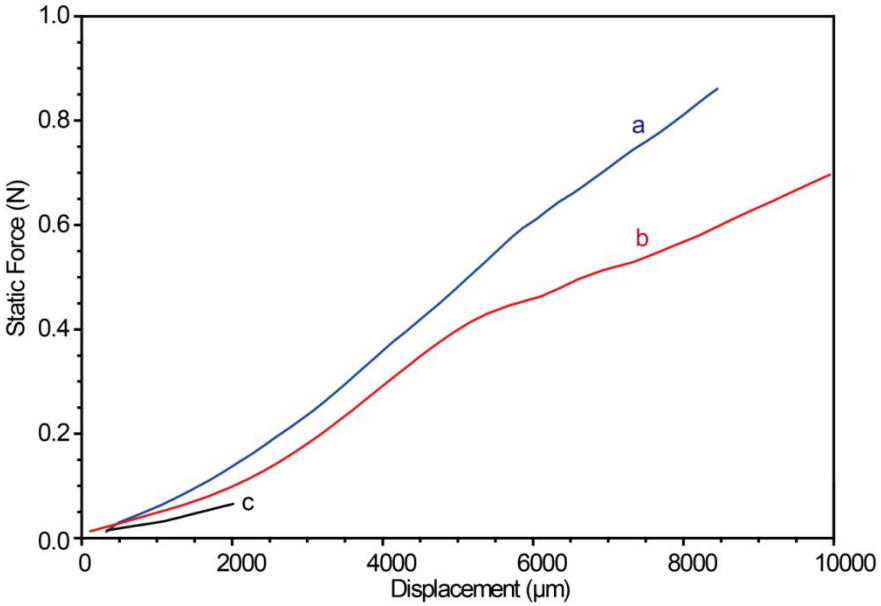

Figure 3.9 Force-displacement curves of a) nylon/PHB-GVL gel, b) PVA/PHB-GVL gel, c) PHB-GVL gel

3.3.4 Discussion

In this investigation, the aim was to improve the mechanical property of the organogels to achieve a better application, a simple method implemented by combination of organogel with electrospun mat was proposed. In detail, the precursor solution of organogel dropped on the tissue serves as soak solution to immerse electrospun tissue which placed on the bottom and top. The porous of electrospun tissue were partly filled by the precursor gel solution, in which the precursor gel solution acted as a ‘‘glue” to hold together the fibrous layers. The obtained combination gels showed an appearance of whitish, opaque and sandwich structure. Single cantilever tests of combined gels indicated a significant enhance of mechanical bending property over normal organogel. The SEM morphology showed the combined gels have irregular surfaces and various porous networks, which might be allow a larger contact area with varnish. TGA was applied for verifying the evaporation of the gels at room temperature condition which related to the solvent retention ability. The results showed the electrospun combined gels allowed to speed the solvent release, due to the high surface area and rich of porous structure which have been observed in the SEM images. The uncontrollable release in cleaning could induce serious risk to the artworks by swelling and leaching, however the

appropriate solvent release could control by application time and reach a more efficient cleaning result. The cleaning efficiency of different gels were evaluated on the standard samples and investigated in the next part.

3.4 The cleaning work on painting for removal of dammar varnish

3.4.1 Mock-ups preparation

The mock-up was prepared according to traditional painting techniques, and nature aged over 2.5 years before using. The preparation layer was made of gypsum and rabbit glue, dissolving 1.0 g of animal glue in 5.0 mL of hot distilled water and mix with 6.0 g grinded gypsum. The pigment layer was obtained by dissolving 2.0 g red burnt ochre in 2.0 mL 10% w/w of rabbit glue solution. The varnish layer was prepared by dissolving 1.0 g dammar in 2.5 mL turpentine, a layer of mix dammar solvent was applied on the painting surface and drying under the room temperature. Two different thickness dammar layer coated painting mock-ups A and B were prepared with above recipe. The ATR spectra of dammar layer mock-ups were showed in figure 3.10 and the vibrational assignments were listed in table 3.2. The thickness of dammar layer was measured by observing the cross-section through optical microscope. The dammar layer was applied by brush, the thickness of dammar layer can’t be homogenous everywhere, samples were taken from closing to the treatment area to get an average thickness of before cleaning. As shown in figure 3.11, the varnish on sample A was measured and the thicknesses are in the region of 17-25 μm, and the average thickness of sample B is 22 μm. The varnish on sample B is thicker, the thicknesses are in the region of 32-51 μm and the average thickness of sample B is 40 μm.

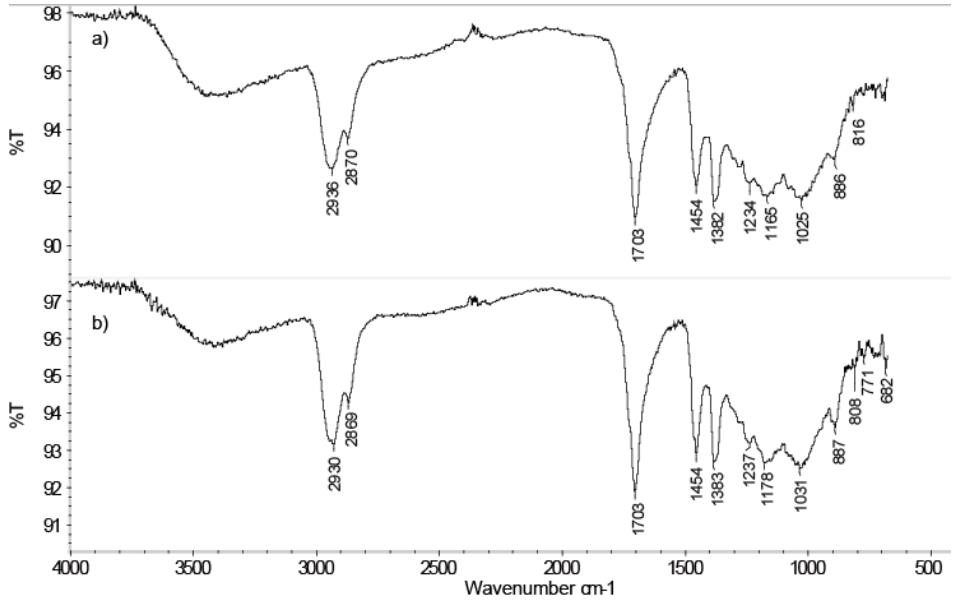

Figure 3.10 ATR spectra of a) thin layer dammar covered glue tempera mock-up; b) thick layer dammar covered glue tempera mock-up

Table 3.2 Principal vibrational assignments of all the glue tempera mock-ups

thin layer dammar covered glue tempera mock-up	Assignment	thick layer dammar covered glue tempera mock-up	Assignment
3414 cm^{-1}	v O-H	3411 cm^{-1}	v O-H
2936 cm^{-1}	v_a C-H_2	2930 cm^{-1}	v_a C-H_2
2870 cm^{-1}	v_s C-H_2	2869 cm^{-1}	v_s C-H_2
1703 cm^{-1}	v C=O	1703 cm^{-1}	v C=O
1454 cm^{-1}	δ C-H_2	1454 cm^{-1}	δ C-H_2
1382 cm^{-1}	δ C-H_2	1383 cm^{-1}	δ C-H_2
1234 cm^{-1}	δ C=C	1237 cm^{-1}	δ C=C
1165 cm^{-1}	v C-C ring	1178 cm^{-1}	v C-C ring
1025 cm^{-1}	v C-C ring	1031 cm^{-1}	v C-C ring
886 cm^{-1}	δ C=C	887 cm^{-1}	δ C=C
816 cm^{-1}	v C-C-OH	808 cm^{-1}	v C-C-OH
		771 cm^{-1}	v C-C ring

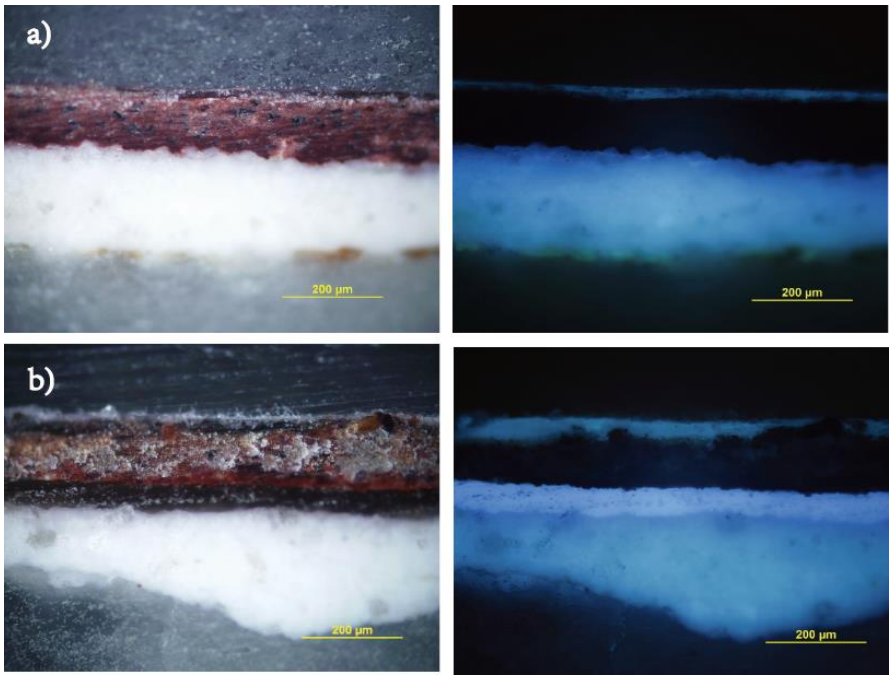

Figure 3.11 Cross-section microphotographs of glue paint reconstructions varnished with dammar, image under visible light (left) and image under UV illumination (right), a) mock-up A, b) mock-up B

3.4.2 Evaluation the cleaning efficiency on mock-up

Different thickness aged dammar layer mock-ups were investigated during the cleaning, the results allowed us to overview the performance of the combined gels and normal gel. The evaluation of the cleaning efficacy of the gel was carried out on two standard glue tempera painting samples, one coated with a thin layer of dammar around 20 µm (mock-up A), another one coated with a thicker layer of dammar around 40 µm (mock-up B). PHB-GVL gel, PVA/PHB-GVL gel and nylon/PHB-GVL gel were applied sandwiched in between two piece of rice paper or directly applied on the samples surface for 5 min, a light pressure provided a good adhesion of the gel with the treated area, then removed the gel and cleaned with three dry cotton swabs. The cleaning efficiency of PHB-GVL gel and electrospun combined gels were evaluated by FTIR-ATR directly on the surface after 24 h from treatment. Optical microscope was also used to check the cross section of dammar varnish before and after cleaning in visible and ultraviolet light mode.

3.4.2.1 Cleaning of thin dammar layer mock-up

Mock-up A application without rice paper

Results obtained by Optical microscope show a good performance for the removal of varnish after the application of PVA/PHB-GVL gel, nylon/PHB-GVL gel and PHB-GVL gel, all the fluorescence layers related to varnish layer completely disappeared (figure 3.12). The results were further investigated by ATR.

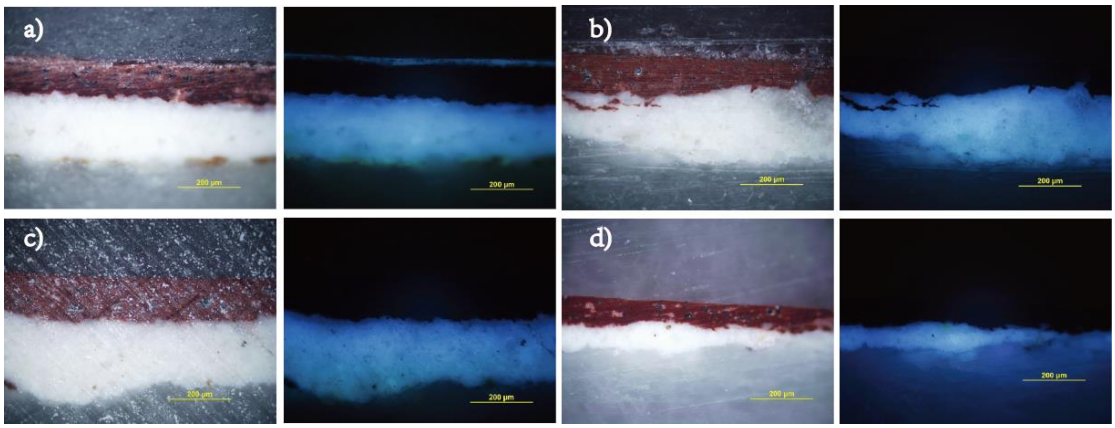

Figure 3.12 Cross-section microphotographs of glue paint A reconstructions varnished with dammar, image under visible light (left) and image under UV illumination (right), (a) varnished area before cleaning, (b) after cleaning by PHB-GVL gel, (c) after cleaning by PVA/PHB-GVL gel, (d) after cleaning by nylon/PHB-GVL gel

ATR was performed on the areas before and after cleaning, as shown in figure 3.13, the diagnostic bands of dammar at 2936 cm^{-1} and 2870 cm^{-1} (C-H stretching), the C=O stretching band at 1703 cm^{-1}, the C-H bending bands at 1454 cm^{-1} and 1382 cm^{-1}, as well as the C-C ring bands at 1165 cm^{-1} and 1025 cm^{-1} were clearly observed on the mock-up before cleaning. While after cleaning by the gels, the characteristic C=O stretching band of dammar at 1703 cm^{-1} was disappeared, the characteristic signals of the glue binder (mainly amide I and II at around 1650 cm^{-1}, 1540 cm^{-1}) were detected. However the characteristic band of GVL at 1767 cm^{-1} was observed after cleaning by all gels, meaning that after cleaning redundant amount of solvent were released during the cleaning.

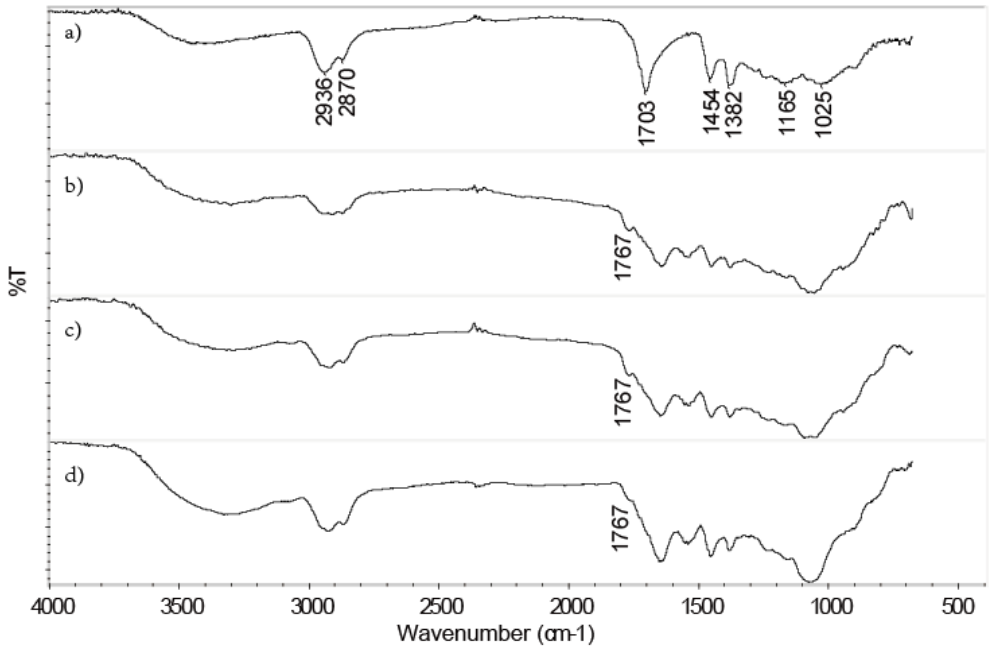

Figure 3.13 FTIR ATR spectra acquired on the surface of the dammar varnished mock-up A; (a) varnished area before cleaning, (b) after cleaning by PHB-GVL gel, (c) after cleaning by PVA/PHB-GVL gel, (d) after cleaning by nylon/PHB-GVL gel

Mock-up A application with rice paper

Considering directly applied the gels on the mock-up surface, all the dammar varnish were completely removed, but the GVL residues were still observed after 24 h from the treatment. In this case, rice paper was selected for the further cleaning tests, rice paper usually served as a barrier could partly avoid the risk of PHB residues left on the treated surface and further to control the solvent release.

As shown in figure 3.14, after cleaning by the electrospun combined gels and PHB-GVL gel, the characteristic C=O stretching band of dammar at 1703 cm^{-1} was disappeared, the characteristic signals of the glue binder (mainly amide I and II at around 1650 cm^{-1}, 1540 cm^{-1}) were detected, as observed in unvarnished areas. Moreover, no GVL and PHB residues were detected after cleaning. This result reflected the cleaning efficiency of the gels including electrospun combined gels and PHB-GVL gel. Results obtained by Optical microscope were also confirmed the good cleaning performance of combined gels and PHB-GVL gel (figure 3.15), all the fluorescence layers related to varnish layer disappeared. The results have been confirmed by ATR investigation above, demonstrating all the synthesis gels were efficiency

for the removal of aged thinner layer of dammar varnish. There was no significant difference from the cleaning results between nylon and PVA combined gel and PHB-GVL gel.

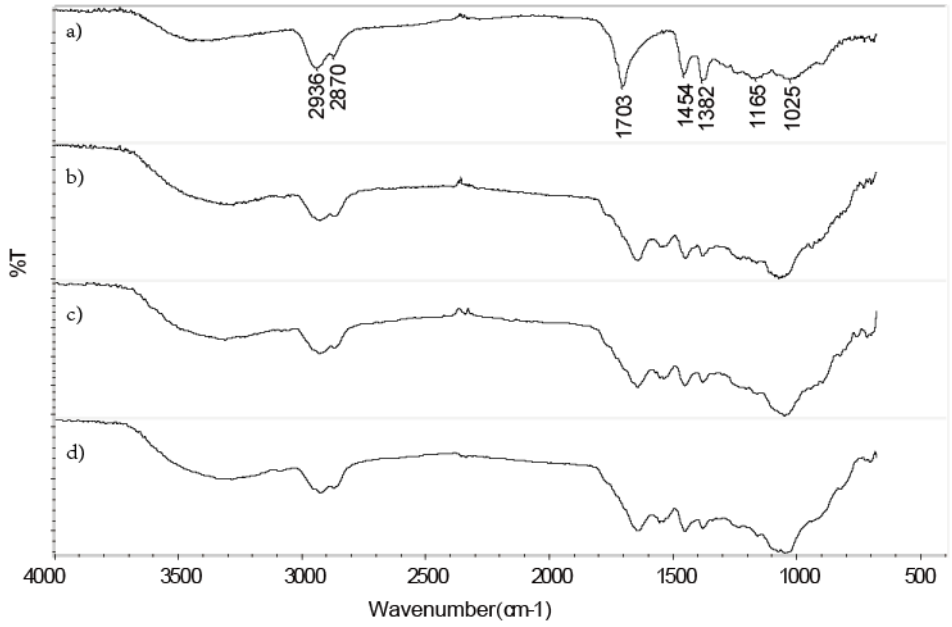

Figure 3.14 FTIR ATR spectra acquired on the surface of the dammar varnished mock-up A; (a) varnished area before cleaning, (b) after cleaning by PHB-GVL gel, (c) after cleaning by PVA/PHB-GVL gel, (d) after cleaning by nylon/PHB-GVL gel

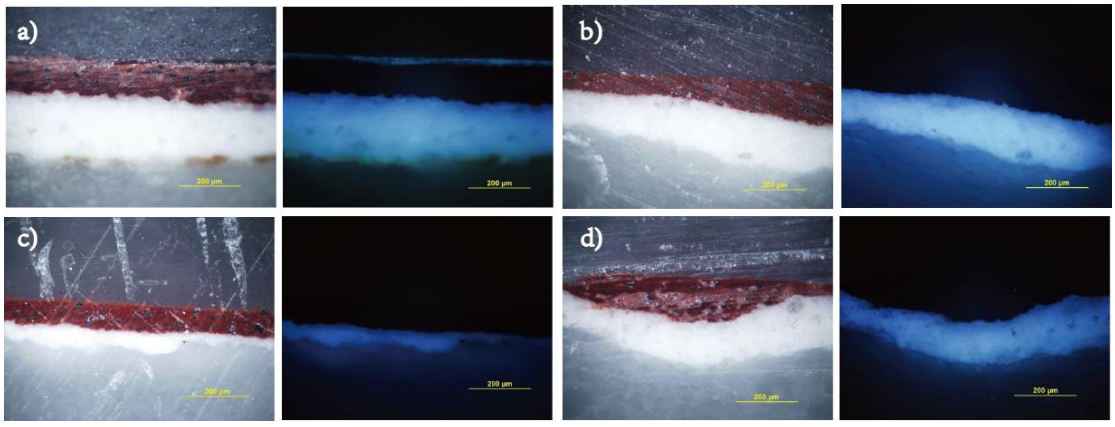

Figure 3.15 Cross-section microphotographs of glue paint A reconstructions varnished with dammar, image under visible light (left) and image under UV illumination (right), (a) varnished area before cleaning, (b) after cleaning by PHB-GVL gel, (c) after cleaning by PVA/PHB-GVL gel, (d) after cleaning by nylon/PHB-GVL gel

3.4.2.2 Cleaning of thick dammar layer mock-up

Mock-up B application without rice paper

In order to test the capacity of electrospun combined gels for removal of thicker dammar varnish layer sample. Mock-up B which decorated with around 40 μm dammar varnish was selected for the cleaning treatment. PVA/PHB-GVL gel, nylon/PHB-GVL gel and PHB-GVL gel were directly applied on the samples surface for 5 min, a light pressure provided a good adhesion of the gel with the treated area, then removed the gel and cleaned with dry cotton swabs. The cleaning results were preliminary investigated by Optical microscope, cross-section samples' microphotographs including before and after treatment with various gels are shown in figure 3.16, all the fluorescence layers of dammar varnish disappeared after cleaning by PVA and nylon combined gel, demonstrated the good performance of electrospun combined gels for the removal of thick dammar coating. However, after same cleaning procedure by PHB-GVL, a part of fluorescence dammar components still present on the painting surface.

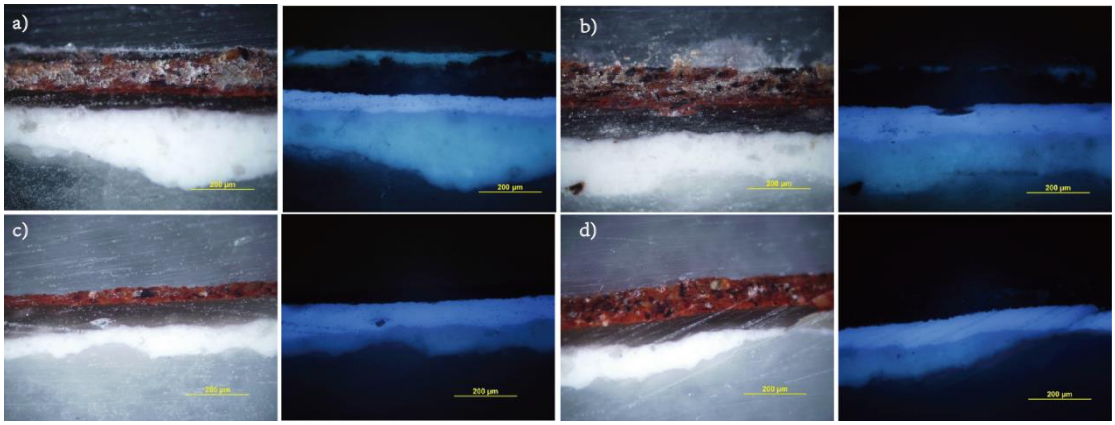

Figure 3.16 Cross-section microphotographs of glue paint B reconstructions varnished with dammar, image under visible light (left) and image under UV illumination (right), (a) varnished area before cleaning, (b) after cleaning by PHB-GVL gel, (c) after cleaning by PVA/PHB-GVL gel, (d) after cleaning by nylon/PHB-GVL gel

The results were further confirmed by ATR, ATR crystal in direct contact with the mock-up surface after 24 h from the treatments. As shown in figure 3.17, after cleaning by PHB-GVL gel, the characteristic band of dammar at 1703 cm^{-1} (C=O stretching) is obviously reduced but

it is still present, and the band at 1770 cm^{-1} attributed to GVL (C=O stretching) was also visible, this result confirmed with the above optical microscope result indicated powerless cleaning of thicker aged dammar by PHB-GVL gel. It is noticeable, after cleaning by electrospun fibres combined gels, the dammar C=O stretching band at 1703 cm^{-1} was completely disappeared. In the meantime, no residue of GVL and PHB was observed, the glue binder characteristic bands of amide I at 1650 cm^{-1} and amide II at 1540 cm^{-1} were detected as observed in the unvarnished paint layer, demonstrating the high efficiency of the electrospun combined gel system in removing the dammar coating, without leaving solvent residues.

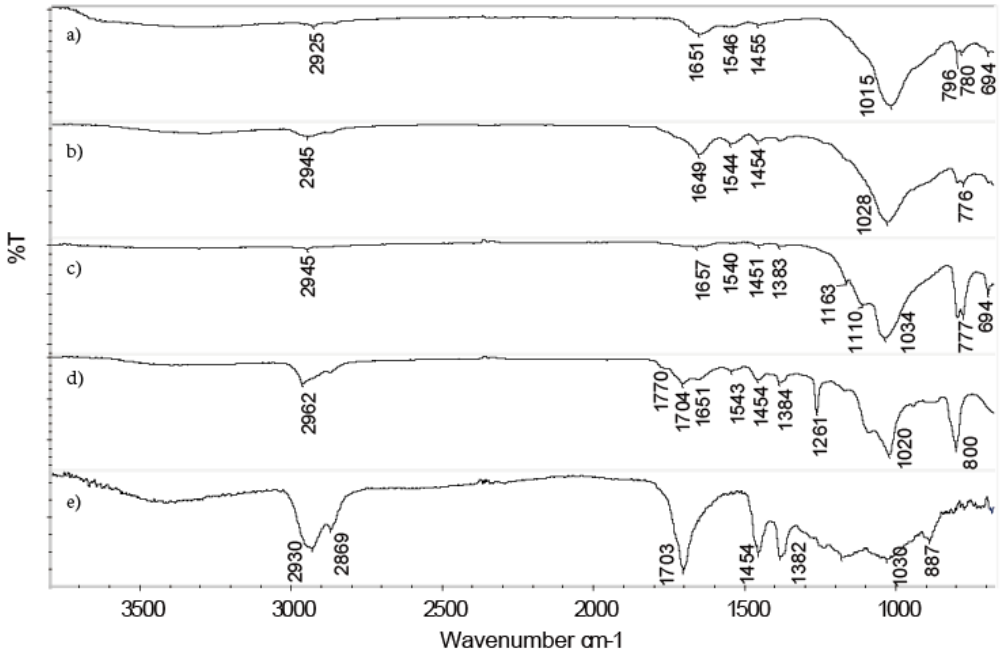

Figure 3.17 FTIR ATR spectra acquired on the surface of the dammar varnished mock-up B, (a) an unvarnished area, (b) after PVA/PHB-GVL gel, (c) after nylon/PHB-GVL gel, (d) after PHB-GVL gel, (e) dammar varnish area

In order to understand how the gel works during cleaning and why the electrospun tissue combined gel showed higher cleaning efficiency, SEM morphology was applied for further investigation, the gels both including PVA/PHB-GVL gel, nylon/PHB-GVL gel and PHB-GVL gel were collected before and after application and then air-dried under oven at 40 ℃ condition. As shown in figure 3.18**,** after cleaning, the small spherical morphology which related to the dammar was observed on the gels' surface. It can be observed that while on the PHB-GVL gel the round particles are just adherent to the surface, forming a roughness of the wrinkled morphology during the drying process. As to the PVA/PHB-GVL gel and

nylon/PHB-GVL gel, the widespread adherent thick the dammar particles varnish covered not only on the surface but also get into the porous space between the fibres, moreover, the dammar particles accumulated to a thick film on the gel surface, which looks less wrinkle and more cracks, this could be due to the increasing of film thickness the reducing of the flexibility of the film surface, cracks formed when the tensile stress exceeds ultimate film strength during the drying process. This result suggested the rough and porous combined gels readily to adsorb more dammar than normal gel, it could be an important reason that the combined gels showed more efficiency for removal of dammar varnish, highlighting the important role of tissue played in the cleaning procedure.

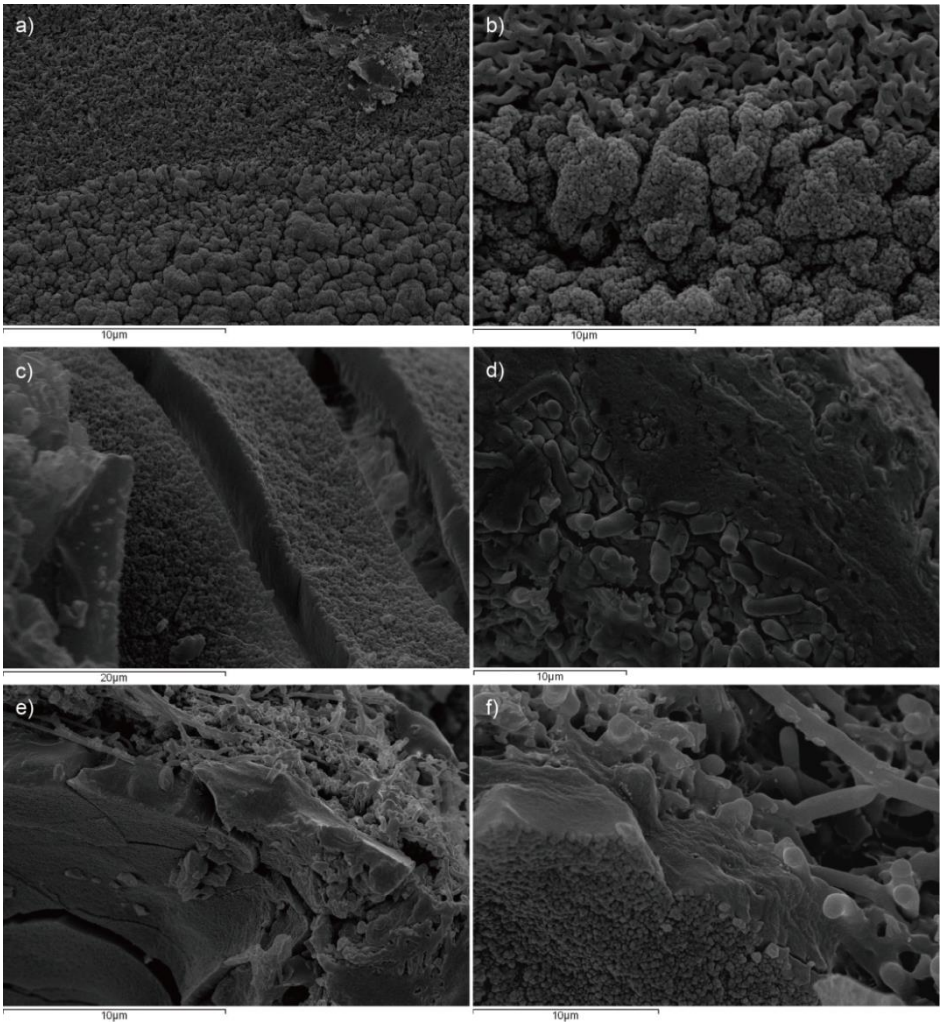

Figure 3.18 SEM micrographs of the dry gels after cleaning, a) PHB-GVL gel after application; b) large magnification of PHB-GVL gel after application; c) nylon/PHB-GVL gel after application; d) large magnification of nylon/PHB-GVL gel after application; e) PVA/PHB-GVL gel after application; f) large magnification of PVA/PHB-GVL gel after

application

Mock-up B application with rice paper

In this test, rice paper was applied with PHB-GVL gel and electrospun combined gel, in order to check the cleaning result when in presence of a barrier film between gel and painting surface. After cleaning (figure 3.19), dammar coating is clearly visible in the treatment area, all the three gels were unable to completely remove the thicker dammar in the presence of rice paper. For the further cleaning step, we length the application time of the gel, a second application for 5 minutes was also tested achieving a better removal of the varnish. The cleaning performance were achieved by analyses of fragments sampled before and after the cleaning procedures with Optical microscope both in visible and UV-Vis light (figure 3.20), we observed few fluorescence spots was still present after cleaning by PHB-GVL gel, however, all the fluorescence layers of dammar varnish disappeared after cleaning by PVA/PHB-GVL gel and nylon/PHB-GVL gel, demonstrating the good efficiency of electrospun combined gels for removal of thick dammar coating over PHB-GVL gel, even in presence of the rice paper. Further investigations of the cleaning performance were characterized by FTIR microscopy in ATR mode (figure 3.21). The ATR results revealed that after length of the gel application time, the cleaning results improved a lot, the characteristic C=O stretching band of dammar at 1703 cm^{-1} was disappeared, the characteristic signals of the glue binder of amide I and II at around 1650 cm^{-1} and 1540 cm^{-1} were detected. Moreover, no GVL and PHB residues observed after cleaning. Comparison with the results of Optical microscope, dammar fluorescence was observed after cleaning PHB-GVL gel, but we failed to obtain the FTIR spectra of the dammar residue, this could be explained by the random selected test points didn’t cover the dammar residue spots. On the other hand, there are only very few amount of dammar still present after cleaning by PHB-GVL gel. As a result, in the presence of rice paper, a thicker dammar coating can be removed by applying a total of 10 minutes with electrospun tissue combined gels, for PHB-GVL gel, it would take longer time.

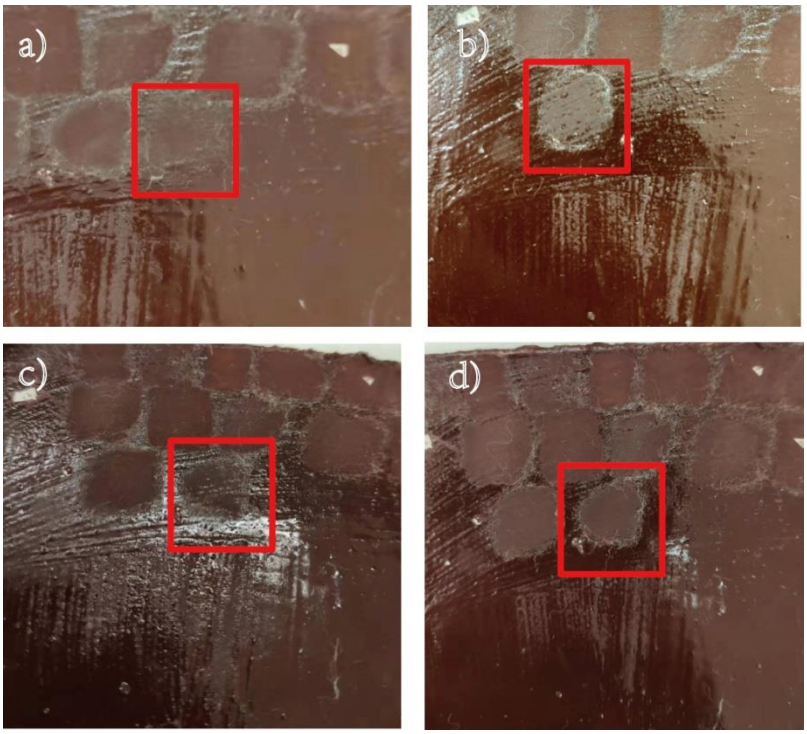

Figure 3.19 Photograph of mock-up B after cleaning by gels for 5 min with rice paper, red square represents the treatment area, a) after application of PHB-GVL gel; b) after application of nylon/PHB-GVL gel; c) after application of PVA/PHB-GVL gel; d) an area of dammar varnish completely be removed

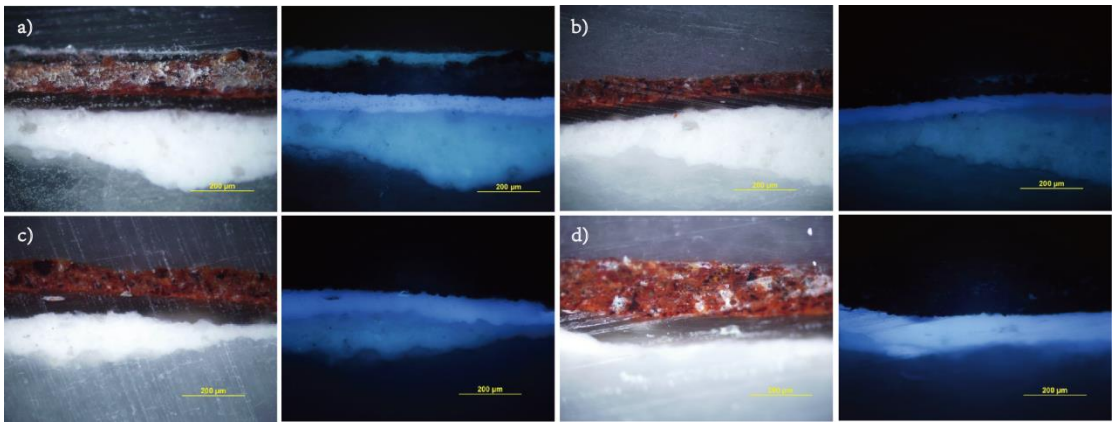

Figure 3.20 Cross-section microphotographs of glue paint B reconstructions varnished with dammar, image under visible light (left) and image under UV illumination (right), (a) varnished area before cleaning, (b) after cleaning by PHB-GVL gel, (c) after cleaning by PVA/PHB-GVL gel, (d) after cleaning by nylon/PHB-GVL gel

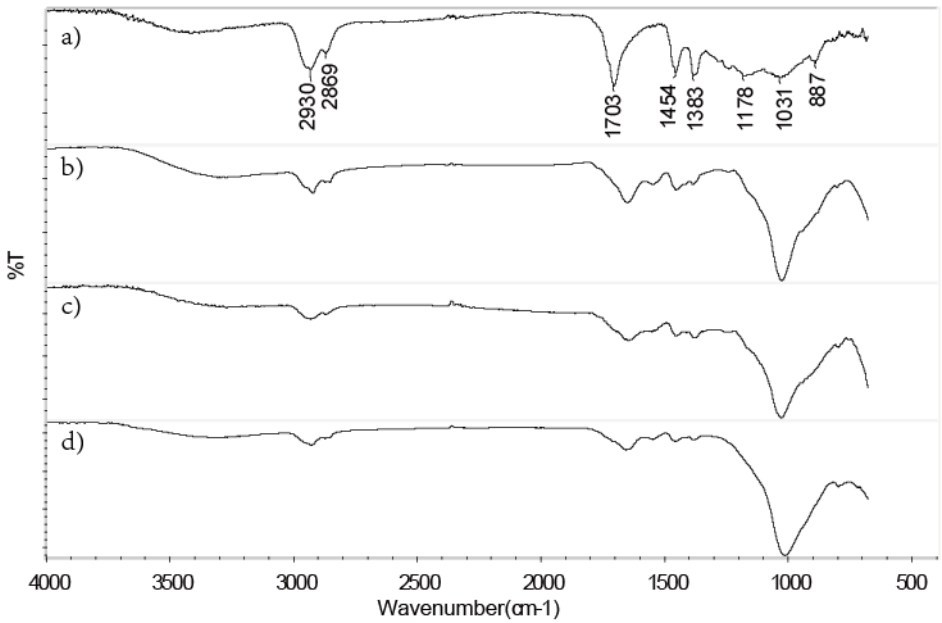

Figure 3.21 FTIR ATR spectra acquired on the surface of the dammar varnished mock-up B; (a) varnished area before cleaning, (b) after cleaning by PHB-GVL gel, (c) after cleaning by PVA/PHB-GVL gel, (d) after cleaning by nylon/PHB-GVL gel

3.4.3 Evaluation the gel residues

The residues left on the painting surface could lead to a series of adverse effects, in order to assess and control the risk to the original paint, it's necessary to detect the amount of residues. In this research, cleaning was performed on the thick dammar layer mock-up B by combined gels and PHB-GVL gel, since PHB-GVL gel was not able to remove all the varnish in the first 5 min application, a second application of 5 min was implemented for a completely removal of the varnish. ATR was applied for evaluation the cleaning, in particular for the detection of GVL residues. Figure 3.22 showed the spectra after 2 h and 24 h from the treatments, most of the dammar was disappeared except in the PHB-GVL gel cleaning area, a small amount of dammar still presents related to the C=O stretching at 1704 cm^{-1}. The GVL characteristic band at 1767 cm^{-1} was detected after 2 h from cleaning treatment, except PVA combined gel cleaning area, demonstrating the best solvent retention ability of PVA/PHB-GVL gel. After 24 h from cleaning, GVL can't be detected in the PVA and nylon combined gels' cleaning areas, however, it can still be detected in the PHB-GVL gel cleaning area.

HS-SPME was also applied to evaluate and quantitate the GVL component which left on the painting surface. With this aim, γ-butyrolactone (BL) was used for internal standard sample

because of its relative similar structure with GVL, a calibration curve was carried with the different ratio of concentration of GVL with 1000 ppm of BL and their areas ratio in GC-MS, they are linear relation with the slope of 0.1377 and intercept of 0.2254, the correlation coefficient square reached to 0.993 (figure 3.23). Afterwards, sampling a fragment in different gel treatment area, extraction of the analytes with carbon fiber, and then analyzed by GC-MC. The amount of residual GVL detected after 2 h and 24 h from the treatment are shown in table 3.3. According to the result, the GVL residues tend to decrease with the time, nylon/PHB-GVL gel cleaned area showed a slightly higher amount of residues than PVA/PHB-GVL gel cleaned area after 2 h from treatment, whereas after 24 h from treatment only very small amount of residual was detected on the area cleaned by both combined gels, they reduced to the same negligible level, and the negligible amount residues are too low to be detected by FTIR-ATR. However, in the PHB-GVL gel cleaned area remained a significantly higher amount of residual than combined gels in particular after the double cleaning processes. This result revealed that PVA and nylon combined gels are more efficiency in the removal of the dammar varnish, not only showed performance in reducing the application time, but also showed a lower amount of solvent residues after completely removal of the varnish.

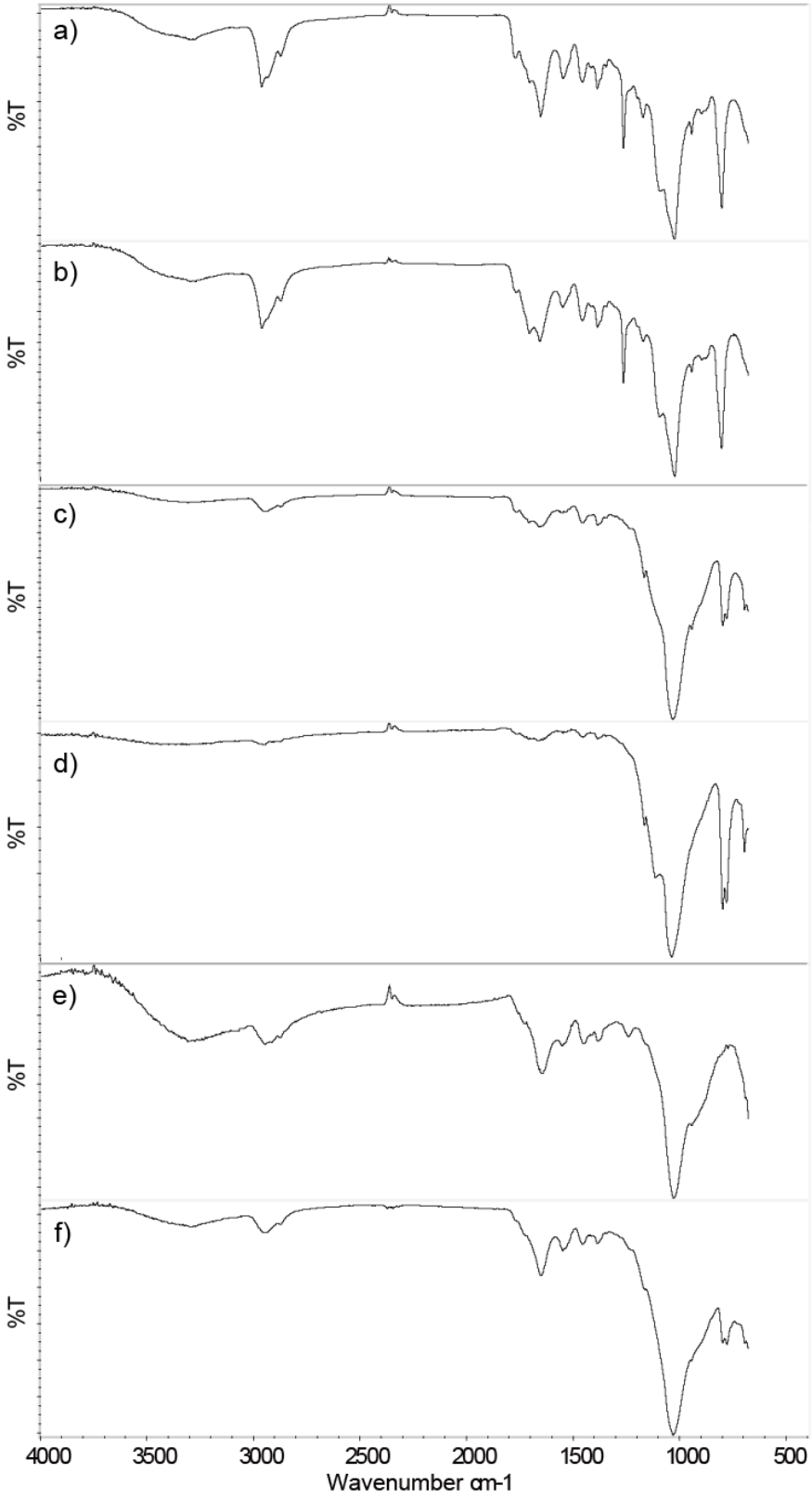

Figure 3.22 FTIR-ATR spectra acquired on the after cleaning area of the dammar varnished mock-up B; a) after 2 h from PHB-GVL gel application; b) after 24 h from PHB-GVL gel application; c) after 2 h from nylon/PHB-GVL gel application; d) after 24 h from nylon/PHB-GVL gel application; e) after 2 h from PVA/PHB-GVL gel application; f) after 24

h from PVA/PHB-GVL gel application

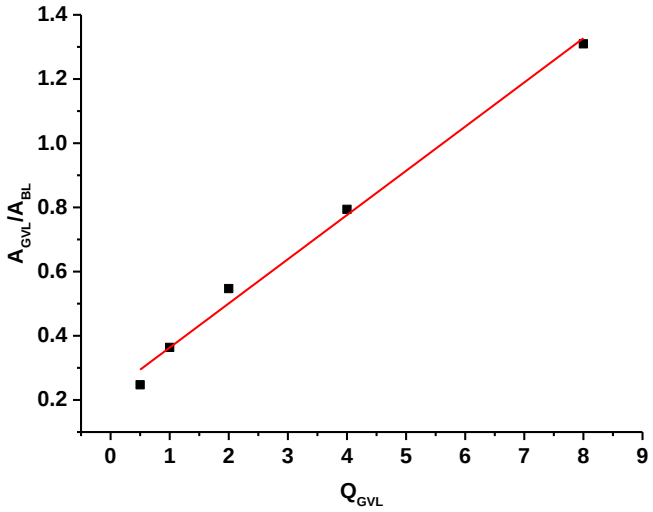

$$y = 0.1377x + 0.2254 \qquad R^2 = 0.993$$

Figure 3.23 Calibration curve of GVL with internal standard BL; axis X represents the GC-MS peak area ratio of GVL and BL, axis Y represents the prepared GVL and BL concentration ratio

Table 3.3 Amount of GVL residues (wt%) after 2 h, 24 h from the cleaning treatment.

Cleaning system	application	wt% after 2 h	wt% after 24 h
PHB-GVL	10 min	0.54 ±0.06	0.34 ±0
PHB-GVL	5 min	0.45 ±0.12	0.27 ±0.13
PVA/PHB-GVL	5 min	0.16 ±0	0.14 ±0.02
Nylon/PHB-GVL	5 min	0.27 ±0.03	0.17 ±0.02

3.4.4 Discussion

Electrospinning fabrication tissue was first time used to combine with organogel for cleaning purpose in cultural heritage field. The combined gels displayed both the advantages of nanometer scale tissue and organogel which reflected in mechanical property and cleaning efficiency aspects. The large porous and delicate microstructures of combined gels contain more space for loading the dammar which demonstrated by the SEM morphology of before and after gel application. In this case, the good performance of combined gels for removal of dammar varnish from painting mock-up has been described by optical microscope and

FTIR-ATR. Moreover, negligible solvent residues were detected by HS-SPME and guaranteed the safety to artworks. As a result, the new developed electrospinning combined organogels showed the advancements over normal organogel both in mechanical property and cleaning efficiency, which provided a new method to design advance gel cleaning system for conservation.

Chapter 4 DES-agar gel for the removal of proteinaceous coating from oil painting

4.1 Introduction

The removal of superficial layers on artworks including grease, dirty, various natural or synthetic varnishes that used in the past, is one of the most important tasks in conservation of heritage properties [1].

Thanks to the properties such as flexibility, versatility, natural produced and inherent adhesive properties, many proteinaceous materials including animal glue, egg, and casein from milk have traditionally been used for preparation of binders, coatings, and adhesives in painting or other artifacts [139]–[141].

Usually polar solvents, such as water, ethanol, ketones, aromatic and chlorinated hydrocarbons, can be used to solubilize the proteinaceous materilas [142]. But this kind of wet cleaning approach may induce drawbacks mainly owing to the unrestricted action of the solvent, which leads to its penetration into porous matrices, producing undesired phenomena, such as water could attaches to many inorganic pigments, and will infiltrate paint several particles deep in a short time and turned the oil milky with water clusters [124].

In the last decade, chemical and physical gels used for the removal of aged varnishes or coatings from artwork surfaces have gained considerable popularity, due to their control delivery of solvent ability. Recently, new kind of agar-gauze bacteria gel systems were developed for removal of proteinaceous [94]. However, limited attention has been devoted to the impact that such cleaning systems might have on the long application time and bacteria residues treatment.

To introduce powerful and sustainable alternatives for cleaning artworks, a new biocompatible cleaning system for paintings based on the use of fully green components of the deep eutectic solvent (DES), which obtained with choline chloride and urea, mixed with agar was developed for removal of proteinaceous coating from oil painting.

Deep eutectic solvents are salts formed from an eutectic mixture of acids and bases, they are characterized by a melting point much lower than either of the individual components [143]. As eco-friendly solvent, DESs have similar physical-chemical properties with common ionic liquids (ILs) and they have several advantages over traditional ILs such as low price, easy

storage and easy preparation [144]. DESs have been applied in many areas of chemistry, including catalysis and organic synthesis [145]–[147], separation technology [148], electrochemistry [149] and pharmaceutical [150] due to the excellent chemical-physical properties with low vapor pressure, non-flammability, good solubility and conductivity, wide electrochemical window and large liquid range [143],[144]. It has been already demonstrated the efficacy of DES for the extraction of proteins [148]. On these bases, an ongoing research work is currently aimed at developing a new green gel containing DES for the removal of proteinaceous coating from paintings. A good cleaning method should minimum effect the painting layer, in order to control the release of DES solvent during the cleaning procedure, an appropriate substance material should be selected to load the cleaning agent. Agar is a polysaccharide able to form rigid gels, it produces from marine seaweed of the red algae mainly tengusa and ogonori. Agar is composed of two types of polysaccharides, Agarose and Agaropectin. Agarose is a linear polymer made up of repeating units of agarobiose and enables to form gel, due to its high molecular weight (100.000-150.000 Daltons) and low percentage of sulphate groups (0.15%). We found in a certain condition, DES mixed with agar could produce a high viscous gel without any water addition. In this research, the new kind of rigid and peel able DES-agar gel was applied for removal of proteinaceous coating from oil painting.

Moreover, a new nondestructive analytical technique was evaluated in this research for investigation of diffusion behavior with the cleaning agent in painting layer. It is widely known that the use of not confined solvents for the cleaning of paintings may produce negative effects towards the painting such as swelling, softening and thus affecting the optical and mechanical properties of the painting layer. The correct evaluation of solvent diffusion and retention into paint layers is of crucial importance in assessing new cleaning procedures. Here, we propose micro-Spatially Offset Raman Spectroscopy (micro-SORS) as a valuable alternative non-destructive method to explore the diffusion of DES in painting.

Micro-SORS Raman is a new technique was recently developed, the technique combines conventional macroscale SORS with microscopy permitting the non-invasively resolve thin, micrometre scale layers such as painted stratigraphy in the Cultural Heritage field and turbid stratified systems in polymer, catalytic, biological, biomedical and forensics sciences [151]–[153]. Micro-SORS represents an essential tool in situations where a non-invasive molecular analysis is required, i.e. when dealing with precious, unique samples or objects in art field and

forensic science or in quality control processes to reduce time and costs in the manufacturing activity.

In this research, egg tempera samples were selected as the substances instead of using the oil painting samples, mainly because of the oil painting has very high interference of background fluorescence which limited the sensitivity of Raman spectroscopy, on the other hand, the DES residues can induce a long term effect with proteinaceous binder paint. In this case, DES solvent and DES-agar gel were selected for studying the presence and diffusion of DES in the egg tempera mock-up after wetting or simulation cleaning procedure.

4.2 Materials and methods

Reagents	Grade of purity.	Manufacturer
Choline Chloride	≥98%	Sigma-Aldrich
Urea	99.0-100.5%	Sigma-Aldrich
Agar	-	C.T.S
Rabbit glue	-	Phase, Bologna
Gypsum	-	Zecchi
Red ochre	-	Kremer
Egg	-	Coop

Rheology experiments were carried out on an Anton Paar Rheometer MCR 102 using a Cone plate configuration (23 mm diameter, 1 °). Experiments were performed at constant temperature of 28 °C controlled by the integrated Peltier system and a Julabo AWC100 cooling system. A solvent trap (H-PTD200) was used to avoid solvent evaporation during the measure. Frequency sweep measurements were carried out at 5% strain. The storage and loss moduli (G' and G'', respectively) and complex viscosity were measured over the frequency range 0.01 to 100 s^{-1}. Rheological measurements were performed on a set of 3 replicates for each type of gel system studied and the trend shows no significant differences.

Optical microscopy in visible and ultraviolet light (Olympus Optical Microscope BX51,

Tokyo, Japan) was applied on cross section before and after cleaning procedure to evaluate the thickness of varnish.

Thermo Scientific Nicolet iN10 Infrared Microscope in total attenuated reflectance (ATR) mode was performed directly over the surface after treatment, without any sample preparation, in order to implement the non-invasive analysis for assess the cleaning efficiency and the residues after treatment. A Thermo Nicolet (Thermo Fisher Scientific, Waltham, MA, USA), iN™10MX imaging microscope, fitted with a mercury-cadmium-telluride (MCT) detector cooled by liquid nitrogen, was used for spectroscopic analyses. Measurements were performed using a slide-on ATR objective, equipped with a conical germanium crystal, in the range 4000-675 cm^{-1}, at a spectral resolution of 4 cm^{-1} with 64 scans and an optical aperture of 150×150 μm. Spectroscopic analysis was performed on 3 different areas treated with the same cleaning procedure and 4 spectra were recorded before and after treatment. Moreover FTIR analyses in reflection-absorption spectroscopy (RAS) on gold sheet were performed for the analysis of DES, spreading a thin layer DES solvent on the gold sheet, with an Infrared Microscope Thermo Scientific Nicolet iN10MX was used in total reflection mode to record spectra in the range between 675 and 4000 cm^{-1}, with a spectral resolution of 4 cm^{-1} with 64 scans and an optical aperture of 150×150 μm.

Micro SORS-Raman was using a Senterra dispersive Raman microscope (Bruker Optik GmbH) equipped with a Peltier cooled charge coupled device detector (1024 × 256 pixels) and a 785 nm excitation laser. The reference spectra of DES and painting mock-up were performed using a 20x objective, a laser power from 10 to 50 mW at the sample and an acquisition time ranging from 50 s to 100 s. The defocusing micro-SORS measurements were acquired at imaged and defocused positions moving the 20x objective away from the sample in z direction (from 50 to 800 μm of distance), using 10 mW laser power at the sample and an accumulation time of 100 s per spectrum.

4.3 Gel preparation and characterization

4.3.1 Synthesis of DES-agar gel

The DES was synthesized by mixing hydrogen bond acceptor (Choline chloride) and hydrogen bonding donor (Urea), at the mole ratio 1:2 in a Petri dish. The mixture was stirred

at 100 ℃ for 5 min until a homogeneous colorless liquid was obtained. Then add agar in DES with the mass ratio of 1:10, and manually stirring until form the gel.

4.3.2 Synthesis of EtOH-H_2O/agar gel

The EtOH-H_2O/agar gel was synthesized by mixing 1.5 mL of ethanol and 1.5 mL of deionized water in a Petri dish, then add agar 100 mg in the solution, the mixture manually stirred at 70 ℃ for 4 min until form the homogeneous colourless gel.

4.3.3 DES-agar gel characterization

4.3.3.1 FTIR analysis

FTIR in reflection-absorption spectroscopy (RAS) was performed to characterize DES by spreading a thin layer of DES liquid on a gold plate. From the spectrum (figure 4.1), the significant absorption bands of DES were observed at 3337 cm^{-1} (N-H stretching), 1660 cm^{-1} (C=O stretching), 1613 cm^{-1} (N-H scissoring), 1477 cm^{-1} (CH_2 bending), 1444 cm^{-1} (C-N stretching) and 785 cm^{-1} (N-H bending), the bands at 1163 cm^{-1} to 865 cm^{-1} are referred to C-N symmetric stretching. The investigation of DES with FTIR could helpful to recognize the potential residues after cleaning treatment.

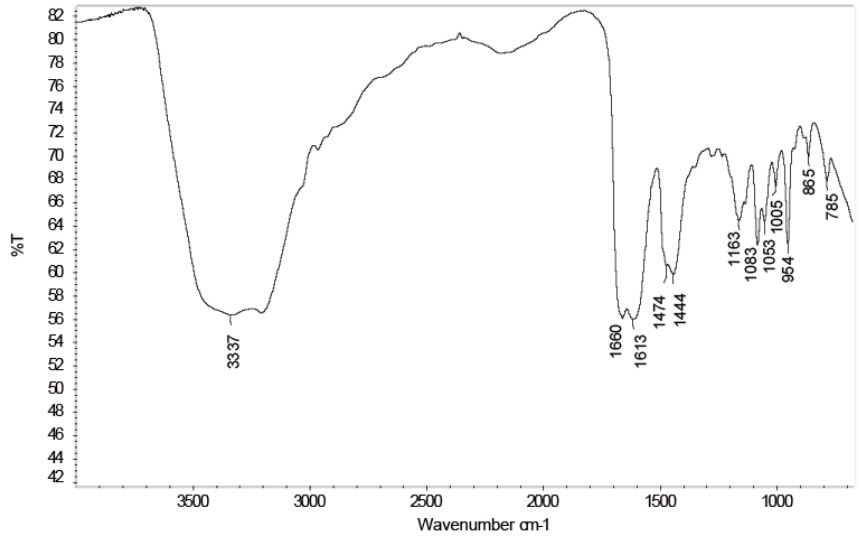

Figure 4.1 The FTIR spectrum of the deep eutectic solvent consists of choline chloride and urea

4.3.3.2 Rheological measurements

The mechanical property of the DES-agar gel was investigated via rheological measurements. Figure 4.2 showed the complex viscosity as a function of the applied frequency. A significant linear decrease in complex viscosity was observed with increasing frequency. This means that the gel is in a very rigid condition. DES-agar gel displayed also a high storage modulus (figure 4.3), indicating good mechanical proprieties in terms of gel stiffness, allowing an easy handling and removal of the gel. The gels presented a gel-like behaviour and in all the cases storage modulus G' was higher than that of the loss modulus G''. The storage modulus quantifies the elastic behavior of the gels, while the loss modulus shows the dissipation ability of the polymer network. This feature proves the ability of DES to form the gel, building a 3D network. The stiffness and rigidity are positively correlated with G' and G''. The intersection of storage and loss modulus was observed with increasing the shear strain, over the shear strain of intersection, it losses the gel property and shows liquid condition. From the results, DES-agar gel is a rigid gel which could be easy to peel off and leave a low (up to none) extent of residues behind.

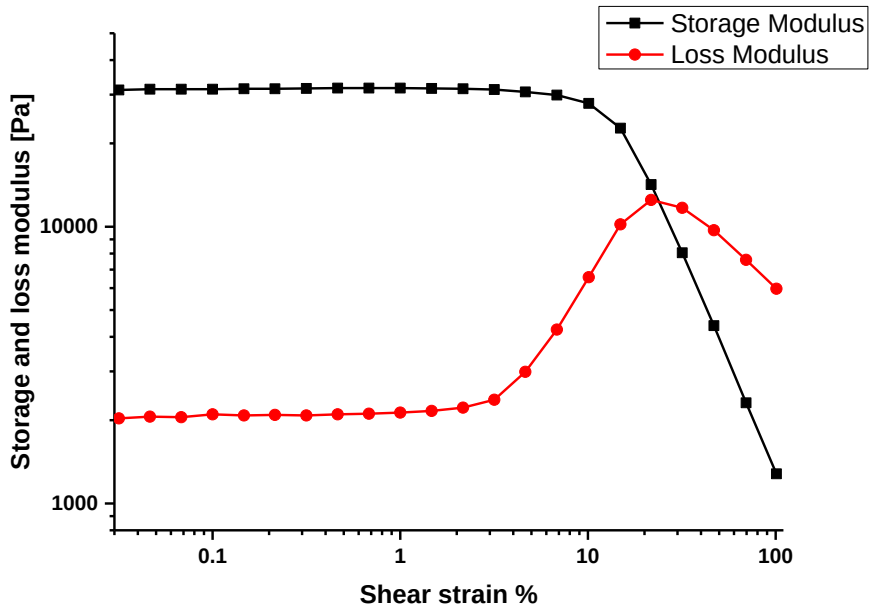

Figure 4.2 Storage (G') and loss modulus (G'') as a function of shear strain for DES-agar gel

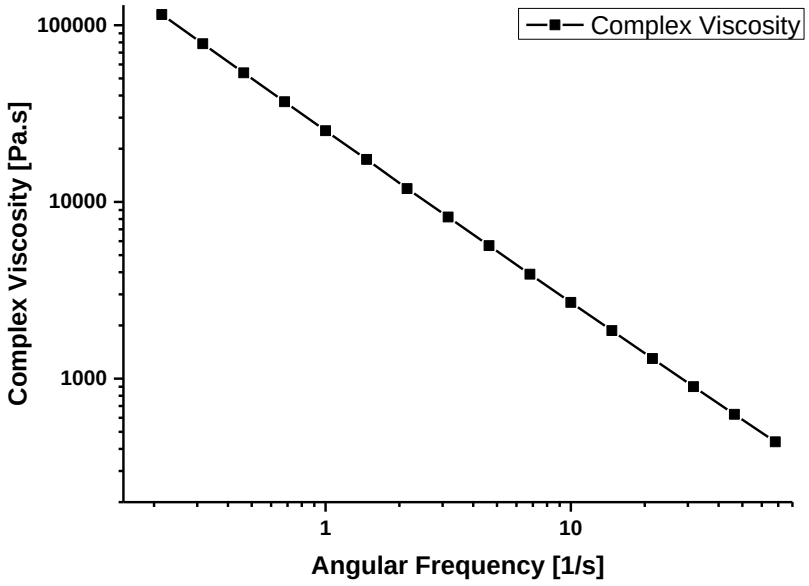

Figure 4.3 Complex viscosity as a function of frequency for DES-agar gel

4.4 The cleaning work on painting

4.4.1 Mock-ups preparation

The oil painting mock-ups were selected for the investigation of cleaning efficiency of the new developed DES-agar gel system. The painting mock-ups composed by three layers including ground layer, painting layer and varnish layer. In detail, the ground layer was prepared by a mixture of gypsum and rabbit glue. First 1.0 g of glue was melted in hot water (5.0 mL), as soon as the solution was homogeneous, 6.0 g of gypsum were added and well mixed. Then brushed appropriate thickness mixture on wood board, after drying several minutes, a thin layer of glue closing (the well dissolved glue solution) was applied on the ground layer. Oil painted layer was prepared by adding 1.0 g of burnt ochre pigment to 0.5 mL of linseed oil. Two kinds of proteinaceous coatings were applied over different binding media: whole egg and rabbit glue varnishes. Whole egg coating was composed by egg white, yolk, and water in a 1:1:1 (v/v) ratio. Glue coating was composed by mixing rabbit glue with water in a 1:10 (m/v) ratio. The ATR spectra of oil painting mock-up, whole egg covered oil painting and rabbit glue covered oil painting were shown in figure 4.4, and the vibrational

assignments were listed in table 4.1.

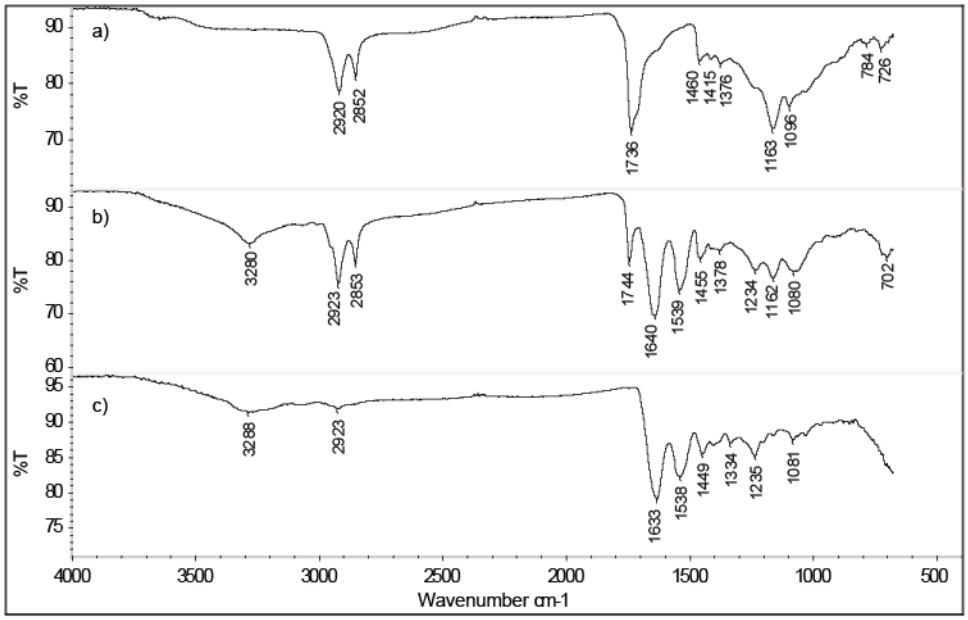

Figure 4.4 ATR spectra of a) oil painting mock-up; b) whole egg covered oil painting; c) rabbit glue covered oil painting

Table 4.1 Principal vibrational assignments of all the mock-ups

Oil painting mock-up	Assignment	Whole egg covered mock-up	Assignment	Glue covered mock-up	Assignment
2920 cm^{-1}	v_a C-H_2	3280 cm^{-1}	v N-H	3288 cm^{-1}	v N-H
2852 cm^{-1}	v_s C-H_2	2923 cm^{-1}	v_a C-H_2	2923 cm^{-1}	v_a C-H_2
1736 cm^{-1}	v C=O	2853 cm^{-1}	v_s C-H_2	1633 cm^{-1}	v C=O amide I
1460 cm^{-1}	δ CH_2	1744 cm^{-1}	v C=O	1538 cm^{-1}	δ N-H_2 and C-N amide II
1415 cm^{-1}	wag(CH_2)-CH_2-C O-O	1640 cm^{-1}	v C=O amide I	1449 cm^{-1}	δ C-H
1376 cm^{-1}	wag(CH_2)	1539 cm^{-1}	δ N-H_2 and C-N amide II	1403 cm^{-1}	wag(CH_2)-CH_2-C O-O
1163 cm^{-1}	v_a(C-O)	1455 cm^{-1}	δ C-H	1334 cm^{-1}	wag(CH_2)
1096 cm^{-1}	v Si-O	1378 cm^{-1}	wag(CH_2)	1235 cm^{-1}	v C-O

784 cm^{-1}	v Si-O-Si	1234 cm^{-1}	v C-O	1081 cm^{-1}	v Si-O
726 cm^{-1}	γ -(CH_2)-	1162 cm^{-1}	v_a C-O		
		1080 cm^{-1}	v Si-O		
		702 cm^{-1}	wag N-H		

Egg tempera mock-ups were selected to characterize the diffusion behavior of the DES solvent. The mock-up was prepared according to traditional painting techniques. The ground layer was made of gypsum and rabbit glue, dissolving 1.0 g of animal glue in 5.0 mL of hot distilled water and mix with 6.0 g grinded gypsum. Painting layer was whole-egg tempera, briefly, a mixture of egg white, yolk, and water in a 1:1:1 (v/v) ratio, was used as binder and mixed with red ochre with ratio 1:1 (v/m). The preparation layer was made of gypsum and rabbit glue, dissolving 1.0 g of animal glue in 5.0 mL of hot distilled water and mix with 6.0 g grinded gypsum. The ATR spectrum of egg tempera mock-up was shown in figure 4.5, and the vibrational assignments were listed in table 4.2.

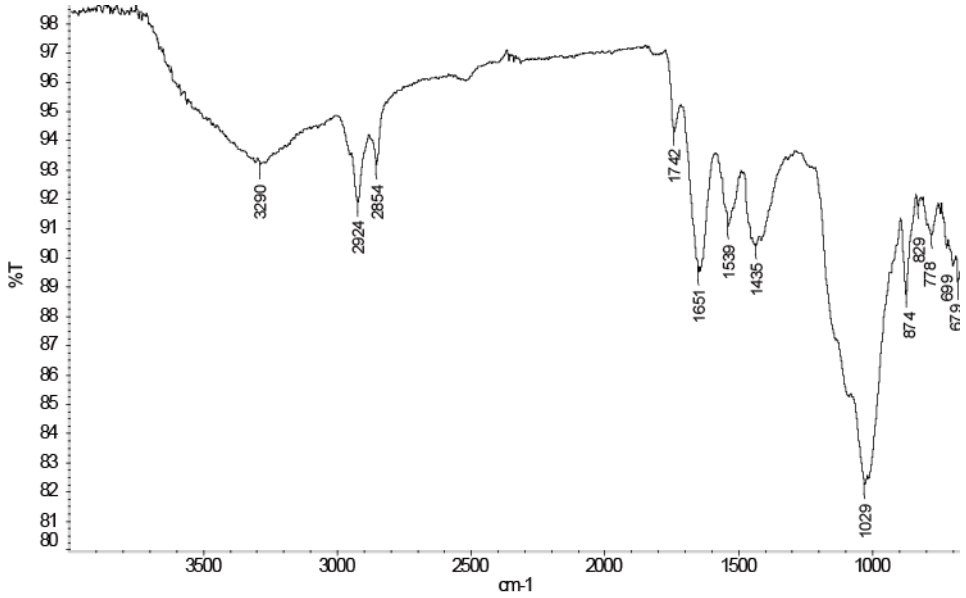

Figure 4.5 ATR spectra of egg tempera mock-up

Table 4.2 Principal vibrational assignments of all the egg tempera mock-ups

Oil painting mock-up	Assignment
3290 cm^{-1}	v N-H
2924 cm^{-1}	v_a C-H_2

2854 cm^{-1}	v_s C-H_2
1742 cm^{-1}	v C=O
1651 cm^{-1}	v C=O amide I
1539 cm^{-1}	δ N-H_2 and C-N amide II
1435 cm^{-1}	δ C-H
1029 cm^{-1}	v Si-O
874 cm^{-1}	γ CO_3^{2-}
778 cm^{-1}	v Si-O-Si
699 cm^{-1}	wag N-H

4.4.2 EtOH-H_2O/agar gel for the removal of residues

The DES we used for cleaning is a kind of hardly volatile liquid consists of two salts by hydrogen bond, it's difficult to completely removal of only by mechanical cotton swab, other methods should be developed for an auxiliary cleaning. DES has good solubility in high polar solvents such as water, ethanol and methanol, however, the more volatile ethanol and methanol can't form gel with agar, in this case, water was selected to combine with ethanol to obtain a solution both enable to produce a gel with agar and good volatilization ability. The EtOH-H_2O/agar gel shows good mechanical property with rigid and easy peel off advantages. The experiments were carried on the oil painting mock-up surface which already implemented DES wet cotton swab (1 wet cotton swab for wetting the surface) and dry cotton swabs (3 wet cotton swabs for cleaning the surface), figure 4.6 showed ATR spectra of after different EtOH-H_2O/agar gel application time. Before the gel application, DES bands at 1676 cm^{-1} (C=O stretching) and 1627 cm^{-1} (N-H scissoring) were clearly seen, after 2 min, 30 s and 10 s gel application respectively, the DES characteristic bands disappeared, the results revealed that EtOH-H_2O/agar gel showed good performance for cleaning the DES residues, with a shot application time (10 s) the DES residues could be completely removed. This strategy provided a powerful substance for removal of the potential DES residues in the cleaning process.

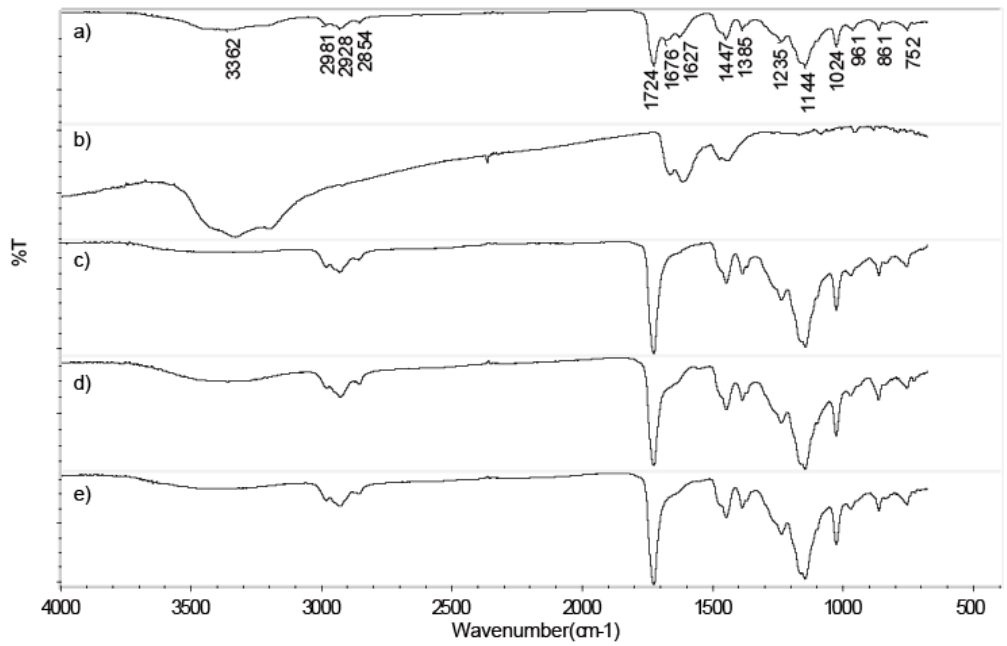

Figure 4.6 ATR spectra of EtOH/H_2O-agar gel application for absorption DES residues, a) before EtOH/H_2O-agar gel application; b) DES reference; c) after 2 min EtOH/H_2O-agar gel application; d) after 30 s EtOH/H_2O-agar gel application; e) after 10 s EtOH/H_2O-agar gel application

4.4.3 Evaluation the cleaning efficiency on mock-up

Cleaning method was implemented by applying directly on the samples surface for 5 min, a light pressure provided a good adhesion of the gel with the treated area, then removed the gel and cleaned with dry cotton swabs. Based on the cleaning situation, three times repeat cleaning, totally 15 min treatment with dry cotton swabs and further 10 s application of EtOH-H_2O/agar gel were established for proteinaceous coating removal.

4.4.3.1 DES-agar gel for the removal of whole egg coating

The oil painting mock-up decorated with whole egg coating was used for evaluating the cleaning efficiency of new green DES-agar gel system. In order to understand the cleaning performance of the gel, two cleaning strategies were applied for comparison: 1) application of DES-agar gel for 15 min; 2) application of DES-agar gel for 15 min and further with EtOH-H_2O/agar gel for 10 s. We preliminary checked the cleaning by optical microscope both in visible and UV-Vis light (figure 4.7), four layers in different colour on the mock-up before

cleaning were observed, which including two layers of different brightness fluorescence layer that related to whole egg coating and suspending layer of oil binder. After cleaning by strategy 1), the UV-Vis light microphotograph clearly showed that surface bright fluorescence layer disappeared, only a thin layer of yellowish fluorescence layer presence which referred to suspending oil. This result revealed that DES-agar gel could removal of whole egg coating without damage painting layer. The same situation was observed after strategy 2) cleaning, the further 10 s of EtOH-H_2O/agar gel application didn't change the appearance of the mock-up under optical microscope, and there are no difference be observed between the cleaning of strategy 1) and 2) from OM.

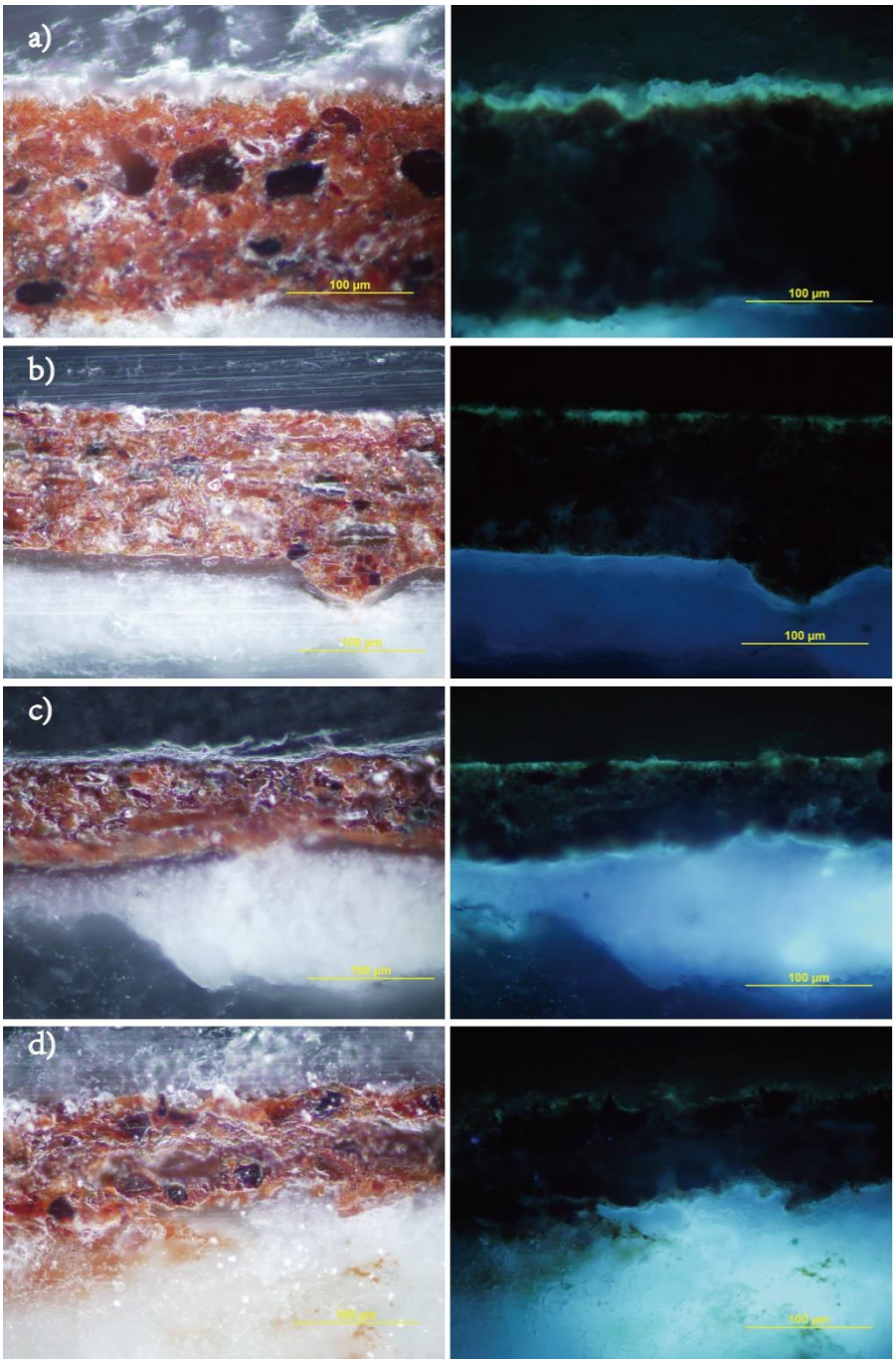

Figure 4.7 Cross-section microphotographs of glue painting reconstructions varnished with whole egg before and after cleaning, image under visible light (left) and image under UV illumination (right); a) before cleaning, b) after 15 min of DES-agar gel application, c) after 15 min of DES-agar gel application and 10 s of EtOH-H_2O/agar gel application, d) unvarnished area

Further analyses before and after the cleaning were performed by the ATR microscopy. Promising results were obtained with the DES agar gel (Figure 4.8), the protein characteristic

bands of amide I and amide II at 1640 and 1539 cm^{-1} completely disappeared, while C=O stretching at 1738 cm^{-1} belong to oil obviously increased, this result revealed DES agar gel could removal of the whole egg coating. However after strategy 1) cleaning, we also detected the double band at 1659 (C=O stretching) and 1620 cm^{-1} (N-H scissoring) that attributed to DES, that's mean there are some residues of DES were left on the surface after DES agar gel cleaning. As shown in figure 4.8e, after strategy 2) cleaning with additional 10 s of EtOH-H_2O/agar gel application, the ATR result showed that the DES double band at 1659 and 1620 cm^{-1} disappeared, as observed in unvarnished area. As a result, the cleaning strategy 2) showed better performance without left any DES residues on the surface.

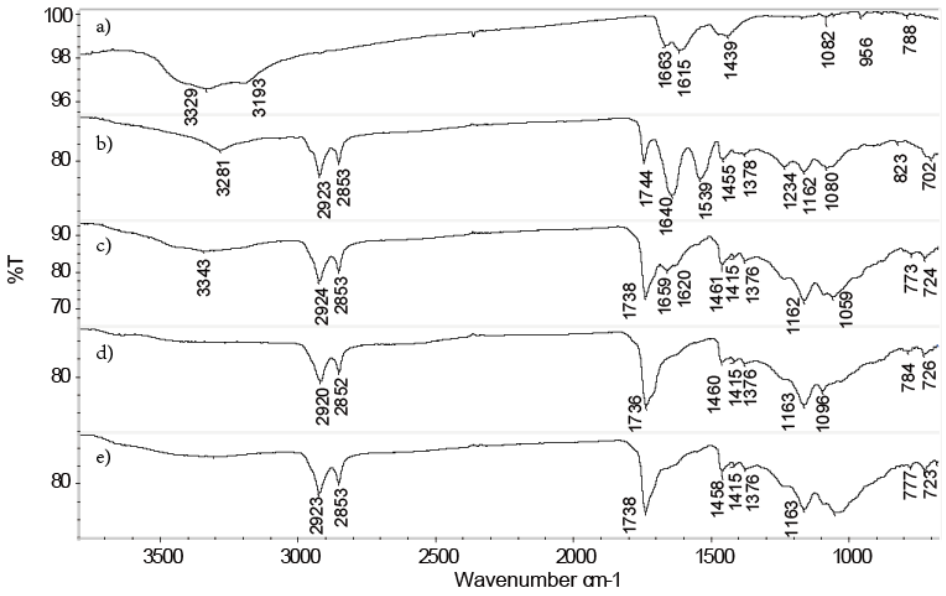

Figure 4.8 ATR spectra acquired on (a) DES reference, (b) before cleaning, (c) after DES-agar gel cleaning, (d) an unvarnished area, (e) after DES-agar gel+EtOH-H_2O/agar gel cleaning

4.4.3.2 DES-agar gel for the removal of glue coating

Animal glue is another common used proteinaceous materials as binder or protective coating in the past, which producing from mammalian or fish collagen, mainly consists of gelatin and lower molecular weight residues of collagen, keratin, and elastin. They usually used in historic and artistic objects, such as painting ground, binders for pigments, and adhesives. Here the oil painting mock-up decorated with rabbit glue was selected for testing the cleaning efficiency of DES-agar gel system. Two cleaning strategies as the same as above removal of

whole egg coating were applied also, in detail, 1) application of DES-agar gel for 15 min; 2) application of DES-agar gel for 15 min and further with EtOH-H_2O/agar gel for 10 s. After the gel application, optical Microscope with visible and UV-Vis light was used for preliminary characterization (figure 4.9), we can observe a significant yellowish coating fluorescence layer, however, it is difficult to distinguish the suspend oil layer and glue coating with both strategies, as shown in figure 4.9bc, the fluorescence layer reduced a lot, but still unable to know whether the glue coating be completely removed or not. ATR crystal directly applied on the treatment surface was useful to identify the components, as shown in figure 4.10, after cleaning by strategy 1), the characterization bands of protein with amide I and amide II at 1640 and 1539 cm^{-1} were completely disappeared, the C=O stretching at 1738 cm^{-1} related to oil came out, however the DES double band at 1666 and 1627 cm^{-1} was still present, demonstrating the DES residues were left on the surface after DES-agar application. Strategy 2) was also tested, as shown in figure 4.10d, after strategy 2) cleaning with additional 10 s of EtOH-H_2O/agar gel application, the ATR result showed that the DES double band at 1666 and 1627 cm^{-1} disappeared, as observed in unvarnished area (figure 4.10e). As the result, the cleaning strategy 2) is more efficiency and without left any DES residues on the surface.

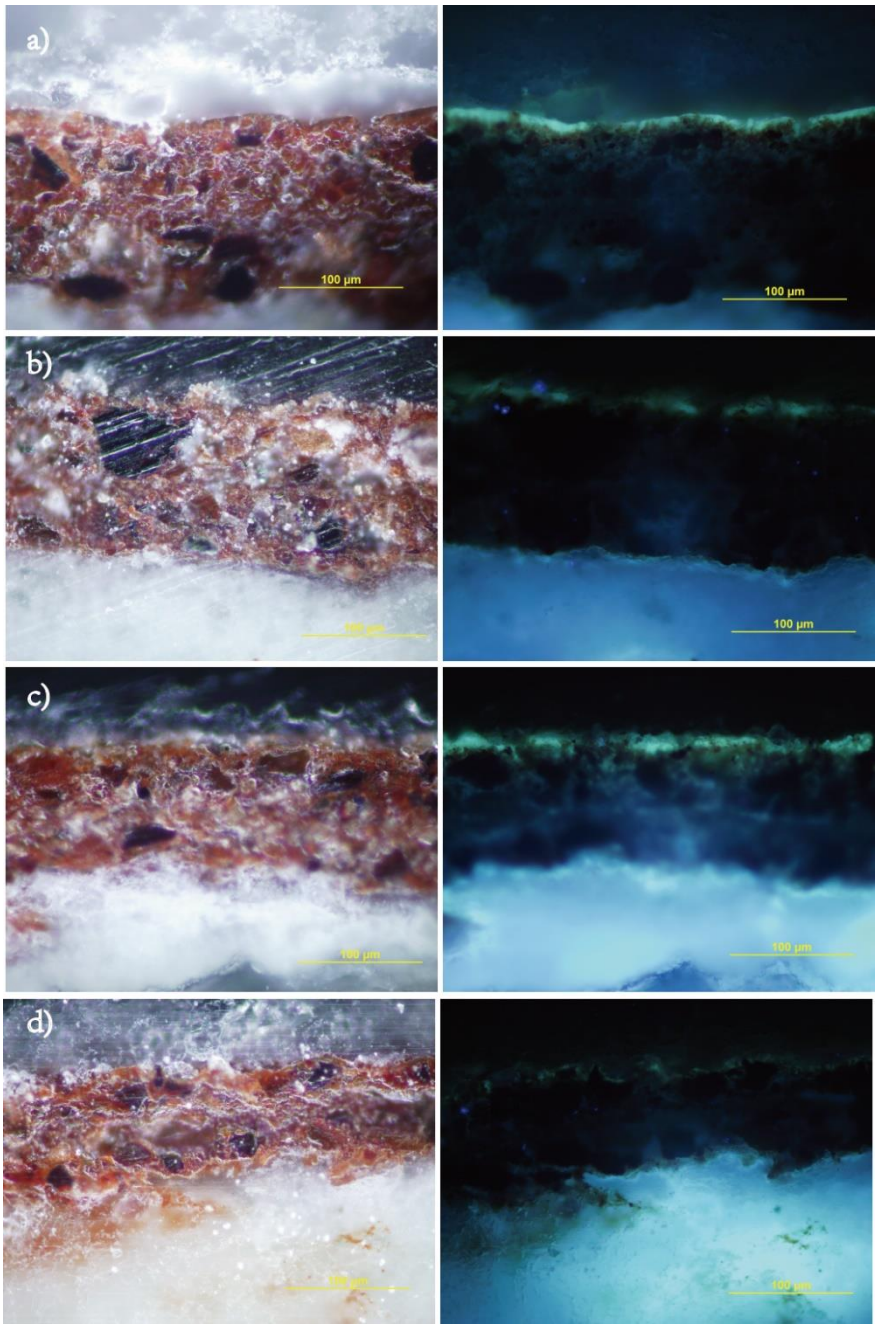

Figure 4.9 Cross-section microphotographs of glue painting reconstructions varnished with glue before and after cleaning, image under visible light (left) and image under UV illumination (right); a) before cleaning, b) after 15 min of DES-agar gel application, c) after 20 min of DES-agar gel application and 10 s of EtOH-H_2O/agar gel application, d) unvarnished area

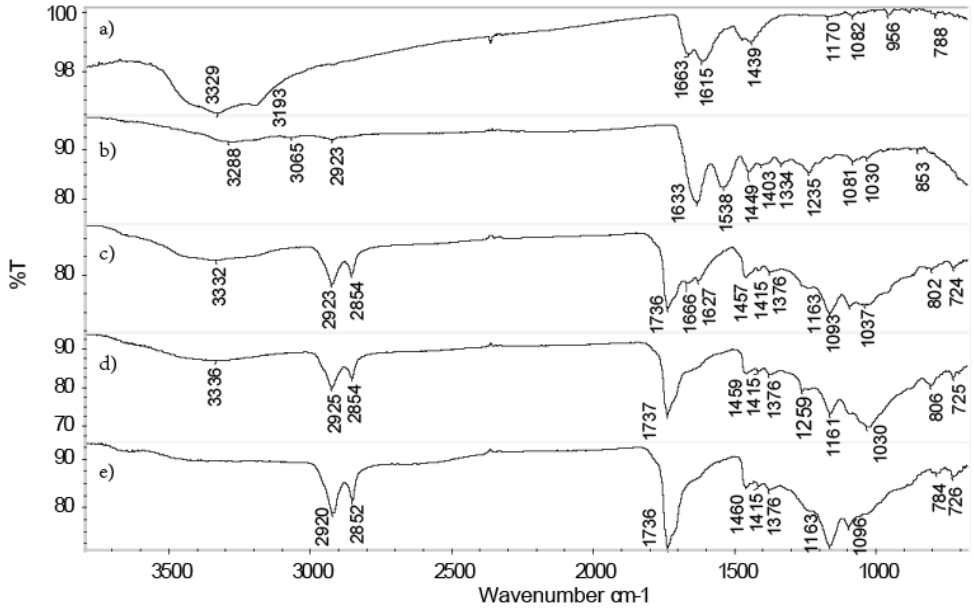

Figure 4.10 ATR spectra acquired on (a) DES reference, (b) before cleaning, (c) after DES-agar gel cleaning, (d) after DES-agar gel+EtOH-H_2O/agar gel cleaning, (e) an unvarnished area

4.4.4 Discussion

Deep eutectic solvent (DES) was selected to serve as a cleaning agent for removal of proteinaceous coating, it's a new kind of eco-friendly solvent consists of the hydrogen bond acceptor (Choline chloride) and hydrogen bonding donor (Urea). Agar was found enable to form gel phase with DES in a heating and stirring condition. Rheological measurements showed DES-agar gel has good mechanical proprieties in terms of gel stiffness. The cleaning tests were performed on whole egg and rabbit glue decorated oil painting mock-ups. A cleaning strategy for removal of proteinaceous coating by using DES-agar gel with dry cotton swabs and 10 s EtOH-H_2O/agar application was implemented. ATR and optical microscopy were applied for evaluation the cleaning efficiency and residues, the results revealed that DES agar gel could completely removal of the whole egg and glue coating without damage the painting layer, and no DES residues were left on the surface after the appropriate cleaning treatment.

4.5 Micro-SORS Raman for characterization DES diffusion behavior of sublayer

Microspatially offset Raman spectroscopy (Micro SORS-Raman) is a new technique was recently developed for noninvasive characterization of the chemical composition of subsurface, the technique combines conventional macroscale SORS with microscopy permitting the study of micrometer-scale turbid layers such as painting [154]. Micro-SORS analysis enable directly performed on artworks with appropriate controlling the focus or defocus under Raman microscope objective, to obtain varying degree of the sub layer Raman signals, which avoid the traditional invasive cross-sectional sampling.

The concept of defocusing micro-SORS is illustrated in Figure 4.11 for a two layer turbid system. The basic measurement relies on collecting at least two Raman spectra using a conventional Raman microscope. The first spectrum is acquired with the sample in a standard 'imaged' position where conventional Raman microscopy would traditionally be performed to analyze the surface of the sample. Then, a second measurement is taken with the sample moved away from the microscope objective by a 'defocusing distance Δz', to a so called 'defocused' position [155].

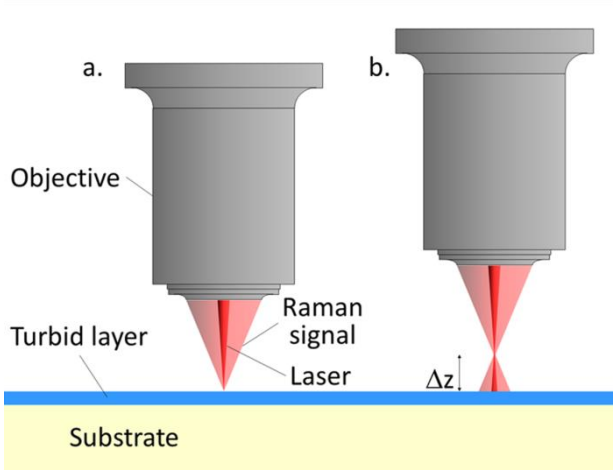

Figure 4.11 Schematic of micro-SORS measurement consists of a) conventional Raman setup, b) defocusing

Based on the previous study with our collaborator, the application of Micro-SORS for detecting the penetration depth of Paraloid B72 and cleaning agent DES on gypsum mock-up was evaluated. In brief, the Monte Carlo simulations were applied to study the micro-SORS signal of liquid which penetrated into the homogeneous mock-up with different degree of

defocusing. For simplicity, the concentration of the liquid is constant from mock-up surface to the diffusion depth and completely zero at a certain depth. This relative rough simplification of liquid concentration during penetration would typically apply on more complex situation, for evaluation the capacity of micro-SORS to distinguish the constant liquid concentration only with different penetration depth. The assumption defocusing SORS illumination and collection geometry, and simulations were carried out using a Monte Carlo code developed before [155]–[157]. From the simulation results, the penetration depth could be deduced from the fall of rate of the dependencies as shallower penetration depths yield faster decay of the enhancement factor with defocusing than for more deeply penetrated agents. In the latter experiments, Paraloid B72 and DES were applied on the gypsum mock-ups with brush and drop respectively, after treatment the mock-ups were defocusing with Micro-SORS, the results revealed the technique was capable of differentiating non-destructively different penetration depths of the products into the matrix. The penetrations are different with many factors such as the application time and the amount of application solvent. However, at this stage of the study, defocusing does not allow the determination of the absolute depth penetration reached by a solvent, instead it establishes if a solvent is more or is less deeply penetrated in a sample compared to another sample.

The present work aims at studying the presence and diffusion of DES in the egg tempera painting mock-up in three different application processes: 1) after the application of a DES drop, 2) after a cleaning simulation performed with a DES wet cotton swab 3) after a cleaning simulation performed with DES-agar gel. Defocusing micro-SORS measurements were performed immediately after the drop application or the cleaning simulations (t_0) and after two hours (t_1). Many defocusing micro-SORS series were acquired at t_0 and t_1 to verify the reproducibility of the results. Here only the most representative outcomes are shown.

4.5.1 The application of micro-SORS Raman for characterization DES diffusion

In this research, DES was applied on an egg tempera mock-up by different ways for study the diffusion of liquid in painting sub layer, such as the most direct with spreading a drop of DES on the surface and simulation cleaning treatments. Before the application, the DES and painting mock-up were characterized by Raman without defocusing (Conventional Raman) respectively, in order to confirm the absorption bands between different materials and identify

the most characteristic band for distinguish each other.

Painting mock-up Raman spectrum showed the presence of both pigment and binder components (figure 4.12), the most characteristic bands at 409 cm^{-1}, 291 cm^{-1} and 224 cm^{-1} referred to red ochre, and egg binder with broad bands distributed in the region between 1200 and 1600 cm^{-1}. Carbonates signals which attributed to calcite (1087 cm^{-1}) and/or dolomite (1094 cm^{-1}) were observed in some area of the painting, probably present in the red ochre pigment. DES Raman spectrum was shown in figure 4.12, the intensity bands at 1450 and 999 cm^{-1} referred to C-N asymmetric and C-N symmetric stretching, respectively, were attributed to urea. Besides, the other C-N asymmetric stretching band at 956 cm^{-1} and C-N symmetric stretching band at 716 cm^{-1} were assigned to choline.

The 716 cm^{-1} Raman band of DES and the 409 cm^{-1} band of red ochre were used for the calculation of the solvent-substrate ratio. The 716 cm^{-1} Raman band was selected because the other intense DES Raman band located 999 cm^{-1} partially overlaps the 1017-15 cm^{-1} band of anhydrite or the 1009 cm^{-1} band of gypsum, that are present in the preparation layer. The 409 cm^{-1} Raman band was selected because it displays the most comparable features (in terms of intensity and band shape) with the DES Raman band.

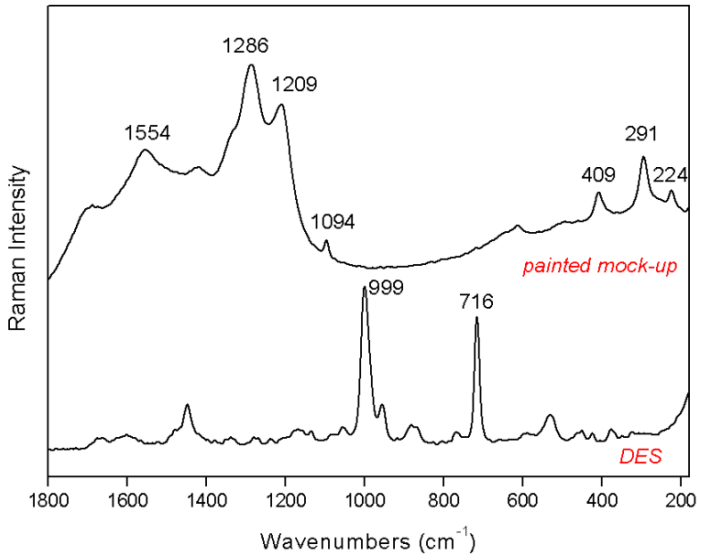

Figure 4.12 Reference Raman spectra of the painted mock-up and DES

4.5.1.1 Application of DES drop on painting surface

A drop of DES was spread on the mock up surface, two micro-SORS sequences have been

repeated starting from the same point at different times include a few seconds after the drop application (t_0) and 2 hours later (t_1). The defocusing micro-SORS measurements were acquired at imaged and defocused positions moving the 20x objective away from the sample in z direction. The same sequential measurements were repeated on different position, the most representative sequences are reported here.

The imaged Raman spectrum acquired at t_0 showed the presence of red ochre, egg (not shown) and DES. Normalizing the spectra to the red ochre band at 409 cm^{-1} (Figure 4.13), it is evident that the gradual incrementing of the defocusing micro-SORS distances, resulting in deeper probing, leads to a rapid relative decrease of DES Raman signal to that of the matrix. This is consistent with the fact that at this initial time DES is expected to be mainly distributed on the painting surface, however, due to the fact that the completion of the entire defocusing micro-SORS sequence took approximately 30 min, during the analysis time DES was partially penetrating into the sub-layer and this could also affect the observed relative intensity variations.

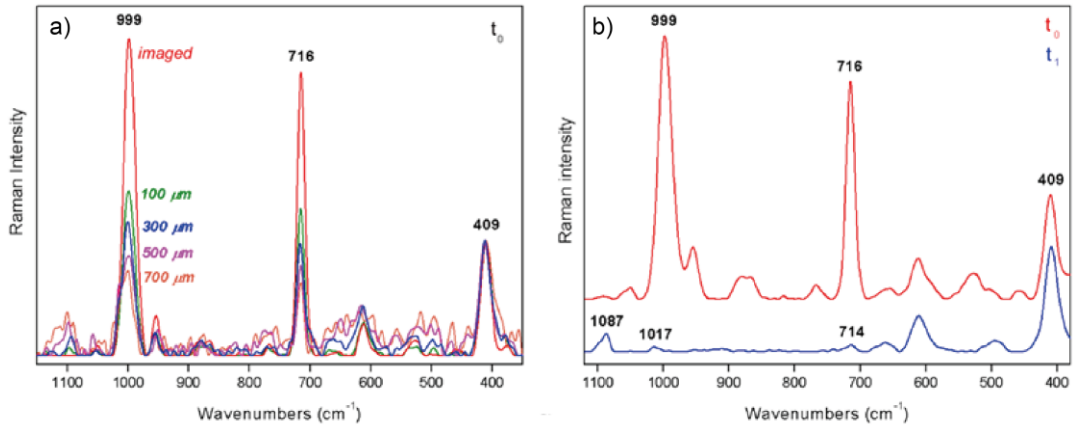

Figure 4.13 a) Micro-SORS sequence acquired at t_0 (started a few seconds after the application of DES drop on the painted mock-up), normalized to the red ochre signal at 409 cm^{-1}; The micro-SORS steps are indicated with colored values from imaged position to 700 µm; b) Raman spectra acquired at t_0 and t_1 at imaged position of the painted mock-up, normalized to the red ochre signal at 409 cm^{-1}

After 2 h from the drop application (t_1), DES was completely absorbed and the diffusion process could be considered completed, a second micro-SORS sequence was acquired in the same area with t_0. Firstly, the presence of calcite (1087 cm^{-1}) which was covered by the DES

drop in the previous micro-SORS sequence, is now visible (Figure 4.13b) together with the 1017 cm^{-1} Raman band ascribed to anhydrite, one of the ingredients of the preparation layer; moreover, the comparison between the imaged spectra acquired at t_0 and t_1 (Figure 4.13) provides the indication of a different intensity ratio between the red ochre signal and DES; at t_1 this ratio dramatically alters, demonstrating that after 2 h a smaller amount of DES is present on the sample surface.

To highlight the DES signal trends in the micro-SORS sequences, the DES/red ochre ratios were calculated (Figure 4.14). At t_0, the fast DES/Red ochre decay rate is related to the fact that the solvent is mainly distributed on the sample surface. At t_1, the 716 cm^{-1} band intensity is very low, reflecting on a small ratio value at imaged position. DES band is detected up to 300 μm of defocusing distance, and the ratio calculated for all the defocusing micro-SORS steps at t_1 shows similar values. This could indicate that DES has been adsorbed within the red ochre layer and the residual amount detectable with Raman is too low that it is not possible to monitor its distribution with micro-SORS.

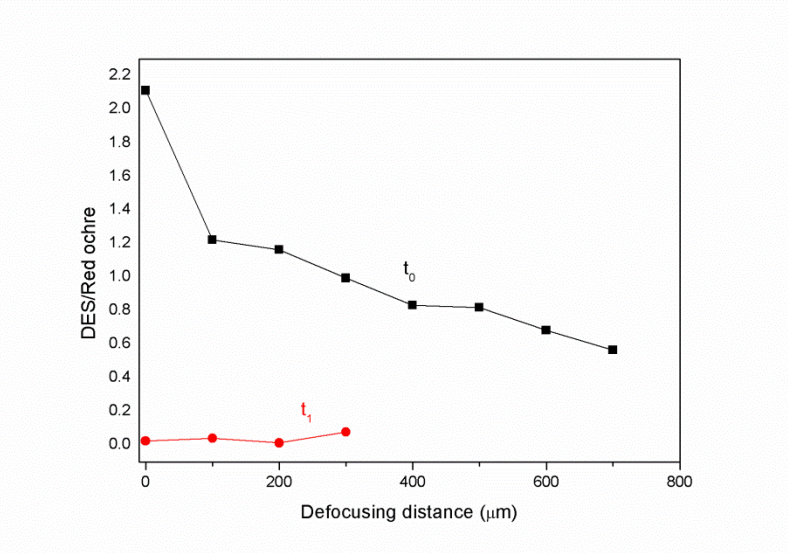

Figure 4.14 DES/ Red Ochre ratios of defocusing micro-SORS sequences acquired at t_0 and t_1

4.5.1.2 DES solvent cleaning

Cotton swab was wet with DES, and the cleaning was carried by rolling to wet a painting mock-up of 1 cm^2, keep the wetting for 5 min and cleaned by other 2 dry cotton swabs. After the cotton swab cleaning, the imaged Raman spectrum acquired at t_0 showed the presence of red ochre, egg (not shown), DES exhibited a less intense signal than in the drop experiment

(Figure 4.15). As observed in the drop case, the gradual increment of the defocusing micro-SORS distance leads to a rapid relative decrease of DES Raman signal to that of the matrix. This is consistent with the fact that at this initial time DES is expected to be mainly distributed on the sample surface. Differently from what is observed in the drop case, here the DES Raman bands are visible only up to 200 µm of defocusing micro-SORS distance, and this is related to the lower amount of DES on the surface. Moreover, in the last steps of defocusing micro-SORS, a 1009 cm^{-1} Raman band is visible. This band referred to gypsum, emerges from the preparation layer. At t_1, the imaged spectrum showed an even weaker 716 cm^{-1} DES Raman band compared to t_0, and its 999 cm^{-1} band is overlapped by gypsum. The 716 cm^{-1} band can be monitored up to 100 µm of defocusing micro-SORS, and the study of DES diffusion is therefore severely limited. The ratio plot in Figure 4.16 displays that at t_1 lower DES/Red ochre values are obtained, and this is related to the absorption of the solvent.

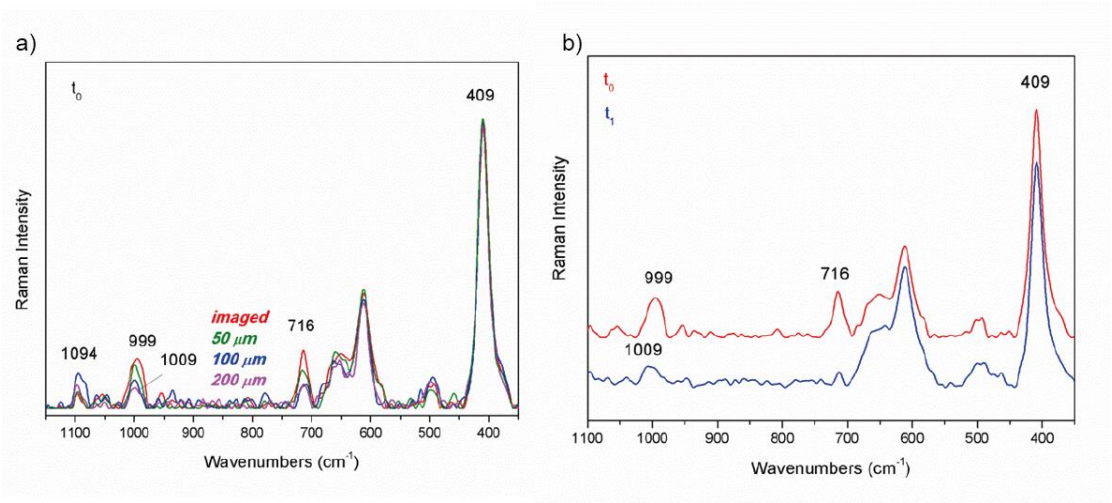

Figure 4.15 a) Micro-SORS sequence acquired at t_0 (started a few seconds after the application of DES drop on the painted mock-up), normalized to the red ochre signal at 409 cm^{-1}; The micro-SORS steps are indicated with colored values from imaged position to 200 µm; b) Raman spectra acquired at t_0 and t_1 at imaged position of the painted mock-up, normalized to the red ochre signal at 409 cm^{-1}

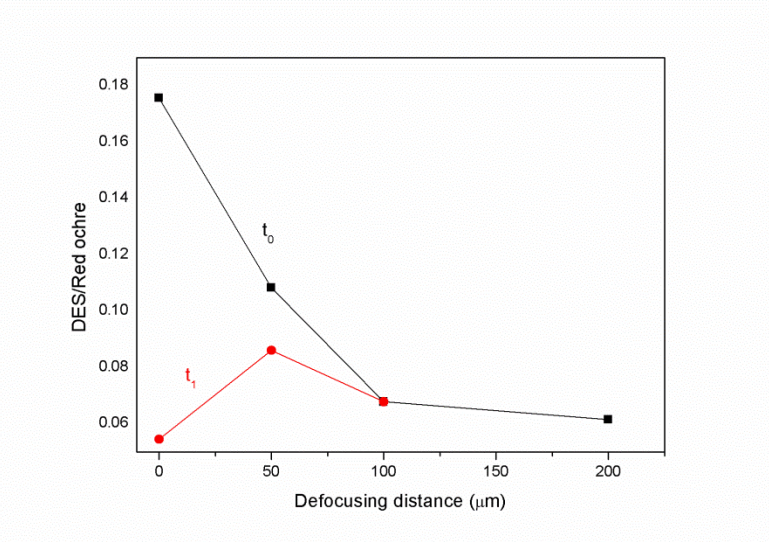

Figure 4.16 DES/ Red Ochre ratios of defocusing micro-SORS sequences acquired at t_0 and t_1

4.5.1.3 DES agar gel cleaning

Cleaning method was implemented by applying DES-agar gel directly on the samples surface for 5 min, then removed the gel and cleaned with 2 dry cotton swabs. In this research, double times cleaning, totally 10 min treatment with dry cotton swabs were performed due to there is no DES signal was detected after the first 5 min cleaning. After the gel application, at t_0, the intensity of the DES 716 cm^{-1} Raman band is very weak and the 999 cm^{-1} Raman band is obscured by the 1009 cm^{-1} band of gypsum (preparation layer). When normalized to the red ochre at 409 cm^{-1}, the DES Raman band showed a progressive decrease from the surface up to 200 μm (Figure 4.17a); after this distance it was not visible anymore. At t_1, a very low DES band (716 cm^{-1}) can be distinguished only at imaged position (Figure 4.17b), whereas in the defocused spectra the Raman band cannot be distinguished anymore. In this case, the ratio values were not calculated due to the very low Raman band of DES.

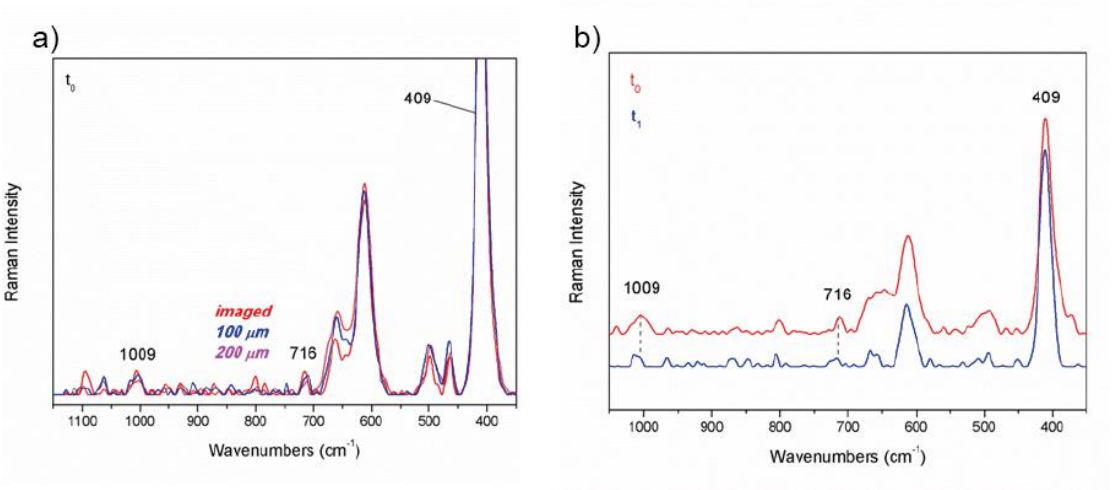

Figure 4.17 a) Micro-SORS sequence acquired at t_0 (started a few seconds after the application of DES drop on the painted mock-up), normalized to the red ochre signal at 409 cm^{-1}; The micro-SORS steps are indicated with colored values from imaged position to 200 μm; b) Raman spectra acquired at t_0 and t_1 at imaged position of the painted mock-up, normalized to the red ochre signal at 409 cm^{-1}

4.5.2 Discussion

In Figure 4.18, the conventional Raman spectra obtained at t_0 and t_1 in the three cases including drop of DES, DES cotton swab cleaning and DES-Agar gel cleaning, were compared to highlight the different intensity of DES Raman bands, related to the different amount of the solvent on the sample surface in the three situations: at t_0 (Figure 4.18a) the DES drop provides the most intense DES bands; between the two cleaning techniques, the Agar gel cleaning provides a lower amount of solvent residues on the surface. At t_1 (Figure 4.18b), the DES Raman band (716 cm^{-1}) is very low and the intensity of this band is similar in the spectra obtained in the three situations. This implies that, regardless to the initial amount of DES present on the sample surface, after the absorption process, the DES residues on the surface is barely detectable. Moreover, the very low intensity of the Raman band of DES at t_1 does not permit an exhaustive study of DES diffusion under the paint layer.

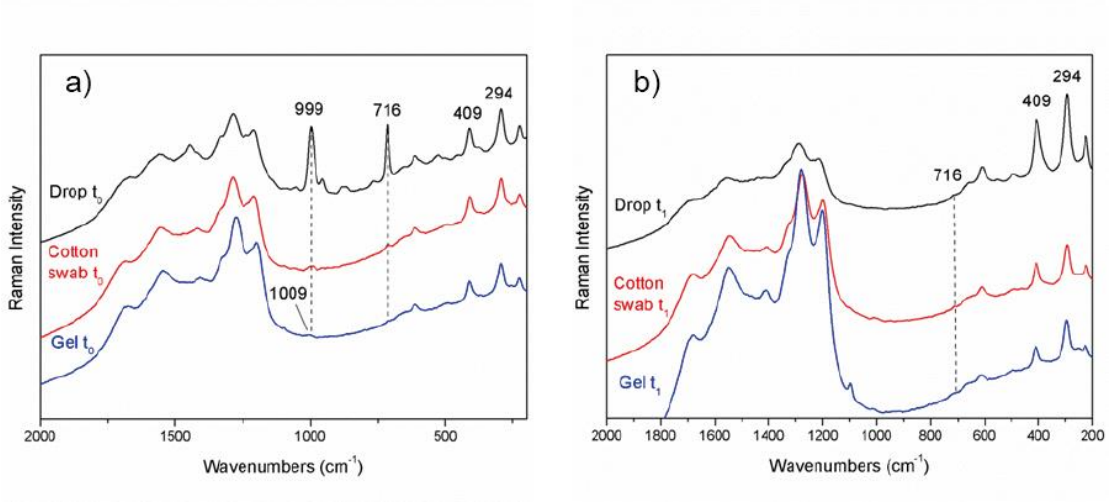

Figure 4.18 a) Conventional Raman spectra obtained at t_0 and b) at t_1 after the drop application, the cleaning with the cotton swab and with the Agar gel

Chapter 5 Conclusion

Varnishes are widely applied for protection of artworks against dirt and mechanical damage, in the meantime, achieving the proper color saturation and gloss appearance. Various varnishes including nature produced and synthetic resins have been used in different periods. However the varnishes are the most vulnerable parts, due to they are directly exposed to the environment. Changes over time, varnishes undergo various aging processes, mainly oxidation, cross-linking, polymerization, degradation and yellowing. Degraded varnishes are usually removed with rather polar solvents, which have significant potential to damage the artworks by swelling and leaching in particular painting artworks. Since 1980s, aqueous gels were introduced for cleaning purpose in conservation field in order to retain the liquid cleaning agents and better control of the cleaning. As a result, many efforts have been focus on developing new gels cleaning system which together with different solvents, enzymes, micelles and surfactants, the advanced gels have been developed with high rigid and viscosity physical property, and showed advantages in easy operation and peelable, they can overcome the serious gel residues problem which widely present in the initial aqueous gels. From the species of cross-link, the gels could be divided into physical and chemical gels, the physical gels were usually developed by weak interaction driving force including hydrophobic, electrostatic, Van der Waals interactions and hydrogen bonds which formed between polymer chains and solvents. The chemical gels were cross-linked by covalent bands which provided strong 3D networks, thus showed outstanding performance in solvents retention and mechanical properties. After years of accumulation, gels were gradually mature, and become a widely recognized method for cleaning some delicate artworks. However, the cleaning always carries on indoor environment with long time handling chemicals, in this case, toxicity issue attracts more and more attentions, including but not limited to reduce environment pollution, protect restorers' health and safe to the artworks. However, up to now, the full green strategies for cleaning are still too less after the investigation. Recently, we have been reported biodegradable PHB based gels with GVL as solvent, for the removal of terpenic and synthetic varnishes from oil and water sensitive egg tempera paintings. This kind of fully green organogel can overcome the soft and sticky drawbacks of aqueous gels, enable readily peel off and leave negligible residues on the surface after the application.

In this thesis, three kind of new advanced green organogels were developed for various aged varnishes removal, including a ternary gel (PHB-DMC/BD) consists of PHB, dimethyl carbonate and biodiesel, the cleaning tests both evaluated on the mock-up prepared by the restorers of Opificio delle Pietre Dure (Florence) and the ancient precious indoor sculpture of Pulpito della Passione (1460 A.C.). FTIR and GC-MS analyses were implemented to investigate the efficiency of the gel and evaluate BD residues after the treatment. The results showed the good performance of the PHB-DMC/BD gel for the removal of fresh and aged beeswax coatings, avoiding problems related to solvent residues and ensuring safety for the works, as well the operators and the environment.

Electrospun fabrication tissue has been the first attempt to couple with organogel for cleaning purpose in cultural heritage field. The combined gels displayed both the advantages of nanometer scale tissue and organogel, resulting in a significant enhance of mechanical bending property and surface microstructures. The results of cleaning tests indicated the combined gels have better cleaning efficiency than uncombined gel, and negligible residual was detected after cleaning treatments. These results would seem to suggest that the combined gels have higher contact surface and spaces promote the release of solvent and the loads of dammar during cleaning. As a result, the new developed electrospun combined organogels can provide helpful guidelines for the design of advance gel cleaning system.

Deep eutectic solvent (DES) is a kind of eco-friendly solvent composed of a salt with a hydrogen bond donor at room temperature that has a lower melting point than either of the individual components. It has been demonstrated the efficiency for the extraction of proteins, in this cases, we developed a new green gel containing DES and agar (DES agar gel) for the removal of proteinaceous coating from paintings. DES agar gel has good mechanical property with high viscosity which easily peels off after treatment. The cleaning efficiency of DES-agar gel was tested on glue and whole egg coating painting mock-up, after DES-agar gel application, residues were further cleaned by a 10 s application with EtOH-H_2O agar gel, FTIR and optical microscope analyses showed the gel enable to remove the proteinaceous coating without leaving residues.

The development of multiscale and multitechnique nondestructive approaches for monitoring surface and sub layer properties of artworks after solvent or gel treatments are useful for assessing the composition and conservation state. These analyses also help to predict future

changes of the surface and to choose the best preservation conditions or the right restoration treatments. The diffusion of the solvent agents on the painting substance could induce the damage of leaching or swelling the painting layer, even lead to the complex reaction between different compositions. In this case, the penetration depth and distribution of the cleaning agents after the conservation treatments are important factors to assess the extent of the change processes and the efficacy of a cleaning system. In this research, the defocusing micro-SORS measurement as a valuable alternative non-destructive method was acquired on an egg tempera mock-up after DES drop, DES wet cotton swabs and DES-agar gel treatments. The 716 cm^{-1} Raman band of DES and the 409 cm^{-1} band of red ochre were used for the calculation of the solvent-substrate ratio, due to the intensity and without overlap with other components. As a result, the gradual increase of the defocusing micro-SORS distance leads to a rapid relative decrease of DES Raman signal, demonstrating the DES is mainly distributed on the sample surface, and always more than sub-layer. Among the different treatments, the DES-agar gel cleaning provides the lowest amount of solvent residues on the surface in the initial time, but after the absorption process, the DES residues on the surface are too few and barely detectable.

In the future work, the real case studies should be performed to evaluate the cleaning efficiency of electrospinning mat combined gels and DES-agar gel, the real case studies could reflect the gels capacity for the removal of aged varnishes and determine whether it is suitable for cleaning valuable paintings.

Bibliography

[1] Chelazzi D, Giorgi R, Baglioni P. Microemulsions, Micelles, and Functional Gels: How Colloids and Soft Matter Preserve Works of Art. *Angew Chemie-Int Ed*. 2018;57(25):7296-7303.

[2] Samor ìC, Galletti P, Giorgini L, Mazzeo R, Mazzocchetti L, Prati S, Sciutto G, Volpi F, Tagliavini E. The Green Attitude in Art Conservation: Polyhydroxybutyrate-based Gels for the Cleaning of Oil Paintings. *ChemistrySelect*. 2016;1(15):4502-4508.

[3] Prati S, Volpi F, Fontana R, Galletti P, Giorgini L, Mazzeo R, Mazzocchetti L, Samor ì C, Sciutto G, Tagliavini E. Sustainability in art conservation: A novel bio-based organogel for the cleaning of water sensitive works of art. *Pure Appl Chem*. 2018;90(2):239-251.

[4] Ramakrishna S, Jose R, Archana PS, Nair AS, Balamurugan R, Venugopal J, Teo WE. Science and engineering of electrospun nanofibers for advances in clean energy , water filtration , and regenerative medicine. *J. Mater. Sci.* 2010;45(23):6283-6312.

[5] Conti C, Botteon A, Colombo C, Realini M, Matousek P. Investigation of Heterogeneous Painted Systems by Micro-Spatially Offset Raman Spectroscopy. *Anal Chem*. 2017;89(21):11476-11483.

[6] Hackney S. The Art and Science of Cleaning Paintings. Smithsonian Institution. 2012;(November 2010).

[7] Stulik D, Miller D, Khanjian H, Khandekar N, Wolbers R, Carlson J, Petersen WC. *Solvent Gels for the Cleaning of Works of Art: The Residue Question*. 2004.

[8] Pereira MC, Sandu ICA, S MH De. Ancient ‘gilded’ art objects from European cultural heritage: a review on different scales of characterization. *Interface Anal*. 2011;43(8): 1134-1151.

[9] Glanville H. Varnish, grounds, viewing distance, and lighting: some notes on seventeenth-century Italian painting technique. 1995.

[10] Wallert A, Hermens E, Peek M. *Historical Painting Techniques, Materials, and Studio Practice: Preprints of a Symposium, University of Leiden, the Netherlands, 26-29 June 1995*. Getty Publications; 1995.

[11] Langenheim JH. *Plant Resins: Chemistry, Evolution, Ecology, and Ethnobotany*.

Oregon, US: Timber Press; 2003.

[12] Maclaren N, Werner A, Maclaren N, Werner A. Some Factual Observations about Varnishes and Glazes. *The Burlington Magazine*, 1950;92(568):189-192.

[13] De la Rie ER. Old master paintings: a study of the varnish problem. *Anal Chem*. 1989;61(21):1228A-1240A.

[14] Pollard AM, Heron C. *Archaeological chemistry*, 239-70. 1996.

[15] Stout SA. Resin-derived hydrocarbons in fresh and fossil dammar resins and Miocene rocks and oils in the Mahakam Delta, Indonesia. *Amber, resinite, Foss resins*. 1995;617:43-75.

[16] Van der Doelen GA, van den Berg KJ, Boon JJ. Comparative chromatographic and mass-spectrometric studies of triterpenoid varnishes: fresh material and aged samples from paintings. *Stud Conserv*. 1998;43(4):249-264.

[17] Colombini MP, Modugno F, Giannarelli S, Fuoco R. GC-MS characterization of paint varnishes. *Microchem J*. 2000;67(1-3):385-396.

[18] White R. The application of gas-chromatography to the identification of waxes. The application of gas-chromatography to the identification of waxes. *Stud. Conserv*. 1978; 23(2):57-68.

[19] Kosec T, Legat A, Miloev I. The comparison of organic protective layers on bronze and copper. *Prog Org Coatings*. 2010;69(2):199-206.

[20] Le Roux JH. Fischer-tropsch waxes. II. Crystallinity and physical properties. *J Appl Chem*. 1969;19(3):86-88.

[21] Colinart S, Drilhon F, Scherf G, Gaborit J-R, Ligot J. *Sculptures En Cire de l'ancienne Egypte à l'art Abs Trai*. 1987.

[22] Swartz N, Clare T L. On the protective nature of wax coatings for culturally significant outdoor metalworks: microstructural flaws, oxidative changes, and barrier properties. *J Am Inst Conserv*. 2015; 54(3):181-201.

[23] Olszewski EJ, Armenini GB. *On the True Precepts of the Art of Painting*. Franklin; 1977.

[24] Harley R D. Portrait painting in England: studies in the technical literature before 1700. 1982.

[25] Langenheim JH. Plant resins. *Am Sci*. 1990;78(1):16-24.

[26] Mills JS, White R. Natural resins of art and archaeology their sources, chemistry, and identification. *Stud Conserv*. 1977;22(1):12-31.

[27] Mayer L, Myers G. A note on the early use of dammar varnish. *Stud. Conserv.* 2002; 47(2):134-138.

[28] Colombini MP, Modugno F. *Organic Mass Spectrometry in Art and Archaeology*. John Wiley & Sons; 2009.

[29] Van der Doelen GA. *Molecular Studies of Fresh and Aged Triterpenoid Varnishes*. Universiteit van Amsterdam; 1999.

[30] Dietemann P, Ka M, Zumbu S, Knochenmuss R, Wu S, Zenobi R. A Mass Spectrometry and Electron Paramagnetic Resonance Study of Photochemical and Thermal Aging of Triterpenoid Varnishes. *Anal. Chem.* 2001;73(9):2087-2096.

[31] Vahur S, Teearu A, Haljasorg T, Burk P, Leito I. Analysis of dammar resin with MALDI-FT-ICR- MS and APCI-FT-ICR-MS. *J. Mass Spectrom.* 2012;47(3):392-409.

[32] Horie C V. Materials for conservation: organic consolidants. *Adhes Coatings, London*. 1987.

[33] Feller RL. New solvent-type varnishes' in Recent Advances in Conservation, ed. G. THOMSON. 1963.

[34] Gettens RJ, Stout GL. *Painting Materials: A Short Encyclopaedia*. Courier Corporation; 1966.

[35] Lawman SJ. Optical and material properties of varnishes for paintings. Nottingham Trent University. 2011.

[36] Routledge V. The development of MS2A reduced ketone resin in painting conservation. 2000.

[37] Leitgeb R, Hitzenberger CK, Fercher AF. Performance of fourier domain vs. time domain optical coherence tomography. *Opt. Express.* 2003;11(8):889-894.

[38] Rie ER De, Lomax SQ, Palmer M, Glinsman LD, Maines CA. An investigation of the photochemical stability of urea-aldehyde resin retouching paints: removability tests and colour spectroscopy. *Stud Conserv*. 2000; 45(sup1):51-59.

[39] Turri B, Vicini S, Margutti S, Pedemonte E. Calorimetric analysis of the polymerisation process of linseed oil. *J. Therm. Anal. Calorim.* 2001;66:343-348.

[40] Sutherland KR. *Solvent Extractable Components of Oil Paint Films*. FOM Institute for

Atomic and Molecular Physics Amsterdam; 2001.

[41] Echard JP, Vaïedelich S. De la peinture de chevalet à l'instrument de musique: vernis, liants et couleurs. *Cité la musique, Paris*. 2008;104-113.

[42] Tirat S, Degano I, Echard J, Derieux A, Tenorio A, Marie A, Serfaty S, Huerou J. Historical linseed oil/colophony varnishes formulations: Study of their molecular composition with micro-chemical chromatographic techniques. *Microchem J*. 2016;126:200-213.

[43] Lehninger AL, Nelson DL, Cox MM, Cox MM. *Lehninger Principles of Biochemistry*. Macmillan; 2005.

[44] Creighton TE. *Proteins: Structures and Molecular Properties*. Macmillan; 1993.

[45] McWilliams M. *Foods: Experimental Perspectives.* MacMillian Publishing Company; 1989.

[46] Campbell L, Raikos V, Euston SR. Review Modification of functional properties of egg-white proteins. *Food/Nahrung.* 2003;47(6):369-376.

[47] McCully KA, Mok C-C, Common RH. Paper Elegtrophoretic Characterization of Proteins and Lipoproteins of Hen's Egg Yolk. *Can J Biochem Physiol*. 1962;40(7):937-952.

[48] Harrison SM, Kaml I, Prokoratova V, Mazanek M, Kenndler E. Animal glues in mixtures of natural binding media used in artistic and historic objects: identification by capillary zone electrophoresis. *Anal. Bioanal. Chem.* 2005;382(7):1520-1526.

[49] Schellmann NC, Schellmann NC. Animal glues: a review of their key properties relevant to conservation. *Stud Conserv*. 2007;52(sup1): 55-66.

[50] Doerner M. Malmaterial und seine Verwendung im Bilde. The Materials of an Artist and Their Use in Painting. *Repr*. 1938.

[51] Valencia UP De, Gritt S, Laudenbacher K, Hackney S. New Insights into the Cleaning of Paintings International Conference. 2010;(3).

[52] Ruhemann H, Plesters J. *The Cleaning of Paintings. Problems and Potentialities*. 1968.

[53] Teas JP. Graphic analysis of resin solubilities. *J Paint Technol*. 1968;40(516):19-25.

[54] Hedley G. Solubility parameters and varnish removal: a survey. *Conserv*. 1980;4(1):12-18.

[55] Signorini E. Surface Cleaning of Paintings and Polychrome Objects in Italy: The Last 15 Years. In: *New Insights into the Cleaning of Paintings: Proceedings from the Cleaning 2010 International Conference, Universidad Politecnica de Valencia and Museum Conservation Institute*. Smithsonian Institution; 2013.

[56] Phenix A, Sutherland K. The cleaning of paintings: effects of organic solvents on oil paint films. *Stud Conserv*. 2001;46(sup1):47-60.

[57] Stolow N. The action of solvents on drying-oil films: parts i and ii. *J Oil Colour Chem Assoc*. 1957;40(5-6):377-402.

[58] Tsang AJ, Erhardt D, Tsang J, Erhardt D. Current Research on the Effects of Solvents and Gelled and Aqueous Cleaning Systems on Oil Paint Films. *J Am Inst Conserv*. 1992;31(1):87-94.

[59] Noble P, Boon JJ, Parkin HM. Metal soap degradation of oil paintings: aggregates, increased transparency and efflorescence. In: *AIC Paintings Specialty Group Postprints, Providence, Rhode Island, June 16-19, 2006*. Vol 19.;2007:1-15.

[60] Sutherland K. Measurements of Solvent Cleaning Effects on Oil Paintings. *J Am Inst Conserv*. 2006;45(3):211-226.

[61] Casoli A, Berzioli M, Cremonesi P. The chemistry of egg binding medium and its interactions with organic solvents and water. In: *New Insights into the Cleaning of Paintings: Proceedings from the Cleaning 2010 International Conference, Universidad Politecnica de Valencia and Museum Conservation Institute*. Smithsonian Institution; 2013.

[62] Ploeger R, Chiantore O. Characterization and Stability Issues of Artists' Alkyd Paints. Smithsonian Institution. 2012;(November 2010).

[63] Zumbühl S, Ferreira ESB, Scherrer NC. The Nonideal Action of Binary Solvent Mixtures on Oil and Alkyd Paint: Influence of Selective Solvation and Cavitation Energy. Smithsonian Institution. 2012.

[64] Schawlow AL. Lasers. *Science*. 1965;149(3679):13-22.

[65] Asmus JF, Murphy CG, Munk WH. Studies on the interaction of laser radiation with art artifacts. In: *Developments in Laser Technology II*. Vol 41. *International Society for Optics and Photonics*. 1974;19-30.

[66] Bracco P, Lanterna G, Matteini M, Nakahara K, Sartiani O. Er: YAG laser: an

innovative tool for controlled cleaning of old paintings: testing and evaluation. *J. Cult. Herit*. 2003;4:202-208.

[67] Georgiou S, Zafiropulos V, Anglos D, Balas C, Tornari V, Fotakis C. Excimer laser restoration of painted artworks: procedures, mechanisms and effects. *Appl. Surf. Sci*. 1998;127:738-745.

[68] Pouli P, Selimis A, Georgiou S, Fotakis C. Recent studies of laser science in paintings conservation and research. *Acc Chem Res*. 2010;43(6):771-781.

[69] Bordalo R, Morais PJ, Gouveia H, Young C. Laser Cleaning of Easel Paintings : An Overview. *Laser Chemistry*. 2006;2006.

[70] Scholten JH, Schipper DA. Advanced workstation for controlled laser cleaning of paintings. Optics and Lasers in Biomedicine and Culture. Springer, Berlin, Heidelberg, 2000;183-187.

[71] Madden O, Paul TJ, Trust G, Abraham M. The Effects of Laser Radiation on Adhesives , Consolidants , and Varnishes. Lasers in the Conservation of Artworks. Springer, Berlin, Heidelberg, 2005;247-254.

[72] Cooper M. *Laser Cleaning in Conservation: An Introduction*. Butterworth-Heinemann Oxford; 1998.

[73] Zafiropulos V. Laser ablation in cleaning of artworks. In: *Laser Cleaning*. World Scientific. 2002;343-392.

[74] Castillejo M, Martín M, Oujja M, Silva D, Torres A, Manousaki A, Zafiropulos V, Brink O, Heeren R, Teule R, Silva A, Gouveia H. Analytical Study of the Chemical and Physical Changes Induced by KrF Laser Cleaning of Tempera Paints. *Anal. Chem.* 2002;74(18):4662-4671.

[75] Oujja M, García A, Romero C, de Aldana JRV, Moreno P, Castillejo M. UV laser removal of varnish on tempera paints with nanosecond and femtosecond pulses. *Phys Chem Chem Phys*. 2011;13(10):4625-4631.

[76] Hildenhagen J, Dickmann K. Nd: YAG laser with wavelengths from IR to Uv (ω, 2 ω, 3ω , 4ω) and corresponding applications in conservation of various artworks. *J. Cult. Herit*. 2003;4:174-178.

[77] Pouli P, Emmony DC, Madden CE, Sutherland I. Studies towards a thorough understanding of the laser-induced discoloration mechanisms of medieval pigments. *J.*

Cult. Herit. 2003;4:271-275.

[78] Siano S, Agresti J, Cacciari I, Ciofini D, Mascalchi M, Osticioli I, Mencaglia AA. Laser cleaning in conservation of stone, metal, and painted artifacts: state of the art and new insights on the use of the Nd: YAG lasers. *Appl. Phys. A.* 2012;106(2): 419-446.

[79] Cruz A De, Wolbarsht ML, Hauger SA. Laser removal of contaminants from painted surfaces. *J. Cult. Herit*. 2000;1:173-180.

[80] Perla M, Andreotti A, Lanterna G, Rizzi M. A novel approach for high selective micro-sampling of organic painting materials by Er: YAG laser ablation. *J. Cult. Herit*. 2003;4:355-361.

[81] Carretti E, Salvadori B, Baglioni P, Dei L. Microemulsions and micellar solutions for cleaning wall painting surfaces. *Stud Conserv*. 2005;50(2):128-136.

[82] Baglioni M, Rengstl D, Berti D, Bonini M, Giorgi R, Baglioni P. Removal of acrylic coatings from works of art by means of nanofluids : understanding the mechanism at the nanoscale. *Nanoscale*. 2010;2(9):1723-1732.

[83] Baglioni M, Jàidar Y, Berti D, Giorgi R, Keiderling U, Baglioni P. Journal of Colloid and Interface Science An amine-oxide surfactant-based microemulsion for the cleaning of works of art. *J Colloid Interface Sci*. 2015;440:204-210.

[84] Ramírez J L, Santana M A, Galindo-Castro I, Gonzalez A. The role of biotechnology in art preservation. *Trends Biotechnol.* 2005;23(12):584-588.

[85] Koshland Jr DE. The key-lock theory and the induced fit theory. *Angew Chemie Int Ed English*. 1995;33(23-24):2375-2378.

[86] Cremonesi P. Rigid Gels and Enzyme Cleaning. New Insights into the Cleaning of Paintings: Proceedings from the Cleaning 2010 International Conference, Universidad Politecnica de Valencia and Museum Conservation Institute. Smithsonian Institution, 2013.

[87] Bellucci R, Cremonesi P, Pignagnoli G. A preliminary note on the use of enzymes in conservation: the removal of aged acrylic resin coatings with lipase. *Stud Conserv*. 1999;44(4):278-281.

[88] Romão PMS, Alarcão AM, Viana CAN. Human saliva as a cleaning agent for dirty surfaces. *Stud Conserv*. 1990;35(3):153-155.

[89] Andrews TM, Andrews WW, Baker C. An investigation into the removal of enzymes from paper following conservation treatment. *J Am Inst Conserv*. 1992;31(3):313-323.

[90] Ramírez JL, Santana MA, Galindo-Castro I, Gonzalez A. The role of biotechnology in art preservation. *TRENDS Biotechnol*. 2005;23(12):584-588.

[91] Gomes V, Dionísio A, Pozo-antonio JS. Progress in Organic Coatings Conservation strategies against graffiti vandalism on Cultural Heritage stones : Protective coatings and cleaning methods. *Prog Org Coatings*. 2017;113(June):90-109.

[92] Caselli E, Pancaldi S, Baldisserotto C, Petrucci F, Impallaria A, Volpe L, D'Accolti M, Soffritti I, Coccagna M, Sassu G, Bevilacqua F, Volta A, Bisi M, Lanzoni L, Mazzacane A. Characterization of biodegradation in a 17 th century easel painting and potential for a biological approach. *PLoS One*. 2018;13(12):1-18.

[93] Ranalli G, Alfano G, Belli C, Lustrato G, Colombini MP, Bonaduce I, Zanardini E, Abbruscato P, Cappitelli F, Sorlini C. Biotechnology applied to cultural heritage : biorestoration of frescoes using viable bacterial cells and enzymes. *J. Appl. Microbiol.* 2005;98(1):73-83.

[94] Ranalli G, Zanardini E, Rampazzi L, Corti C, Andreotti A, Colombini MP, Roig P, Lustrato G, Giantomassi C, Zari D, Virilli P. Editor's Choice Onsite advanced biocleaning system for historical wall. *J. Appl. Microbiol.* 2019;126(6):1785-1796.

[95] Baglioni P, Bonelli N, Chelazzi D, Chevalier A, Dei L, Domingues J, Fratini E, Giorgi R, Martin M. Organogel formulations for the cleaning of easel paintings. *Appl Phys A*. 2015;121(3):845-856.

[96] Burnstock A, White R. A preliminary assessment of the agingidegradation of Ethomeen c-12 residues from solvent gel formulations and their potential for inducing changes in resinous paint media. *Stud Conserv*. 2000;45(sup1):34-38.

[97] Pizzorusso G, Fratini E, Eiblmeier J, Giorgi R, Chelazzi D, Chevalier A, Baglioni P. Physicochemical Characterization of Acrylamide/Bisacrylamide Hydrogels and Their Application for the Conservation of Easel Paintings. *Langmuir*. 2012;28(8):3952-3961.

[98] Domingues JAL, Bonelli N, Giorgi R, Fratini E, Gorel F, Baglioni P. Innovative Hydrogels Based on Semi-Interpenetrating p(HEMA)/PVP Networks for the Cleaning of Water-Sensitive Cultural Heritage Artifacts. Langmuir, 2013;29(8):2746-2755.

[99] Carretti E, Fratini E, Berti D, Dei L, Baglioni P. Nanoscience for Art Conservation: Oil-in-Water Microemulsions Embedded in a Polymeric Network for the Cleaning of Works of Art . Angew. Chem.-Int. Edit., 2009;48(47):8966-8969.

[100] Natali I, Carretti E, Angelova L, Baglioni P, Weiss RG, Dei L. Structural and Mechanical Properties of "Peelable" Organoaqueous Dispersions with Partially Hydrolyzed Poly (vinyl acetate)-Borate Networks: Applications to Cleaning Painted Surfaces. Langmuir, 2011;27(21):13226-13235.

[101] Baglioni M, Domingues JAL, Carretti E, Fratini E, Chelazzi D, Giorgi R, Baglioni P. Complex Fluids Confined into Semi-interpenetrated Chemical Hydrogels for the Cleaning of Classic Art omplex Fluids Confined into Se*ACS Appl Mater Interfaces*. 2018;10:19162-19172.

[102] Domingues J, Bonelli N, Giorgi R. Chemical semi-IPN hydrogels for the removal of adhesives from canvas paintings. *Applied Physics A.* 2014;114(3):705-710.

[103] Bonelli N, Montis C, Mirabile A, Berti D, Baglioni P. Restoration of paper artworks with microemulsions confined in hydrogels for safe and efficient removal of adhesive tapes. *PNAS.* 2018;115(23):5932-5937.

[104] Bonelli N, Poggi G, Chelazzi D, Giorgi R, Baglioni P. Poly-(vinyl alcohol)/poly-(vinyl pyrrolidone) hydrogels for the cleaning of art. *J Colloid Interface Sci*. 2019;536: 339-348.

[105] Khandekar N. Asurvey of the conservation literature relating to the development of aqueous gel cleaning on painted and varnished surfaces. *Stud Conserv*. 2000;45(1):10-20.

[106] Sutherland K. Measurements of solvent cleaning effects on oil paintings. *J Am Inst Conserv*. 2006;45(3):211-226.

[107] Casoli A, Diego Z Di, Isca C. Cleaning painted surfaces: evaluation of leaching phenomenon induced by solvents applied for the removal of gel residues. *Environ. Sci. Pollut. Res.* 2014;21(23):13252-13263.

[108] Angelova L V, Ormsby B, Richardson E. Diffusion of water from a range of conservation treatment gels into paint films studied by unilateral NMR Part I : Acrylic emulsion paint. *Microchem J*. 2016;124:311-320.

[109] Di Tullio V, Sciutto G, Proietti N, Prati S, Mazzeo R, Colombo C, Cantisani E, Rom è

V, Rigaglia D, Capitani D. ^{1}H NMR depth profiles combined with portable and micro-analytical techniques for evaluating cleaning methods and identifying original, non-original, and degraded materials of a 16thcentury Italian wall painting. *Microchem J*. 2018;141:40-50.

[110] Raudino M, Giamblanco N, Montis C, Berti D, Marletta G, Baglioni P. Probing the Cleaning of Polymeric Coatings by Nanostructured Fluids : A QCM-D Study. *Langmuir*. 2017;33(23):5675-5684.

[111] Pietropolli A. Salute e restauro: utilizzo dei prodotti chimici nel restauro: aspetti nocivi per la salute degli operatori: situazione attuale e possibili alternative: 30 novembre 1999, Dolo, Villa Ferretti Angeli. 2000.

[112] Cremonesi P. DEA, la sorella cattiva della TEA. *Progett restauro*. 2008;13(47):2-3.

[113] Lagalante AF, Hall RL, Bruno TJ. Kamlet-Taft Solvatochromic Parameters of the Sub- and Supercritical Fluorinated Ethane Solvents. *J. Phys. Chem. B.* 1998;5647 (98):6601-6604.

[114] Jessop PG. Searching for green solvents. *Green Chem.* 2011;13(6): 1391-1398.

[115] Mendoza AR, Corvo F. Outdoor and indoor atmospheric corrosion of non-ferrous metals. *Corrosion Sci*. 2000;42:1123-1147.

[116] Ćurković H, Kosec T, MaruŠić K, Legat A. An electrochemical impedance study of the corrosion protection of artificially formed patinas on recent bronze. *Electrochim. Acta*. 2012;83:28-39.

[117] Scott DA. Copper and bronze in art: corrosion, colorants, conservation. Getty publications; 2012.

[118] Otieno-Alego V, Hallam D, Viduka A, Heath G, Creagh D. Electrochemical impedance studies of the corrosion resistance of wax coatings on artificially patinated bronze. In: *Conférence Internationale Sur La Conservation Des Métaux*. 1998;315-319.

[119] Bierwagen G, Shedlosky TJ, Stanek K. Developing and testing a new generation of protective coatings for outdoor bronze sculpture. *Prog Org Coatings*. 2003;48 (2-4):289-296.

[120] Couture-Rigert DE, Sirois PJ, Moffatt EA. An investigation into the cause of corrosion on indoor bronze sculpture. *Stud Conserv*. 2012;57(3):142-163.

[121] Baglioni P, Carretti E, Chelazzi D. Nanomaterials in art conservation. *Nat Publ Gr*. 2015;10(4):287-290.

[122] Frank G. Matero AAT. Cleaning, Iron Stain Removal, and Surface Repair of Architectural Marble and Crystalline Limestone: The Metropolitan Club. *J Am Inst Conserv*. 1995;34:49-68.

[123] Phenix A. The Swelling of Artists' Paints in Organic Solvents. Part 1, a Simple Method for Measuring the In-Plane Swelling of Unsupported Paint Films. *J Am Inst Conserv*. 2002;41(1):43.

[124] Michalski S. A Physical Model of The Cleaning of Oil Paint. *Stud Conserv*. 1990;35:85-92.

[125] Phenix A. Effects of organic solvents on artists' oil paint films: swelling. *Smithson Contrib to Museum Conserv*. 2013;3:69-76.

[126] Chelazzi D, Giorgi R, Baglioni P. Microemulsions , Micelles , and Functional Gels : How Colloids and Soft Matter Preserve Works of Art. *Angew. Chem.-Int. Edit.* 2018;57(25):7296-7303.

[127] Stulik D, Miller D, Khanjian H, Carlson J, Khandekar N, Wolbers R. *Solvent Gels for the Cleaning of Works of Art: The Residue Question*. Getty Publications; 2004.

[128] Baglioni P, Berti D, Bonini M, Carretti E, Dei L, Fratini E, Giorgi R. Micelle, microemulsions, and gels for the conservation of cultural heritage. *Adv Colloid Interface Sci*. 2014;205:361-371.

[129] Parisi EI, Bonelli N, Carretti E, Giorgi R, Ingo GM. Invited paper Film forming PVA-based cleaning systems for the removal of corrosion products from historical bronzes. *Pure Appl. Chem.* 2018;90(3):507-522.

[130] Bucci DZ, Tavares LBB, Sell I. PHB packaging for the storage of food products. *Polym Test*. 2005;24(5):564-571.

[131] Meher LC, Vidya Sagar D, Naik SN. Technical aspects of biodiesel production by transesterification-A review. *Renew Sustain Energy Rev*. 2006;10(3):248-268.

[132] Samorì C, Basaglia M, Casella S, Favaro L, Galletti P, Giorgini L, Marchi D, Mazzocchetti L, Torri C, Tagliavini E. Dimethyl carbonate and switchable anionic surfactants: two effective tools for the extraction of polyhydroxyalkanoates from microbial biomass. *Green Chem*. 2015;17(2):1047-1056.

[133] Samor ìC, Abbondanzi F, Galletti P, Giorgini L, Mazzocchetti L, Torri C, Tagliavini E. Extraction of polyhydroxyalkanoates from mixed microbial cultures: impact on polymer quality and recovery. *Bioresour Technol*. 2015;189:195-202.

[134] Agarwal S, Wendorff JH, Greiner A. Use of electrospinning technique for biomedical applications. *Polymer (Guildf)*. 2008;49(26):5603-5621.

[135] Dai H, Gong J, Kim H, Lee D. A novel method for preparing ultra-fine alumina-borate oxide fibres via an electrospinning technique. *Nanotechnology*. 2002;13(5):14-18.

[136] Li Q, Xi S, Zhang X. Conservation of paper relics by electrospun PVDF fiber membranes. *J Cult Herit*. 2014;15(4):359-364.

[137] Matthews JA, Wnek GE, Simpson DG, Bowlin GL. Electrospinning of Collagen Nanofibers. *Biomacromolecules.* 2002;1(Iii):232-238.

[138] Azuma Y, Yoshie N, Sakurai M, Inoue Y, Ch ûj ô R. Thermal behaviour and miscibility of poly-(3-hydroxybutyrate)/poly-(vinyl alcohol) blends. *Polymer (Guildf)*. 1992;33(22): 4763-4767.

[139] Leo G, Cartechini L, Pucci P, Sgamellotti A, Marino G, Birolo L. Proteomic strategies for the identification of proteinaceous binders in paintings. *Anal. Bioanal. Chem.* 2009;395(7):2269-2280.

[140] Nevin A, Osticioli I, Anglos D, Burnstock A, Cather S, Castellucci E. Raman Spectra of Proteinaceous Materials Used in Paintings: A Multivariate Analytical Approach for Classification and Identification. *Anal. Chem.* 2007;79(16):6143-6151.

[141] Tai BH. Stradivari's Varnish: A Review of Scientific Findings-Part II. *J. Violin Soc. Am.* 2009;22:1-31.

[142] Casoli A, Berzioli M, Cremonesi P. The Chemistry of Egg Binding Medium and Its Interactions with Organic Solvents and Water. Smithsonian Institution, 2012; (November 2010).

[143] Smith EL, Abbott AP, Ryder KS. Deep Eutectic Solvents (DESs) and Their Applications. *Chem. Rev.* 2014;114(21):11060-11082.

[144] Ru ß C, K önig B. Low melting mixtures in organic synthesis-an alternative to ionic liquids? *Green Chem.* 2012;14(11):2969-2982.

[145] Phadtare SB, Shankarling GS. Halogenation reactions in biodegradable solvent: Efficient bromination of substituted 1-aminoanthra-9, 10-quinone in deep eutectic

solvent (choline chloride: urea). *Green Chem.* 2010;12(13):458-462.

[146] Pawar PM, Jarag KJ, Shankarling GS. Environmentally benign and energy efficient methodology for condensation: an interesting facet to the classical Perkin reaction. *Green Chem.* 2011;13(8):2130-2134.

[147] Gore S, Koenig B. Efficient synthesis of 3, 4-dihydropyrimidin-2-ones in low melting tartaric acid-urea mixtures. *Green Chem.* 2011;13(4):1009-1013.

[148] Zeng Q, Wang Y, Huang Y, Ding X, Chen J, Xu K. Deep eutectic solvents as novel extraction media for protein partitioning. *Analyst.* 2014;139(10):2565-2573.

[149] Gómez E, Cojocaru P, Magagnin L, Valles E. Electrodeposition of Co, Sm and SmCo from a Deep Eutectic Solvent. *J. Electroanal. Chem.* 2011;658(1-2):18-24.

[150] Serrano MC, Gutiérrez MC, Jiménez R, Ferrer ML, del Monte F. Synthesis of novel lidocaine-releasing poly-(diol-co-citrate) elastomers by using deep eutectic solvents. *Chem Commun.* 2012;48(4):579-581.

[151] Conti C, Colombo C, Realini M, Zerbi G. Subsurface Raman Analysis of Thin Painted Layers. *Appl. Spectrosc.* 2014;68(6):686-691.

[152] Conti C, Colombo C, Realini M, Matousek P. Subsurface analysis of painted sculptures and plasters using micrometre-scale spatially offset Raman spectroscopy (micro-SORS). *J Raman Spectrosc*. 2015;46(5):476-482.

[153] Conti C, Botteon A, Colombo C, Realini M, Matousek P. Investigation of Heterogeneous Painted Systems by Micro-Spatially. *Anal. Chem.* 2017;89(21): 11476-11483.

[154] Botteon A, Conti C, Realini M, Colombo C, Matousek P. Discovering Hidden Painted Images: Subsurface Imaging Using Microscale Spatially Offset Raman Spectroscopy. *Anal Chem*. 2017;89(1):792-798.

[155] Matousek P, Conti C, Realini M, Colombo C. Micro-scale spatially offset Raman spectroscopy for non-invasive subsurface analysis of turbid materials. *Analyst.* 2016;141(3):731-739.

[156] Conti C, Realini M, Colombo C, Matousek P. Comparison of key modalities of micro-scale spatially offset Raman spectroscopy. *Analyst*. 2015;140(24):8127-8133.

[157] Das BB, Liu F, Alfano RR. Time-resolved fluorescence and photon migration studies in biomedical and model random media. *Reports Prog Phys*. 1997;60(2):227.

Acknowledgements

I would like to thank my supervisor Prof. Rocco Mazzeo, my co-supervisor Dott.ssa. Gorgia Sciutto and Prof. Silvia Prati. They gave me the opportunity to start my PhD study, providing me the guidance not only on my research activities but also pass on the positive attitude and thought in my study.

I'm grateful to have this study experience, and really thanks to China scholarship council provide me the scholarship. Thanks to Chongqing Cultural Heritage Research Institute and my colleagues in China, they gave me many supports with my life and study.

Thanks to our collaborators Dott.ssa Claudia Conti and Alessandra Botteon in Consiglio Nazionale delle Ricerche in Milano for the help in Micro-Spatially Offset Raman Spectroscopy study. Thanks to our collaborators from Opificio delle pietre dure in Florence for providing the samples.

Thanks to our University of Bologna collaborators Dott.ssa Chiara Samor ìand Daniele for the supporting in GC-MS and SPME analysis. Thanks to Dott.ssa Chiara Gualandi and Giorgia for helping me in preparing electrospinning mats and many instrumentations support. Thanks to Flavia Fiorillo for the Raman analysis. Thanks to Dott.ssa Laura Mazzocchetti for the gel characterization.

I am appreciated to have the long-term help from Dr. Eimilio Catteli and all the colleagues in M2ADL family group Dott.ssa Francesca, Diego, Marco, Lucrezia, they are kindly and warmly, I am so happy to work with them. Thanks to Analisa, Eunice, Yibing and Yang Nan who have been provided the contributions in my research activities and thesis. Many thanks to Gianluca for the well management of laboratory instruments and regents, a special thanks to Amelia and Agnese provide the warmly coffee every day and give me energy.

Thanks to all my graduate and undergraduate Chinese friends recognised in Ravenna, they enriched my life.

Thanks to my relatives, friends, and everyone who has helped me throughout my study career for their always being there, and for their never-ending support.